THE EFFECT OF UNDER ICE CRUDE OIL SPILLS ON SYMPAGIC BIOTA OF THE ARCTIC: A MESOCOSM APPROACH

By

Kyle B. Dilliplaine, B.S.

A Thesis in Partial Fulfillment of the Requirements

for the Degree of

Master of Science

in

Marine Biology

University of Alaska Fairbanks

May 2017

APPROVED:

Rolf Gradinger, Committee Co-Chair

Bodil Bluhm, Committee Co-Chair

Eric Collins, Committee Member

Hajo Eicken, Committee Member

Sarah Hardy, Chair

Department of Marine Biology

Bradley Moran, Dean

College of Fisheries and Ocean Sciences

Michael Castellini, *Dean of the Graduate School*

Abstract

The Arctic marine environment is facing increasing risks of oil spills due to growing maritime activities such as tourism and resource exploration. Encapsulation and migration of spilled oil through the brine channel system in sea ice poses significant risk to ice-associated biological communities. The first objective of this study was to establish mesocosms that allow the growth of artificial sea ice leading to sea ice physical properties similar to young natural sea ice. In addition, the mesocosms should be capable of growing and maintaining a sea ice community. Six sea water tanks with 360 l capacity each were inoculated with biological cultures collected from landfast sea ice near Utqiaġvik , AK in April 2014 (year 1) and March 2015 (year 2). The two experiments lasted 24 and 27 days, and final ice thickness reached a mean value of 33 cm. The light conditions under the ice mimicked natural spring irradiances of 15 µmol photons m^2 s^{-1}. Different inoculation approaches for ice biota were used. In year 1 we did not observe any algal growth. In year 2, biological characteristics in the ice prior to oil release (chlorophyll *a*, Extracellular Polymeric Substance (EPS) concentrations and algal and bacterial abundances) were similar to natural concentrations from early spring first year ice. The second objective was to evaluate the impact of Alaska North Slope crude oil on sea ice biota. Two different oil spill scenarios were tested in the mesocosms: discrete oil lenses and dispersed emulsions. Tanks were sampled prior to oil release and 13 or 10 days post-release in year 1 and year 2, respectively. In year 1, bacterial abundances increased after oil release, while establishment of algal populations was unsuccessful. In year 2, algal growth rates and EPS production increased over time in the control tanks, while they did not change in the oil exposed tanks. Differential response of bacteria and algae between year 1 and 2 not only point to the potential of nutrient competition, but also to the need of measuring several biological properties to detect effects of oil exposure in the event of a spill. Future studies can build upon the developed experimental framework including biological responses to low, sub-lethal oil dosing.

Table of Contents

Page

List of Figures

Page

List of Tables

Page

Acknowledgments

I would like to thank my co-advisors Bodil Bluhm and Rolf Gradinger for their unending patience, feedback and support throughout my entire graduate career. Their always positive attitude brought along a unique perspective when approaching my project and the general woes of graduate school. It is something I strive to emulate in my own life. Thank you both for taking a gamble and bringing me on as a student without a clear project at the start. I hope that one day I can be as great of a role model as you both have been for me. Thank you to my graduate committee members Hajo Eicken and Eric Collins who provided invaluable feedback at all steps of the project that ultimately led to its success. Thank you to Marc Oggier, the crazed Swiss man, who tackled this project in stride with me as the second graduate student working on this project, and who held this project together with quality caffeine, alcohol and assorted meats and cheeses when the hours got long and the sleep was far off. Thank you to the entire faculty at the University of Alaska Fairbanks who I bothered on many occasions seeking feedback and equipment. Thank you to Ana Aguilar-Islas for her invaluable feedback on experimental fermentations and efficient use of spent grains. To the countless students who sacrificed their evenings or weekends to assist me with processing time sensitive samples, thank you. Financial support for this project was provided in part by the Coastal Marine Institute and the Kathleen and Robert Byrd Award who made this project possible. Thank you to my friends, Alexis, Puka and Runa who have made my time at UAF the best I have had.

1. Introduction

Large unexploited oil reserves have been estimated to occur in the Arctic and a recent discovery of a 10 billion barrel reserve near Utqiaġvik, Alaska confirms the continued discovery of potential resource for exploitation (Gautier et al. 2009). These reserves can increasingly be exploited given the lengthening ice free season. The most visible representation of climate change in the Arctic is the loss of approximately 3 million km^2 of summer sea ice extent from 1980-2012 (Wang and Overland 2012). Less visible is the 75% reduction of sea ice volume in the Arctic since 1979 (Overland and Wang 2013). These losses led Harsem et al. (2013) to predict an additional three ice-free months per year by 2040 in the Chukchi and Beaufort seas. Increased oil and gas exploration and shipping activity are possible due to these ice losses, which enable greater accessibility for exploration and exploitation (Arctic Council 2009). Despite the expectation of an ice-free summer (<1 million km^2) within 50 years, sea ice will continue to form during the Arctic winter each year (Overland and Wang 2013). Landfast sea ice is present along coastal northern Alaska for up to nine months each year, while pack ice can drift inshore even during the summer ice-free period (Mahoney et al. 2007; Mahoney et al. 2014).

The presence of sea ice represents a hazard to the petroleum exploration and marine shipping industries, and an obstruction to oil spill responders. Recent Arctic oil research has focused on detection of spilled oil in ice (Bassett et al. 2016), the interaction and distribution of oil with and within the porous sea ice medium (Petrich et al. 2013) and clean up techniques and technology (Buist et al. 2011). With regard to biological consequences of oil spills, research has focused on the ability of microbes to degrade oil in Arctic conditions (McFarlin et al. 2014; Garneau et al. 2016), response of ice-associated cod to oil exposure (Bender et al. 2016; Hansen et al. 2016), and toxicity to key Arctic invertebrates (Gardiner et al. 2013). Acute toxicity of water soluble components from oil increases with colder ice due to the decreased flushing of sea ice brine with the underlying water mass (Faksness and Brandvik 2008), and *in situ* burning of oil does not decrease the water soluble components of oil in seawater (Faksness et al. 2012). Still, very little is known about the response of sea ice organisms to oil exposure while still in the ice matrix, particularly under the variety of conditions that can arise due to diverse interactions of oil and ice (Fig. 1). The present study, therefore, investigated the biological response to oil inside sea ice.

The Arctic sea-ice cover is host to a diverse biological community which includes bacteria, algae and metazoan meiofauna (Gradinger and Zhang 1997; Gradinger et al. 1999). The organisms occupying the Brine Channel System (BCS), liquid inclusions existing as both discrete pores and convoluted channels connecting with the underlying seawater, can grow to abundance and biomass concentrations

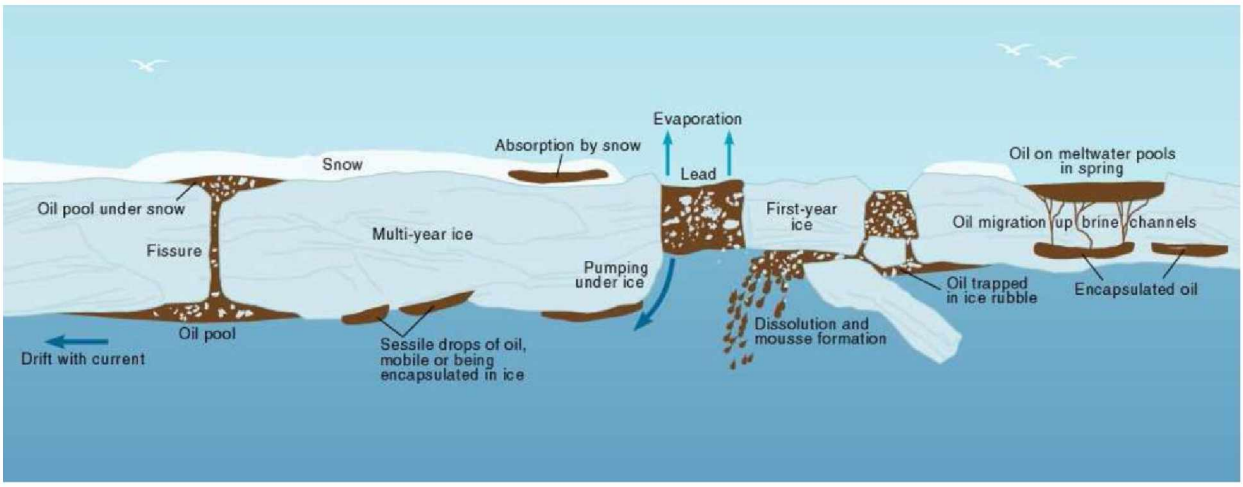

Figure 1. Oil interactions with sea ice. Reprinted from (AMAP 2010).

up to 1-3 orders of magnitude greater than in the underlying water column at certain times of the year (Lee et al. 2008; Manes and Gradinger 2009). On an annual basis, primary production in sea ice contributes 3 to >50% of total annual primary production in the Arctic (Gosselin et al. 1997), and thereby provides a food source for pelagic and benthic fauna (Michel et al. 2006; Boetius et al. 2013). Its significance as a food source is specifically high in early spring, when ice algal blooms contribute to zooplankton nutrition before the onset of the subsequent phytoplankton bloom (Søreide et al. 2010). This food source is not equally abundant and accessible within the BCS since the distribution and activity of ice biota is influenced by sea ice state variables, *i.e.* temperature and bulk salinity, that define brine properties. Within First Year Ice (FYI), brine volume fraction and connectivity is greatest in the bottom-most 10 cm of ice, rendering it the most habitable portion of the ice column, and this is where the majority of the biomass can be found (Lee et al. 2008; Manes and Gradinger 2009).

Oil spilled under sea ice, as might occur from a well blowout or damaged vessel, will rise through the water column and pool at the underside of the ice, accumulating in the recessed undulations (Glaeser and Vance 1972; NORCOR 1975; Figure 1). Oil spilled in open Arctic waters can also find its way under the ice as leads close and force the oil down (MacNeill and Goodman 1987). Ice in dominantly thermodynamic growth, as it occurs in calm weather conditions, can encapsulate the oil over one to two days (NORCOR 1975; Buist and Dickins 1987; Karlsson 2009). After encapsulation, oil is thought to remain encapsulated until increased porosity related to spring warming allows migration of oil to the surface, or under ice ablation re-mobilizes the oil under the ice (NORCOR 1975). The entrainment and further movement of oil within the ice depends on the characteristics of the brine channel network,

including permeability and porosity (Petrich et al. 2013). For example, upward migration of oil by as much as 20 cm was found to occur by March in the NORCOR (1975) experiment. Under more turbulent weather conditions or high current velocities, oil can get naturally emulsified (dispersed) in the upper water column (Tkalich and Chan 2002). The breakup of oil into small droplets can increase the amount of hydrocarbons measured in the water, which is directly related to toxicity (Gardiner et al. 2013; Özhan et al. 2014). More energy will cause smaller droplets to be formed (Li and Garrett 1998), with potentially different effects on biota compared to an oil lens.

The high concentration of sea ice biota at the ice/ocean interface leaves the community particularly vulnerable to oil exposure from below. Oil exposure to sea ice has been shown to inhibit ice algal growth (Brakstad and Nonstad 2008) and decrease meiofauna abundance (Cross and Martin 1987), but ice algal and phytoplankton response to oil exposure varies markedly between Arctic studies. Siron et al. (1993) released oil under sea ice with continuous dilution of the oil in the water column and noted inhibition of phytoplankton growth but no discernable change in the composition. Cross (1987) measured no change in ice algal composition, cell density, biomass or productivity after light oil dosing under ice *in situ* while Fiala and Delille (1999) found inhibited microalgal biomass accumulation to sea ice algae dosed with crude oil *in situ*. Biological response to oil exposure is hard to predict because of species-specific responses within each group of organisms, *e.g.* algae, bacteria etc.. For example, phytoplankton can be both inhibited and stimulated by crude oil exposure depending on the concentration, the source oil and the algal species (Hsiao 1978; Özhan et al. 2014). Varying responses among species can lead to shifts in community composition within algae, bacteria and benthic meiofauna (Gerdes et al. 2005; Gilde and Pinckney 2012; Elarbaoui et al. 2015). Increased abundance of oil-degrading bacteria in the presence of oil is relied on during spill mitigation for biodegradation, and is sometimes supported with nutrient additions to enhance the degradation rate (Bragg et al. 1994). In general, however, few studies have quantified biological effects of oil on sea-ice biota, and even fewer have studied effects on phototrophs and heterotrophs in the same study. More research is needed to discern the responses of ice biota, however *in-situ* experiments face constraints by variable, patchy ice conditions and environmental regulations. The present study contributes to filling this gap by providing a framework for conducting oil exposure experiments under defined simulated *in-situ* conditions.

Mesocosms have long been used as a way to isolate variables for ecological research, or to study the toxicological effects of environmentally sensitive chemicals. Sea-ice tanks have become a good option for experiments because they allow close control over environmental settings, and the ability to grow ice anywhere in the world outside of environmental constraints. Sea-ice mesocosms have been

used for an array of studies including algae exudation (Krembs et al. 2001) and bacterial utilization of Extracellular Polymeric Substances (EPS) (Aslam et al. 2012b), physico-biological interactions (Weissenberger 1998), entrainment processes (Reimnitz et al. 1993; Weissenberger and Grossmann 1998), desalination processes (Cox and Weeks 1975), CO_2 cycling (Kotovitch et al. 2016) and much more. Many of these experiments rely on the use of large scale test basins such as the Arctic Environmental Test Basin (HSVA, 180 m^3) in Hamburg, Germany (Krembs et al. 2001; Aslam et al. 2012b), or are conducted outside under natural light and thermodynamic fluctuations (Siron et al. 1993; Weissenberger 1998). Large-scale tanks are capable of simulating a variety of ice types and growth conditions but have a high cost, require advanced scheduling, and make true replication of multiple experimental treatments challenging. Outdoor tanks allow experiments to proceed under realistic conditions, such as natural fluctuations in light and temperature, but the scientist must sacrifice the precise control over these conditions and limit experimentation to cold climate regions during extended periods of freezing. For this experiment, we designed an easily reproducible medium-scale sea-ice tank that could be set up in a walk-in freezer, providing versatility in timing and location of experiments.

The primary goal of our study was to evaluate the response of algal biomass, EPS and algal and bacterial abundance to a simulated oil spill under two oil release scenarios 1) a calm release with oil lens formation and 2) a physical dispersion in which oil was mechanically emulsified. It was hypothesized that algal biomass, EPS and algal and bacterial abundance would decrease in tanks exposed to oil, with greater declines in the physically dispersed treatment. The secondary goal of our study was to design and build a mesocosm that could quickly grow sea ice similar to level first-year landfast sea ice in the laboratory and would harbor ice biota for experiments.

2. Material and Methods

The design, preparation and implementation of the experiments consisted of three parts: a) design of the mesocosms to conduct oil in ice experiments, b) field collection of natural sea ice communities from landfast ice close to Utqiaġvik, Alaska, as seed for the experiments and c) conducting the experiments in the mescosm tanks themselves. Experiments were conducted in two years (2014, 2015), with a modified approach in 2015 based on the experiences from 2014. Graduate student Marc Oggier (UAF, Geophysical Institute) had equal involvement with the tank design, field collections and in running the experiments.

2.1. Experimental design; treatments

Experimental oil releases under artificial sea ice were conducted in the years 2014 (Year 1) and 2015 (Year 2). Learning outcomes from Year 1 were used to improve the design for year 2, leading to variations in the experimental design between years. Year assignments will be referenced to explain those differences throughout the text (Table 1). Artificial sea ice was grown in mesoscosm tanks located in the Sea Ice and Permafrost walk-in freezer at the Geophysical Institute at the University of Alaska Fairbanks. Tank designs were based on previous work by Karlsson (2009) using an approach to achieve natural ice growth and microstructure while maintaining the capability to set up replicate treatments in a small contained space. Six individual tanks were used simultaneously during experiments to investigate three treatments (each with two replicates) each year. These treatments consisted of one biological control (no oil) and two different oil treatments in both years (Table 1). Each tank was sampled several times; therefore a "repeated measure design" approach was used for treating the data (see section 2.9.3). Tank and cold room functioning was monitored daily for visible signs of failures.

Two different modes of oil release were applied. An oil lens treatment, defined as a gentle oil addition just beneath the ice allowing it to pool, was tested each year varying only the oil volume. In Year 2, a physical emulsification was used to test effects of low volumes of oil representative of a mechanical dispersion process, *i.e.* representative of wave action or turbulent well-head release. Details are provided in section 2.6.

The artificial sea ice was seeded each year with biota (bacteria and algae) collected from landfast ice in Utqiaġvik, Alaska. This field sampling was also used to determine concentrations of basic

Table 1. Summary of tank, equipment, oil and treatment set-up and differences between 2014 (Year 1) and 2015 (Year 2). Acronyms: Biological Control Year 1 (BCY1), Biological Lens Year 1 (BLY1), Oil Lens Year 1 (LY1), Biological Control Year 2 (BCY2), Emulsified Oil Year 2 (EOY2), Emulsified Oil 2 (EOII), Alaska North Slope crude oil (ANS).

		Year 1	Year 2
Treatments		BCY1 BLY1 LY1	BCY2 BLY2 EOY2
Oil	Type	ANS Crude Oil	ANS Crude Oil
	Volume	7l	2l OLY2 0.5l EO
	Releases	1	2
Heat	Power	150W	3 x 10W, 1 x 15W
	Control	Variable Control	On/Off
Algal Growth Nutrients	Nutrient Addition	No	Yes
	Type	na	F/10
Inner Wall Color		White	Black
Initial Salinity		30	26
Core Sectioning		Variable	Conservative
Inoculation Method		Surface Entrainment	Under ice slurry and density layering
Sample Size		n=6	n=3 BCY2; n=6 BLY2, EO

biological variables in natural landfast sea ice for later comparison with the tank biota. Biological samples were collected alongside physical characterization cores prior to the release of oil and on the final day of the experiment. Deviations from this basic sampling regime are explained in detail in section 2.7. and Table 2.

Table 2. Experimental timelines in 2014 (Year 1) and 2015 (Year 2) in respect to Oil Release (OR) and day of experiment. Acronyms: Oil Release (OR), minus symbol (-) indicates days prior to oil release, plus sign (+) indicates days post oil release.

	Year 1		Year 2	
Event	Relation to OR	Day of Experiment	Relation to OR	Day of Experiment
Field Collections	OR-22	-10	OR-21	-8
Biological Inoculation	OR-12	0	OR-13	0
Baseline Coring	OR-2	11	OR-2	12
Oil Release	OR	14	OR	14
Monitor Coring (BCY1 Only)	OR+3	17		
Final Coring	OR+13	27	OR+10	24

2.1.1. Year 1

Six tanks were randomly assigned one of three treatments, each with two replicates. Treatments included Biological Control Year 1 with biota but without oil (BCY1; Biota +, Oil -), Oil Lens Year 1 without biota (LY1; Biota -, Oil +) and Oil Lens Year 1 with biota (BLY1; Biota +, Oil +) containing biota inoculate and an under-ice oil lens (Fig. 2a). After the inoculation with field-collected natural sea-ice biota, ice was slowly grown for ten days to an average thickness of 19 $\pm$ 1 cm to allow for the establishment of a biological ice community. The time of Oil Release (OR) was used as a reference point in the timeline of the experiment, and changes in sea ice and biological activities will be described in relation to this time point (Table 2). An initial coring was conducted two days prior to oil release (OR-2) to obtain baseline values for variables, *e.g.* chlorophyll *a*, bacterial abundance etc., within each tank. Two days after baseline sampling, oil was released into the LY1 and BLY1 tanks. Three days after oil release (OR+3), the BCY1 tanks were once again cored; LY1 and BLY1 tanks were excluded to limit oil contamination of the ice surface. Tanks were allowed to continue growing ice until thirteen days after oil release (OR+13), when the final ice coring was conducted to determine the oil impact to the biological community.

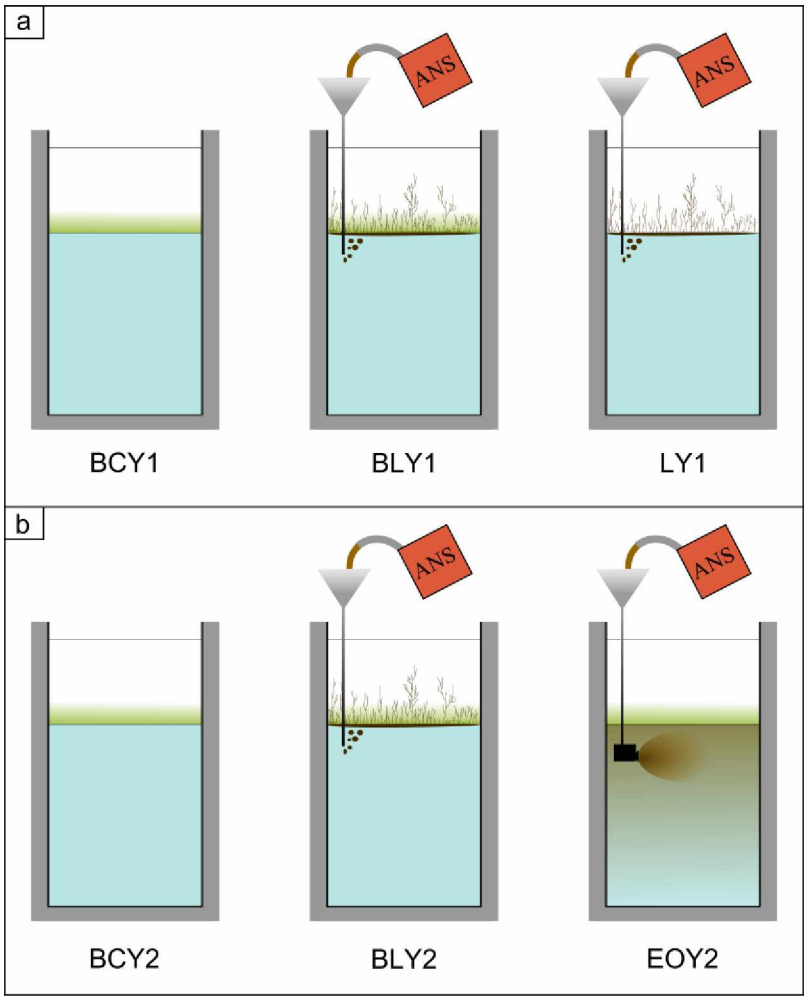

Figure 2. Treatment assignments tested in 2014 (a; year 1) Biological Control Year 1 (BCY1), oil and biota containing Biological Lens Year 1 (BLY1) and the biological free Lens Year 1 (LY1) and 2015 (b; year 2) the non-oiled Biological Control Year 2 (BCY2), oil and biota containing Biological Lens Year 2 (BLY2) and the oil and biota containing Emulsified Oil Year 2 (EOY2). ANS represents Alaska North Slope crude oil used for these experiments and green indicates biological inoculation.

2.1.2. Year 2

For this experiment, the LY1 treatment was replaced with an Emulsified Oil (EOY2, Biota+, Oil+) treatment to examine effects of lower and dispersed oil concentrations (Fig. 2b). The Biological Control Year 2 (BCY2) was retained as in year 1 (BCY1) and the Biological Oil Lens Year 2 (BLY2) treatment had a lower volume of released oil than year 1. Before oil release, ice was allowed to grow for eleven days after biological inoculation to provide more time than in year 1 for biomass accumulation due to low

chlorophyll *a* (chl a) concentrations in year 1. After oil release, ice was allowed to continue growing for 10 days before the final coring (OR+10).

2.2. Tank design

2.2.1. Year 1

Six High Density Poly Ethylene (HDPE) tanks (Greer Tank & Welding), 1 m high and 0.36 m^2 in area (Fig. 3) were coated with foam panel insulation (approximately 5 cm thick) on the outside of the tanks on all sides to prevent ice growth along the tank walls. LED lights (Reef Breeders Super Lux) covering the full photosynthetically active radiation (PAR) spectrum (400-700 nm), with an enhanced irradiance at 450 nm to enhance photosynthesis, were hung 50 cm above the ice surface to stimulate algal growth. The light spectrum was measured using an Ocean Optics USB2000 spectroradiometer at room temperature. PVC scaffolding was placed in the bottom of each tank to mount equipment and instruments. A spherical underwater 4π PAR sensor installed 50 cm from the bottom of a single tank was used to measure under-ice irradiance available to ice algae and phytoplankton cells. An aquarium powerhead (15 l min^{-1}) with a downward inclination prevented the formation of thermal convection cells and kept biota suspended. A 250 watt heater attached to a variable speed controller was used to control ice growth by adjusting the voltage. A 15 l bladder secured to the scaffolding containing antifreeze with a tube running to a collection vessel outside of each tank was inserted to prevent pressure build up during ice growth by passively displacing antifreeze over time. Each tank was filled with 360 l of artificial seawater made from Instant Ocean aquarium salt. A YSI EcoSense EC300A conductivity meter with detachable hand held unit was wired down the side of each tank, approximately 25 cm from the tank bottom, for daily salinity and temperature readings. To reduce evaporation and lessen the strain on the cold room condenser, a thin neutral optical density film (12.5 µm thickness) of transparent plastic (PVC, Reynolds) was placed over the ice surface of each tank to reduce sublimation. The cold room temperature was varied to control ice growth (see section 2.4.).

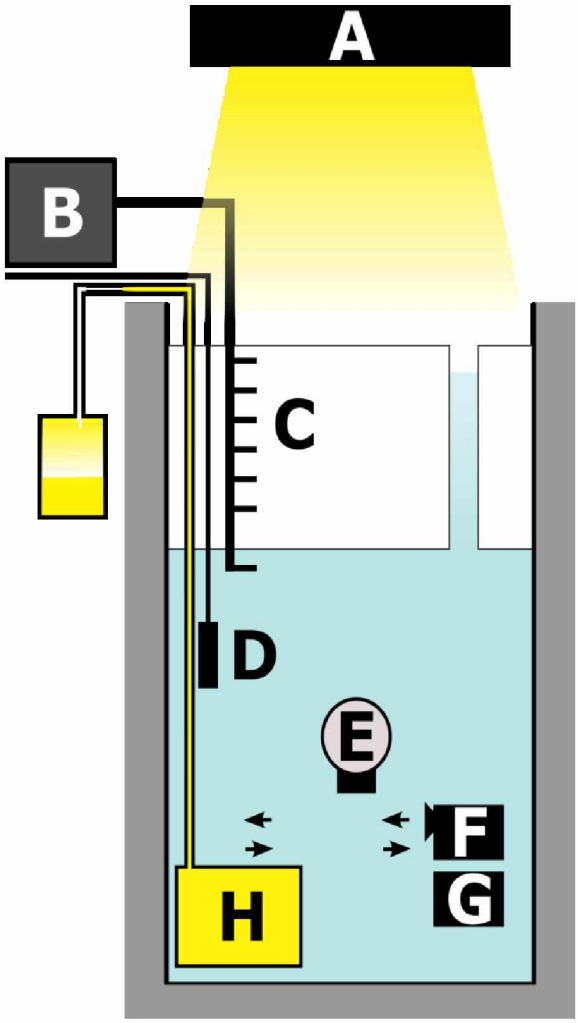

Figure 3. Schematic of tank showing positions of sensors and equipment. *Letters* represent equipment: *A* LED light fixture, *B* datalogger, *C* thermistor chain, *D* temperature and salinity probe, *E* 4π PAR sensor, *F* circulation pump, *G* heater, *H* pressure release bladder.

2.2.2. Year 2

Much of the general tank equipment and experimental conditions remained identical, though the following modifications were made (Table 1). The cold room was held at a constant temperature of -15° C. The mean seawater salinity before freezing was initially lower (Table 1) and increased by the end of the experiment due to brine drainage from the growing ice sheet and evaporation. The tanks were fitted with a black HDPE 152.4 µm thick liner to avoid contact with walls that were oil-contaminated (though cleaned) after year 1. The variable speed controllers used in year 1 for heater control were

replaced with three 10 watt and one 15 watt heater per tank. Heaters were turned on or off in combination to control ice growth.

2.3. Field sampling

2.3.1 Year 1

Field sampling of natural landfast ice communities plus characterization of the *in-situ* environmental conditions occurred in April 2014. Sampling occurred on level landfast ice close to Utqiaġvik, Alaska. Ten snow depth readings were randomly taken within a 1-m^2 quadrat before clearing snow from the ice for coring. Landfast sea ice was collected using a Kovacs Mark II 9-cm Internal Diameter (ID) ice corer. Ice temperature was measured in a single core at 10-cm intervals using a Thermo Scientific Traceable digital thermometer immediately after coring. Salinity samples were collected from an adjacent core by sectioning at 5-cm intervals and salinity was later measured directly from melted sections using an YSI 30 thermoconductivity meter. Irradiance was measured at the ice-air interface using a LICOR 2π PAR sensor, and concurrently at 10 cm below the ice-water interface using a LICOR 4π PAR sensor. The bottom 10 cm of ice was sampled in three replicate cores for quantification of the following biological parameters: chlorophyll a concentration (chl *a*), Extracellular Polymeric Substances (EPS) concentration and bacterial abundance. The 10-cm bottom portion of each ice core was divided into two horizons, 0-2 and 2-10 cm, where 0 represents the ice-water interface. Sections were melted at 4° C with the addition of 100 ml of 0.2 µm-Filtered Sea Water (FSW) per cm of core in the dark to prevent osmotic shock to the ice biota (Garrisson and Buck 1989). Sections were processed once entirely melted (i.e., after 3-30 hours).

At the same time, ice biota were collected for use as an inoculum within the tanks. A custom-built carbon fiber ice corer (Jon's Machine Shop, Fairbanks, Alaska; 20-cm inner diameter) was designed to collect a large volume of ice. From a total of 75 ice cores, the bottom 1 to 3 cm of the core, which typically contain most of the biomass in Alaska landfast ice (Gradinger et al. 2009), was removed and melted with the addition of FSW as a buffer as outlined above. Pooled sections were initially held in an incubator in Utqiaġvik under low light, approximately 20 µmol photons m^{-2} s^{-1} at 1 °C, until transport to the home lab. Half of the collected material was concentrated on a 20-µm sieve to reduce liquid volume for transport and retain the sea ice meiofaunal constituents (Gradinger et al. 2009). Sieves retained a large fraction of the sea ice algae. The other half of the material remained un-concentrated, and

therefore contained the smaller fraction of sympagic biota, *i.e.* small algae and bacteria. The inoculum was transported to Fairbanks, Alaska where it was held at 1° C with a salinity of 28 under constant light conditions, 20 µE m^{-2} s^{-1} with aeration, until use within the tanks. Samples were drawn from the inoculum immediately prior to tank seeding for biological analyses, see section 2.9.2. for details.

2.3.2. Year 2

Field collection was conducted in March of 2015, as described in year 1, with the following modifications. The top and bottom halves of two different cores were used to complete the temperature profile due to rapid cooling in the -19 °C ambient air temperature. Biological analyses of bottom ice were divided into three sections, 0-2, 2-5 and 5-10 cm (0 cm=ice-water interface) for increased vertical resolution. Sixty-four ice cores were collected for inoculation utilizing only the bottom 1-3 cm as described above.

2.4. Control of ice tanks during ice growth

Ice was grown in preliminary trials prior to the two main experiments to ensure ice microstructure was representative of environmental columnar sea ice, which typically dominates most late spring Arctic ice (Lange et al. 2015). To simulate frazil ice, a frazil ice surrogate was used to initiate ice growth within the tanks and provide a disorganized surface layer commonly found in First Year Ice (FYI).

2.4.1. Year 1

Frazil ice was simulated using hoarfrost crystals collected from the surface of lake ice: a 3 cm thick layer was added to the tanks when the water reached the freezing point (-1.8 °C). Ice thickness was monitored using the in-tank thermistor chains by examining ice temperature profiles. Adjustments to the cold room and voltage regulator controlled water heater were made according to these data with a target growth rate of 1 cm day^{-1}. Cold room temperature set points ranged between -5 and -15 °C during the duration of the experiment (Table 3). Ice temperature profiles using the thermistor strings were found to accurately match linear profiles generated from the ice surface and water temperatures.

Table 3. Cold room temperature changes and associated day of experiment.

Day of Experiment	2014	2015
	Temperature Set Point Changes (°C)	
1	-5	-15
2	-8	-15
3	-10	-15
8	-15	-15

Surface and water temperature were used for the interpretation of physical properties, as opposed to thermistor chain data in tanks with them, to maintain equality between the tanks with and without thermistors.

2.4.2. Year 2

Hoarfrost crystals from year 1 contained a pool of organic matter, *e.g.* seed pods etc., that we wished to avoid. Therefore, frazil ice was simulated using clean crushed freshwater ice in direct response to year 1. Surface ice crystals were larger in size (~1 mm) as a result. Ice growth rate was controlled by turning on or off individually three 10 W and one 15 W heaters. By doing so, a large range of combined wattage could be achieved.

2.5. Biological inoculation of the ice tanks

2.5.1 Year 1

The slush ice layer resulting from the hoarfrost crystals provided a surface over which the biological inoculum could be poured, physically trapping the biota in the surface ice. Twenty-two liters of the inoculum were added to each of the six tanks in this way. Ice was allowed to grow for 24 hours after inoculation. Cold room temperature was maintained at -5 °C to reduce osmotic stress to the released biota close to the surface, because ice brine salinity is inversely correlated with temperature (Cox and Weeks 1975; Zhang et al. 1999), and to allow free movement of the organisms with the growing ice.

2.5.2. Year 2

Results from year 1 indicated destructive freezing of biota into surface ice. Therefore a different approach was used in year 2. Algae were cultured at UAF from environmental samples collected three months earlier and used to seed the inoculations. Ice growth was initiated by adding crushed freshwater ice to the water surface once at the freezing point (-1.7° C). Ice was allowed to grow to an initial thickness of 10 cm. At this time, crushed freshwater ice was mixed with half of the inoculum to create an ice slurry similar to year one but with larger crystals. Seven liters of cultured algae were mixed with those collected from the environment at this time, and then injected through a 5-cm diameter hole drilled through the ice in the center of each tank and spread across the ice bottom using a PVC spreading device. After 24 hours, a small hole (1.5 cm diameter) was drilled through the ice close to the edge of the tank and the remaining inoculum, with a lower salinity relative to tank water, was released in direct contact with the ice-water interface, thus creating a stratified layer. The inoculum was thereby held in close contact with the growing ice for four hours in order to promote movement of organisms into the ice. Passive entrainment of immobile organisms was probably also facilitated as the ice presumably grew through this inoculation layer before the pumps that created water movement were turned back on.

2.6. Oil release

2.6.1. Year 1

Alaska North Slope (ANS) crude oil, collected at Pump Station 1 at the Trans-Alaska Pipeline entry point, and provided by the Alyeska Pipeline Services was used for these experiments. Physical characteristics were determined in December of 2014 by SL Ross Environmental Research Ltd. with select properties listed in Table 4. A container of ANS was cooled to -20 °C and mixed with room temperature ANS to a final temperature of -2° C in a double-walled thermos. This was done to prevent substantial differences in temperature that could melt the underside of the ice after release. A 5 cm diameter hole was drilled into the ice in the back left corner of the tank and 7 liters of oil were added gravimetrically. Seven liters are representative of a 2 cm thick oil lens covering the entire ice bottom. As the oil was added, water was drawn from the bottom of the tank to maintain the water level. The core

Table 4. Oil properties determined for the Alaska North Slope crude oil used in this experiment.

			Units
Dynamic Viscosity	At 0°C	40	(mPa·s) @ $180s^{-1}$
Dynamic Viscosity	At 20°C	13	(mPa·s) @ $180s^{-1}$
Pour Point		-18	(°C)
Flash Point		<-10	(°C)

hole was plugged with a replacement ice core made by freezing brackish water in PVC pipes and sealed along its edges with freshwater to prevent oil percolation.

2.6.2. Year 2

Two small holes (1.5 cm diameter) were drilled in the center of the tank for oil release into the lens treatments (BLY2). Vinyl tubing was inserted into the holes where it instantly froze into place providing a water-tight fit. Two liters of oil were added to a hopper above the tank connected to one of the two tubes inserted just below the ice bottom. The second tube was used to vacuum pump water from the bottom of the tank allowing oil to replace the displaced water. In this fashion we were able to carefully control the release of oil and prevent the introduction of air. To prepare the oil emulsification (EOY2), a small impeller was attached to the end of a syringe. The impeller was lowered beneath the ice through a 5-cm diameter hole and 500 ml of oil were injected into the impeller, which mechanically dispersed the oil below the ice.

2.7. Ice core sampling in the experimental tanks

2.7.1. Year 1

All coring was done using a custom-built stainless steel corer, 5 cm ID. The corer was operated by an electric drill and was modeled after a full size sea-ice corer having both flighting surrounding the core barrel for removal of ice shavings and teeth overlapping the inside of the core barrel to prevent cores from freezing into the barrel. The corer drilled holes of approximately seven centimeters in diameter. Five centimeters of buffer zone was left between any two holes or structure transiting the ice, *e.g.* thermistor chain or edge of tank, in order to minimize brine drainage which might impact future

cores. To effectively utilize the limited surface area, a template of twenty-one circles representative of the core hole dimensions and the surface area of the tanks were laid out to preselect coring location and order. Random numbers were selected which corresponded to each drilling location for the entire drilling operation. Six cores in total were extracted during each coring event from each tank. Of those, two cores were used for salinity measurements and oil volume determination, one core for ice microstructure analysis, and three cores were used for biological analysis. Cores were sectioned in order to provide a vertical distribution of each measurement. Salinity cores were cut into 2.5 cm sections immediately upon removal from the tank. Sections were placed into airtight glass containers and frozen at -20 °C until further processing.

Cores for other variables were sectioned to allow differentiation between bottom ice sections (ice-water interface), upper ice sections and location of an oil lens (Fig. 4). At OR-2, cores were cut 10 cm from the ice-water interface creating two sections; the 0-10 cm bottom section and the section from 10 cm to the upper surface which was of variable thickness depending on the ice core length. At OR+3 (BCY1 tanks only) a cut was again made 10 cm from the ice-water interface resulting in the same 0-10 cm sections. As with OR-2, the subsequent (now middle) section of the core was again of variable thickness dependent upon the total length of the individual ice core. Another cut was made 5 cm from the ice-air interface to remove the upper layer, which contained organic matter from entrained biota which would otherwise have biased measurements (Fig. 4b). At OR+13, BCY1 cores were processed identically to OR+3. Cores from the other two treatments, BLY1 and LY1, were sectioned as follows; clean ice under the oil lens was sectioned where no oil was visibly present (Fig. 4c). The next section was an oil lens section, which included ice saturated with oil above the lens and the oil-saturated ice that grew after oil release. Another cut was made 5 cm from the ice-air interface to match the sectioning in OR+3 resulting in a total of four sections from the oil treated cores (Fig. 4c). All sections except the 5 cm surface ice were of variable thickness.

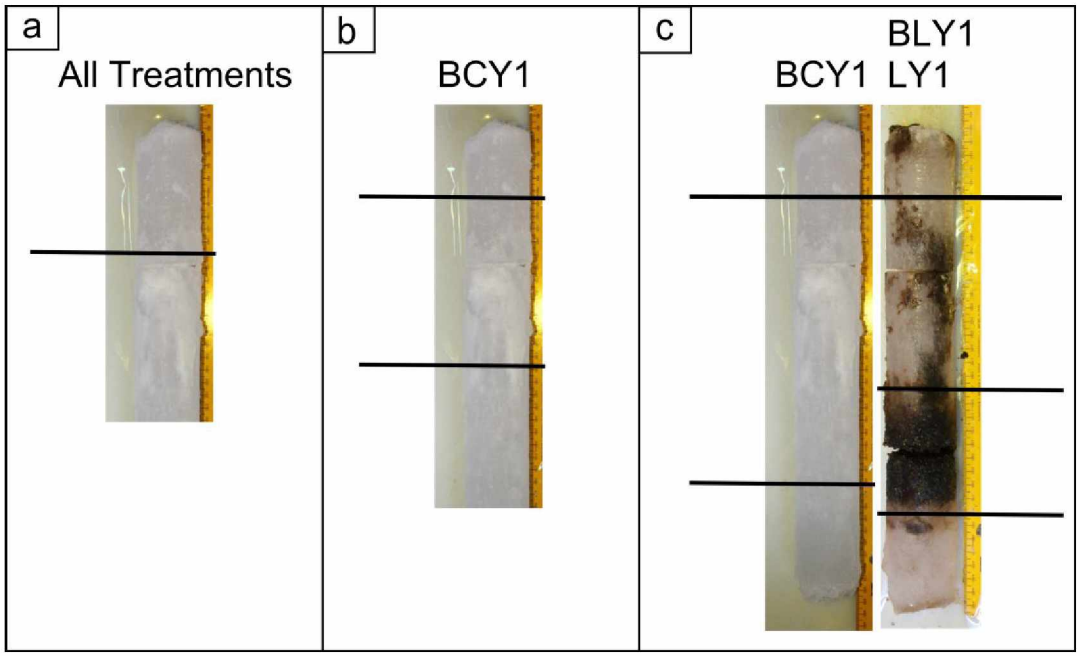

Figure 4. Ice core schematics showing sectioning in year 1, a) two days prior to oil release (OR-2), b) three days after oil release (OR+3), Biological Control Year 1 (BCY1) treatment only and c) thirteen days post oil reals (OR+13) for Biological Lens Year 1 (BLY1) and Lens Year 1 (LY1) and the BCY1 treatments, which were sectioned differently on this day. Lines represent where sections were cut.

2.7.2. Year 2

In contrast to year 1, an intermediate coring day was avoided to prevent oil from getting to the surface ice through core holes in year 2. At OR-2, allocation of the six cores was identical to year 1 but a microstructure core was omitted. At OR+10, six cores were again collected with the addition of an ice block (approximately 25 x 25 cm) being cut from each tank for microstructural analysis. Core holes in these tanks were plugged as above and the block hole was filled using ice shavings with fresh water additions to solidify.

For ice cores taken at OR-2 a cut was made 5 cm from the ice-water interface and again between 9 and 10 cm from the ice-water interface (Fig. 5a). The slight variability in the second cut was to exclude the initial biological inoculation layer, which was visible as a light band in the ice microstructure. This band was excluded to avoid the detritus rich, artefactual layer created by the initial biological inoculation. The ice core sample from tank 6 was too short to yield a second complete section so only the bottom 5 cm were taken from this core. At OR+10, section cuts were identical to those at OR-2 to allow for direct comparison of ice sections. Ice growth between OR-2 and OR+10 yielded a third

section representative of the new ice bottom (Fig. 5b). This bottom ice section was the only section, which was of a variable thickness between cores (Fig. 5b).

2.8. Ice tank physical measurements

2.8.1. Year 1

Light readings from the surface of the ice were taken every 1-3 days on each tank using a LI-COR 2π planar PAR sensor at the same time as the submerged 4π spherical PAR sensor. As ice thickness increased, adjustments to the surface irradiance were made by increasing LED light intensity to maintain an under-ice irradiance between 9.1 and 14.6 µmol photons m^{-2} s^{-1} for the duration of the experiment. This irradiance level is well above the minimum threshold for ice algal growth (<1 µmol photons m^{-2} s^{-1}) and was similar to the environmental measurements (Cota and Smith 1991; Mock and Gradinger 1999). Air, ice surface, and water temperature and salinity were recorded at the same time and frequency as light measurements. Instrument accuracy and resolution are listed in Table 5. The salinity-temperature sensors were not always reliable and obvious deviations from the actual salinity, *i.e.* a drop to 5, were excluded from interpretation ($\pm$ 2.5 units from trend line). Three thermistor chains (Beaded Stream) were attached to a Campbell CR10X data-logger to record ice temperature every five minutes. The thermistor chains, each with six thermistors evenly spaced at 5 cm throughout the ice and upper water layer, were placed in one randomly selected tank per treatment (3 tanks total) 10 cm from the tank edge towards the center.

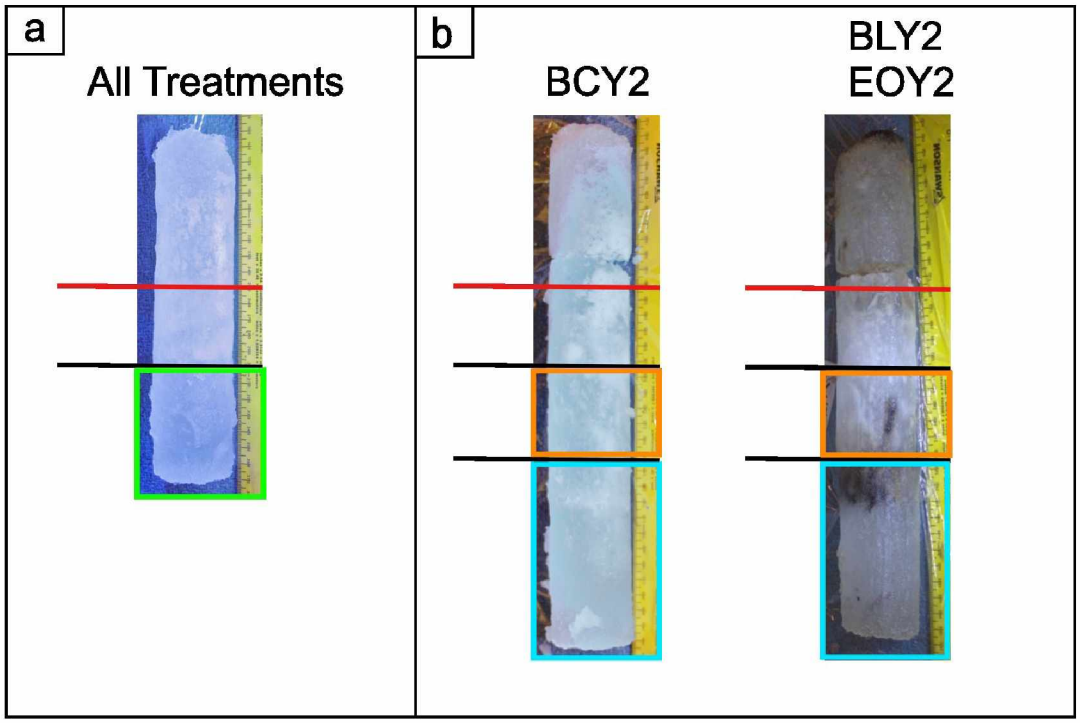

Figure 5. Ice core sectioning showing the conservative (comparison of green and orange box) and the non-conservative divisions (comparison of green and blue box) employed in year 2. a) two days prior to oil release (OR-2), b) ten days post oil release (OR+10) for the oiled Biological Lens Year 2 (BLY2) and Emulsified Oil Year 2 (EOY2) treatments and the non-oiled Biological Control Year 2 (BCY2 treatment). Lines represent where sections were cut, Ice above the red line was present before the biological inoculation and was not included in the biological analyses.

Table 5. Tank instrumentation accuracy and resolution.

Variable	Instrument	Placement	Accuracy	Resolution
Temperature	Fisher Scientific Traceable Thermometer	Air, Ice Surface	± 0.05 °C	0.001 °C
	EcoSense EC300A	Water	± 0.2 °C	0.1 °C
	Beaded Stream Thermistor Chains	Ice	± 0.1 °C	0.01 °C
Salinity	EcoSense EC300A Salinometer	Water	± 2%	0.1
Irradiance	Li-COR 2 π sensor	Ice Surface, Water	± 5%	0.01 µmol photons m^{-2} s^{-1}

2.8.2 Year 2

In year 2, the tank containing the 4π light sensor was lost due to a pressure release failure resulting in an incomplete series of sub-surface light measurements. To reduce the effect of increasing attenuation by the growing ice sheet, LED light irradiance was increased by 3 µmol photons m^{-2} s^{-1} each day.

2.9. Analysis and processing

2.9.1. Physical measurements from ice cores

2.9.1.1. Year 1

Cores sectioned for salinity measurements were melted at room temperature in the original sealed glass container. A YSI EcoSense EC300A was used to measure salinity. Salinity measurement bins (2.5 cm sections) from the salinity cores were compressed or stretched to match core lengths when the salinities were applied to the biological cores for estimation of BVF based on individual core lengths. Ice thickness was measured when cores were extracted (Table 6).

2.9.1.2. Year 2

In year 2, ice blocks were also removed at the end of the experiment and frozen for post-processing of physical parameters. The block was used to supplement information on salinity and microstructure where a larger ice volume was required. Post-processing of physical cores was conducted identically to year 1.

Table 6. Ice thickness at initial and final coring based on extracted core length in 2014 (year 1) and 2015 (year 2). Acronyms: Oil Release (OR), minus symbol (-) indicates days prior to oil release, plus sign (+) indicates days post oil release.

Year	Day	Tank	Ice Thickness (Mean ± SD) in cm	Day	Ice Thickness (Mean ± SD) in cm
1	OR-2	1	17 ± 1	OR+13	33 ± 2
		2	20 ± 1		29 ± 1
		3	19 ± 1		34 ± 5
		4	18 ± 1		28 ± 3
		5	19 ± 1		33 ± 2
		6	19 ± 1		36 ± 1
		All	19 ± 1		33 ± 4
2	OR-2	1	19 ± 0	OR+10	31 ± 1
		2	18 ± 4		34 ± 1
		4	20 ± 1		31 ± 1
		5	25 ± 3		40 ± 1
		6	16 ± 2		27 ± 4
		All	20 ± 4		33 ± 5

2.9.2. Biological measurements from ice cores

2.9.2.1. Year 1

Samples were melted in the dark at 3 °C and immediately processed as soon as they were completely melted over a 72 hour period. Samples containing oil required pre-treatment before processing for analysis. Clear vinyl tubing (4.8 mm ID) was cut into 30 cm sections and sterilized by soaking in a 10% HCl bath for 24 hours followed by rinsing with 0.2 µm FSW. Tubing was connected to a vacuum filtration flask and used to carefully skim oil from the surface leaving only a sheen behind. Fluid accumulation in the vacuum flask revealed this method to remove oil at a ratio of ~ 1:3 parts crude oil: water. The samples were gently homogenized by inverting the container for two minutes and poured into a separatory flask through a large glass funnel, the funnel acts to pre-filter oil through adhesion. All glassware was autoclaved prior to use. The sample was allowed to sit for 60 seconds as small droplets collected at the surface. The sample was then transferred into a new and freshly autoclaved glass container at a rate of 1 l min^{-1} removing much of the visible oil by adhesion to the glass. Samples collected at OR-2 and all of the BCY1 samples were oil free and therefore not subjugated to this process.

Once clean, all samples were processed identically. Most samples were limited in volume, and sample volumes were roughly divided amongst variables as 2.4:1:1.4:1 for Chl *a*:EPS:POM:Bacteria across all sampling events. Samples were gently homogenized by inverting the container for two minutes before allocating the samples. Chl *a,* POM and EPS samples were processed within 3 months of collection and bacteria abundances were determined within 5 months of collection and 3 weeks of filtration.

2.9.2.1.1 Chlorophyll *a*

Chl *a* concentration was determined in the melted samples by filtering 15-360 ml onto Whatman GF/F filters using vacuum filtration $\leq$ 5 psi. Filters were extracted with 7 ml of 90% acetone at -20 °C for 24 hours, samples were warmed to room temperature for 1 hour in the dark before fluorometric measurements were conducted using a TD-700 Turner Design fluorometer (Arar and Collins 1997). Fluorometer calibrations were conducted using pure chl *a* standard (Sigma Aldrich). Chl *a* content per algal cell was calculated by dividing the mean chl *a* concentration by the mean cell abundance per core or section. Passive dilution of chl *a* concentrations on a full core basis were calculated by assuming no further algal growth or entrainment occurred after oil for comparison with actualy OR+10 values. Based on the BCY2 growth rates, predicted chl *a* concentrations were calculated for the time of oil release (OR) and experiment termination (OR+10) and compared with the actual concentrations at OR+10 in BLY2 and EOY2.

2.9.2.1.2. Extracellular polymeric substances

EPS concentrations were determined by the Phenol/Sulfuric Acid (PSA) method of extraction (DuBois et al. 1956; SOKI Wiki 2014). All glassware was soaked in a 10% HCl solution to remove sugar residues, and rinsed with 0.2 µm FSW prior to use. Melted samples were filtered directly onto 25 mm 0.4 µm polycarbonate membrane filters, placed in a borosilicate tube with cap and frozen at -80 °C until further processing. After thawing, 4 ml of 0.5 M sulfuric acid was added directly to the borosilicate tube containing the filter. The tubes were capped tightly and placed in a water bath held at 100 °C for 1 hour, in order to hydrolyze the material retained on the filter. Samples were cooled for 10-20 minutes before centrifugation at 2500 rpm for 5 mins. Two ml of the supernatant was transferred to a fresh borosilicate tube with cap, and processed according to Dubois et al. (1956). Fifty µl of 80% phenol was added followed by 5 ml of concentrated sulfuric acid. The tube was then capped and quickly inverted several

times. Heat generated by this exothermic reaction was allowed to dissipate at room temperature for 15 minutes before being transferred to a water bath held at 27 °C for 15-30 minutes. Samples were pipetted into a 10 mm path length quartz cuvette and absorption was determined for each sample at 450 and 750 nm using a Shimadzu UV-1201 spectrophotometer. Blank filters were included with each processed batch and a standard curve was generated using D (+) Glucose as a standard for conversion of EPS concentration to Glucose Equivalents (GEQV). For comparability with the alternative Alcian Blue method of EPS determination, and in lieu of our own inter-calibration, the equation derived from van der Merwe et al. (2009) was used to convert GEQV l^{-1} ice to Xanthan Gum Equivalents (XGEQV) l^{-1} ice:

μg XGEQV l^{-1} ice = 0.975 x μg GEQV l^{-1} ice + 0.879

2.9.2.1.3. Algal and bacterial enumeration

For bacterial enumeration, 10- to 100-ml aliquots of each melted sample were drawn using a sterile pipette and injected into a clean 100-ml amber glass bottle. 0.2-µm filtered hexamethylenetetramine buffered formaldehyde was added to each bottle to a final concentration of 1%. Samples were stored in the dark at room temperature until later processing for enumeration by epifluorescence microscopy. Bacterial abundance was determined by filtering 10-50 ml of fixed sample onto 0.2 µm Nuclepore filters with a 0.8 µm supporting filter to promote even filtering across the membrane. Each sample was stained by 4', 6-diamidino-2-phenylindole (DAPI) (0.1 μg ml^{-1} sample final concentration) for 5 minutes before filtering (Porter and Feig 1980). The filters were mounted onto microscope slides using immersion oil and frozen until enumeration. Bacterial cell counts were conducted using an Axiovert35 microscope with UV light excitation (excitation: 365 nm, long pass: 397 nm). Bacteria were counted until at least 500 cells were enumerated or 30 fields of view (FOV) were scanned. Diatoms as well as hetero- and phototrophic nanoflagellates were also enumerated but due to their low abundance these data were not used for statistical analyses.

2.9.2.2. Year 2

Nearly all analyses were repeated in year 2, albeit with the following modifications. Volumes of melted sample filtered were as follows; 24-314 ml for chl *a*, 12-255 for EPS and 30 to 96 ml for bacterial fixation. Absorbance measurements for EPS analysis were conducted using a Molecular Devices

SPECTRA max 340PC 96 well microplate reader. Epifluorescent enumeration of bacteria were done with an Olympus BX51 microscope with UV light excitation (excitation: 330/80 nm, long pass: 400 nm). Diatom abundance was high enough to allow enumeration on the same samples. Diatoms were binned according to cellular fluorescent properties into two groups. Group 1, determined intact, showed visible fluorescence of the plasma membrane, plastid and had no defined nucleus. Group 2, determined damaged, showed weak or no plasma membrane or plastid fluorescence and had a well-defined nucleus. Empty frustules were also enumerated; diatom cell counts do not include empty frustules. A proportional percent of frustule abundance is reported as (Frustules/Total Diatoms (excluding frustules)*100).

2.9.3. Statistical analysis

All statistical analyses were conducted using R version 3.2.1. Linear Mixed Effects Regression models (LMER, R package lme4; Bates et al. 2014) with and without treatment as a factor were compared using one way ANOVA for each biological parameter, *i.e.* chl *a*, diatom abundance, EPS and bacterial abundance, for full cores and sections allowing for selection of the best model. LMER accounts for unequal sample size, the repeated measures design where each tank was sampled more than once over time, and the random effect that each tank has on biological concentrations and development. Pairwise comparison of least-squares means were used for post-hoc assignment. A Welch's T-test was applied to the means of projected algal growth rates with actual concentrations. Simple linear regression models were used to correlate EPS with diatom and bacterial abundance. Abundances were log transformed to meet normality requirements and only non-oiled sections were included to eliminate any interference or impact, the adjusted r^2 values are reported.

3. Results

3.1. Landfast ice observations in Utqiaġvik , Alaska

3.1.1. Physical variables

3.1.1.1. Year 1

Level sea ice (71.36675°N, 156.61715°W) was selected for sampling within view of the Seasonal Ice Zone Observing Network mass balance site (http://seaice.alaska.edu/gi/observatories/barrow_sealevel). Snow depth ranged from 9-13 cm, and ice thickness varied between 134 and 138 cm. Light (PAR) transmittance through snow and ice was 1.3% of the incoming radiation (Table 7). The ice temperature showed a nearly linear increase from the ice surface (-14.3 °C) to the ice bottom (-1.75 °C; Fig. 6a). Bulk salinity was highest in the surface and bottom segments of the ice displaying the characteristic "C" profile of FYI before onset of warming and melt (Fig. 6a). Calculated brine salinity based on the ice temperatures and decreased from 172 in the top to 32 in bottommost ice segments (Fig. 6a). The calculated Brine Volume Fraction (BVF) was greatest in the bottom segment of ice and ranged from 2.6 to 24.6% of the total ice volume across the core (Fig. 6a).

3.1.1.2. Year 2

Level ice with visible discoloration from ice algae was selected (71.37182°N, 156.55814°W) near Point Barrow. Snow depth in year 2 was less than in year 1 and ranged from 3 to 6 cm. Ice thickness showed minimal variability and ranged from 126 to 127 cm. Light transmittance through the snow and ice was 1.8% of incoming radiation (Table 7). Physical ice characteristics were similar to year 1 (Fig. 6b). Ice temperature decreased linearly from -16.9 °C at the ice surface to -2.5 °C at the ice bottom (Fig. 6b). A "C" shaped profile was apparent in the bulk salinity profile (Fig. 6b). Calculated brine salinity ranged from 183 to 40 and was generally highest near the surface and lowest near the bottom of the ice (Fig. 6b). The calculated Brine Volume Fraction (BVF) was greatest in the bottom segment of ice and ranged from 2.6 to 20.9% across the ice core (Fig. 6b).

Table 7. Comparison of mean physical data measured during sampling near Utqiaġvik, Alaska in year 1 (2014) and year 2 (2015). For replicate measurements, means only are reported.

Variable	Year 1	Year 2
Air Temperature (°C)	-24.9	-19.0
Ice Thickness (cm)	136	127
Free Board (cm)	10	10
Snow Thickness (cm)	12	4
Water Depth (m)	8.4	7.3
Surface Irradiance (2π) µmol photons m^{-2} s^{-1}	916	470
Under Ice Irradiance (4π) µmol photons m^{-2} s^{-1}	11.4	8.4

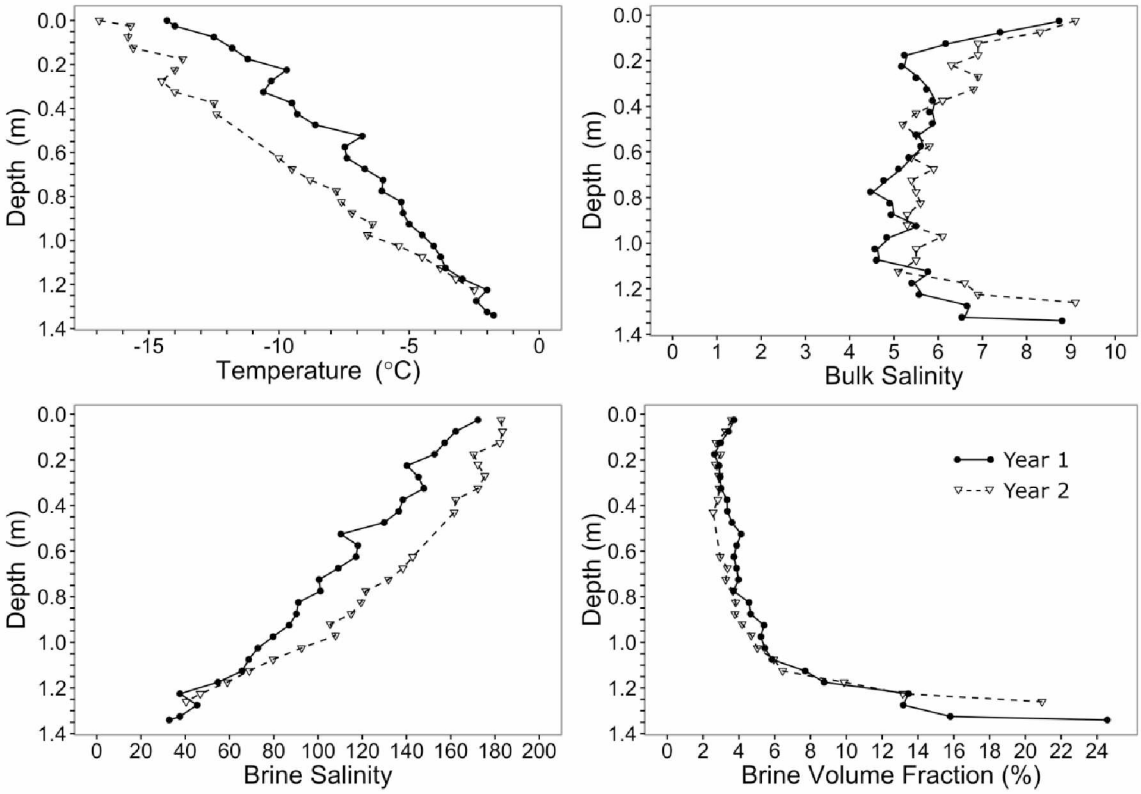

Figure 6. Physical properties of sea ice collected in Barrow, Alaska in year 1 (2014) and year 2 (2015). Temperature and bulk salinity were measured while brine salinity and Brine Volume Fraction (BVF) were calculated according to Cox and Weeks (1983).

3.1.2. Biological variables

3.1.2.1 Year 1

Biological data were collected for the bottom 10cm of the ice cores taken from the landfast ice. Integrated ice chl *a* concentrations for this layer ranged from 27.9 to 37.6 µg chl *a* l^{-1} ice (Table 8). Integrated EPS varied between 6,110 and 8,301 µg XGEQV l^{-1} ice and bacterial abundances ranged from 2.3-3.6 x 10^{8} bacterial cells l^{-1} ice. Within the bottom 10cm, concentrations for all parameters were largest in the lowermost 2 cm of landfast ice (Table 8). Mean values by section and variable are given in Table 8.

3.1.2.2. Year 2

Chl *a* concentration in the bottom 10 cm of landfast ice collected in March of 2015 (Table 8) exceeded the values from year 1 and ranged from 78 to 132 µg chl *a* l^{-1} ice. EPS concentrations were 1.8 times lower in year 2 than in year 1. Sections exhibited strong vertical gradients with highest concentrations occurring in the bottom 2 cm of ice for chl *a* with higher EPS concentrations in the bottom 5 cm.

3.2. Tank experiments

For each of the treatments, variables and years, the baseline coring values before oil release (OR-2) are described first, followed by the data from the monitoring coring (Year 1 BCY1 only at OR+3) and the final coring (Table 2). Due to differences in experimental set-up between years, all results will be presented separately for each of the two years. Algal cell abundances in year 1 were too low throughout the experiment for accurate abundance estimates. The LY1 treatment was not inoculated with sea ice biota, but still had EPS concentrations and bacterial abundance high enough to quantify. In year 2, tanks were inoculated with biota below a segment of already formed artificial ice. This abiotic ice portion (above the inoculation layer) was not sampled and is not included in the full core and section values. Due to variability in sectioning in year 1 between sample days, year 1 data is graphically presented as integrated concentrations across the length of the core. Year 2 data is graphically presented showing the

Table 8. Mean biological parameters of samples taken in 2014 (year 1) and 2015 (year 2) during biological collections from landfast sea ice in Barrow, Alaska. Section 0-10 cm represents the calculated integration of sections spanning 0-10 cm. 0 cm represents the ice-water interface.

Year	Section (cm)	Chlorophyll a (µg Chl a l^{-1} ice)	EPS (µg XGEQV l^{-1} ice)	Bacterial Abundance (Cells x 10^8 l^{-1} ice)
2014	0-2	83.0 + 5.2	17,394 + 4,494	14.6 + 3.2
	2-8	20.8 + 6.1	4,883 + 1,142	0.2 + 0.0
	0-10	33.3 + 4.9	7201 + 1,096	3.0 + 0.6
2015	0-2	246.8 + 10.5	5,388 + 3,504	Not Processed
	2-5	165.9 + 99.5	5,637 + 465	Not Processed
	5-10	28.8 + 2.1	2,540 + 178	Not Processed
	0-10	113.5 + 30.6	3,943 + 601	Not Processed

biologically active bottom sections (below the initial ice layer). All values are reported as mean + SD unless otherwise noted.

3.2.1. Abiotic variables: Ice thickness, temperature, salinity and light

3.2.1.1. Year 1

Total ice thickness at OR-2 in year 1 ranged from 17 to 21 cm from individual cores across all tanks (Table 6). Core length increased by OR+13 to a range of 25 to 40 cm with an average of 42% of the initial thickness at OR-2 for each tank. Variability was lower at OR-2 with a mean of 19 $\pm$ 1 cm across all tanks compared to the mean value of 33 $\pm$ 4 cm at OR+10, (Table 6). Surface irradiance was increased from 20 to 103 µmol photonsm^{-2} s^{-1} throughout the experiment to account for ice growth to maintain reasonably constant under-ice irradiance. Under-ice irradiance ranged from 9 to 15 µmol photonsm^{-2} s^{-1}. Temperature profiles were linear interpolations from the ice surface to the underlying water with steepest slopes in thinner ice (Fig. 7). Bulk salinity profiles in year 1 at OR-2 followed a characteristic "C" profile with the topmost ice section being the most saline in all but one tank (Fig. 8). Calculated brine salinity based on the temperature profile was highest in the uppermost section of ice ranging from 127-136 at OR-2, 148 at OR+3 in BCY2 tanks and 149-160 at OR+13 (Fig. 9). Calculated BVF was largest in the lowermost section of ice, and it varied across all cores ranged from 3.4 to 20.8% at OR-2 and 1.3 to 26.1% at OR+13 (Fig. 10).

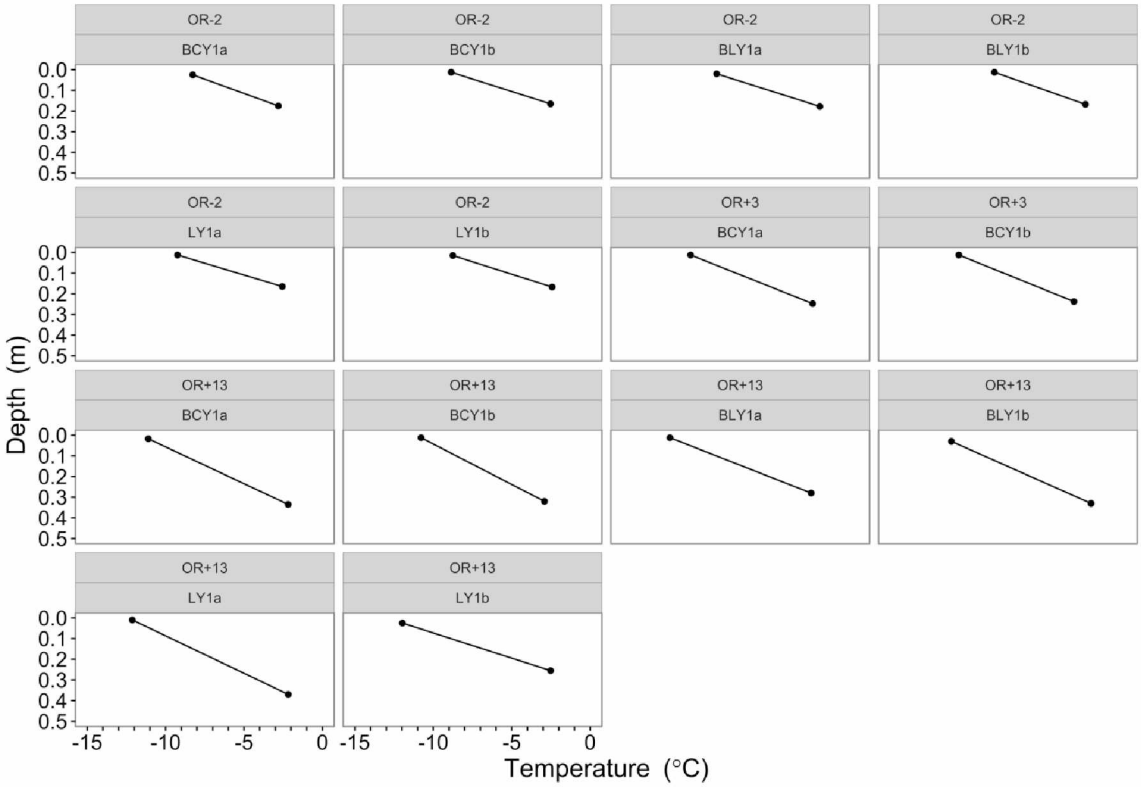

Figure 7. Temperature profile of each sea ice tank in year 1 (2014). Temperature was interpolated from the ice surface to the ice bottom. The letters a and b refer to replicates for each treatment in this and the following figures.

3.2.1.2. Year 2

Ice thickness at OR-2 in year 2 ranged from 15 to 28 cm across all tanks (Table 6). At OR+10, ice thickness had increased in all tanks by an average of 39% compared to OR-2. Ice thickness at OR+10 ranged from 23 to 42 cm across all tanks. Variability across and within tanks was larger in year 2 than in year 1 except for tank 3 at OR-2 in Year 2 which had the smallest standard deviation out of all tanks over both years (Table 6). Surface irradiance was again increased with time from 230 to 307 µmol

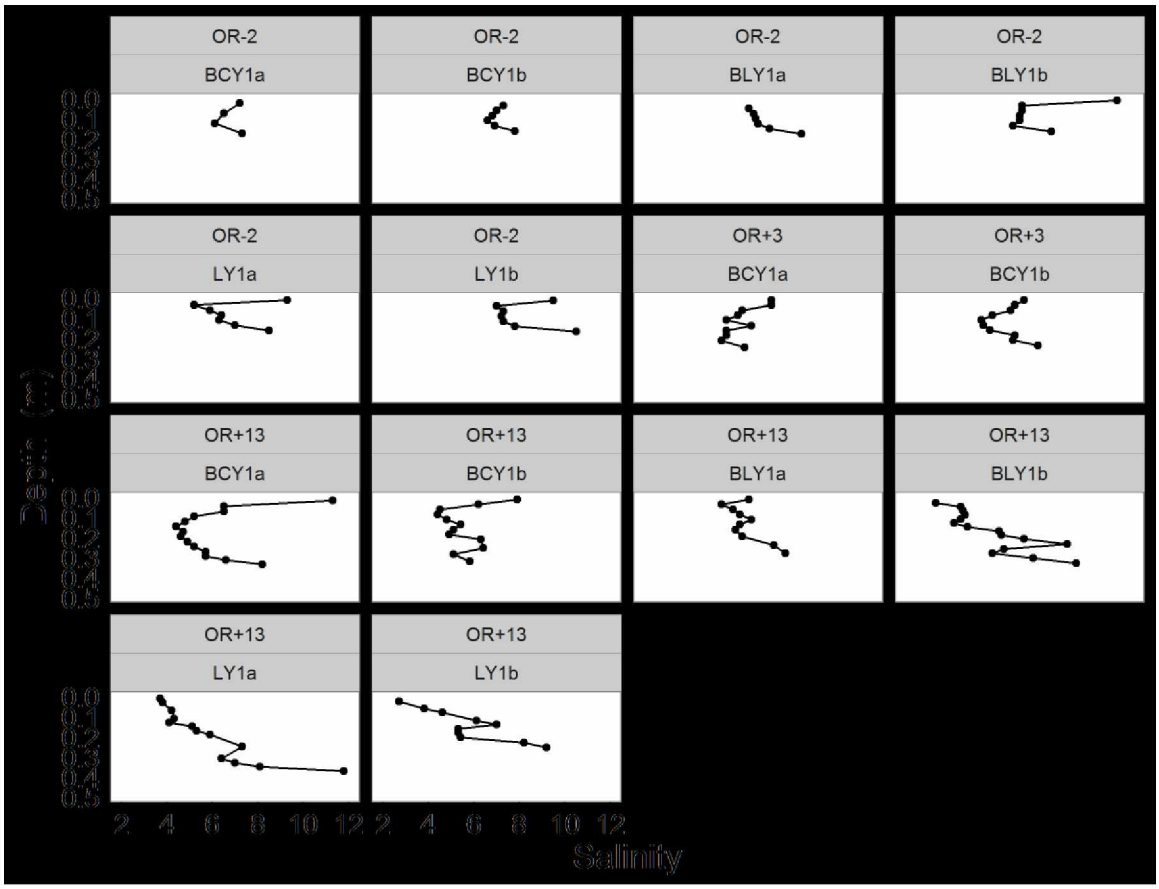

Figure 8. Bulk salinity profile of each sea ice tank in year 1 (2014). Bulk salinity was measured from directly melted samples at a 2.5 cm resolution. The letters a and b refer to replicates for each treatment in this and the following figures.

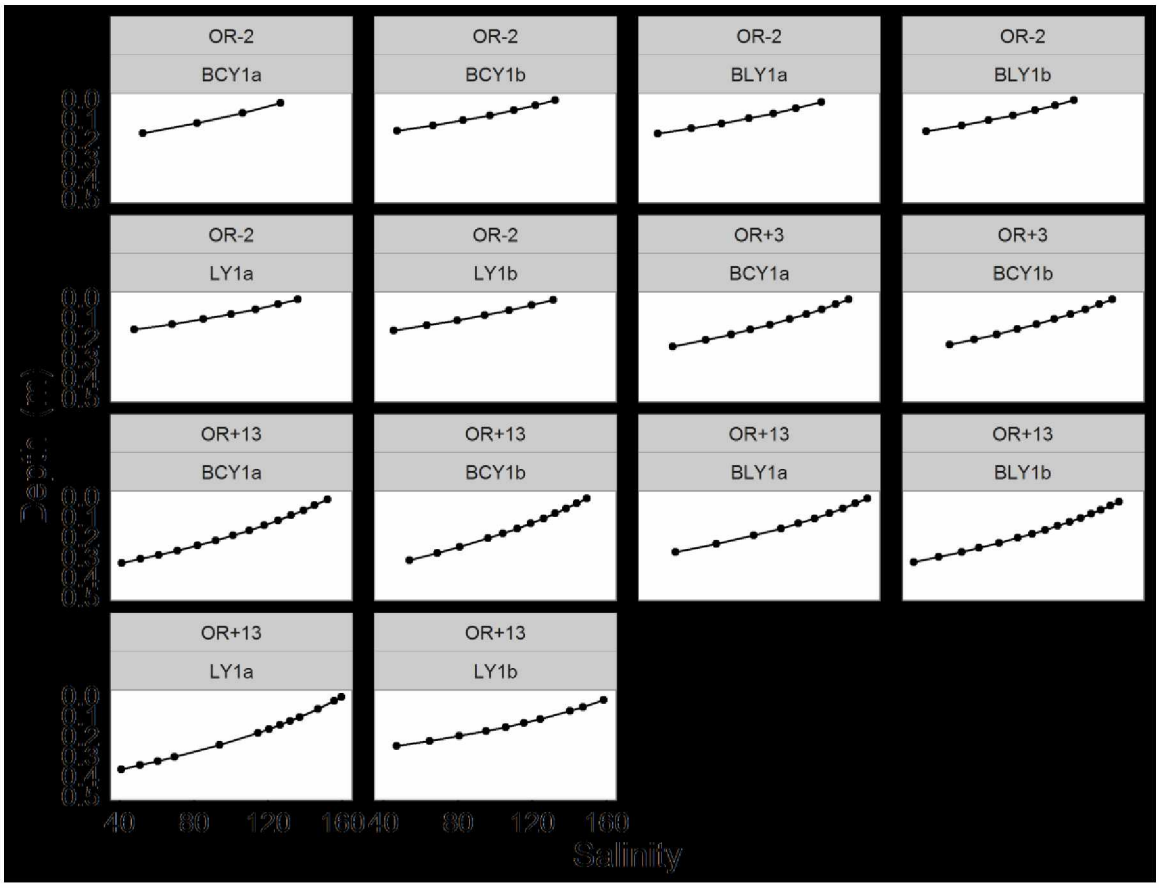

Figure 9. Brine salinity profile of each sea ice tank in year 1 (2014). Brine salinity was calculated according to Cox and Weeks (1983). Vertical line represents a salinity of 90 where algal growth declines can occur. The letters a and b refer to replicates for each treatment in this and the following figures.

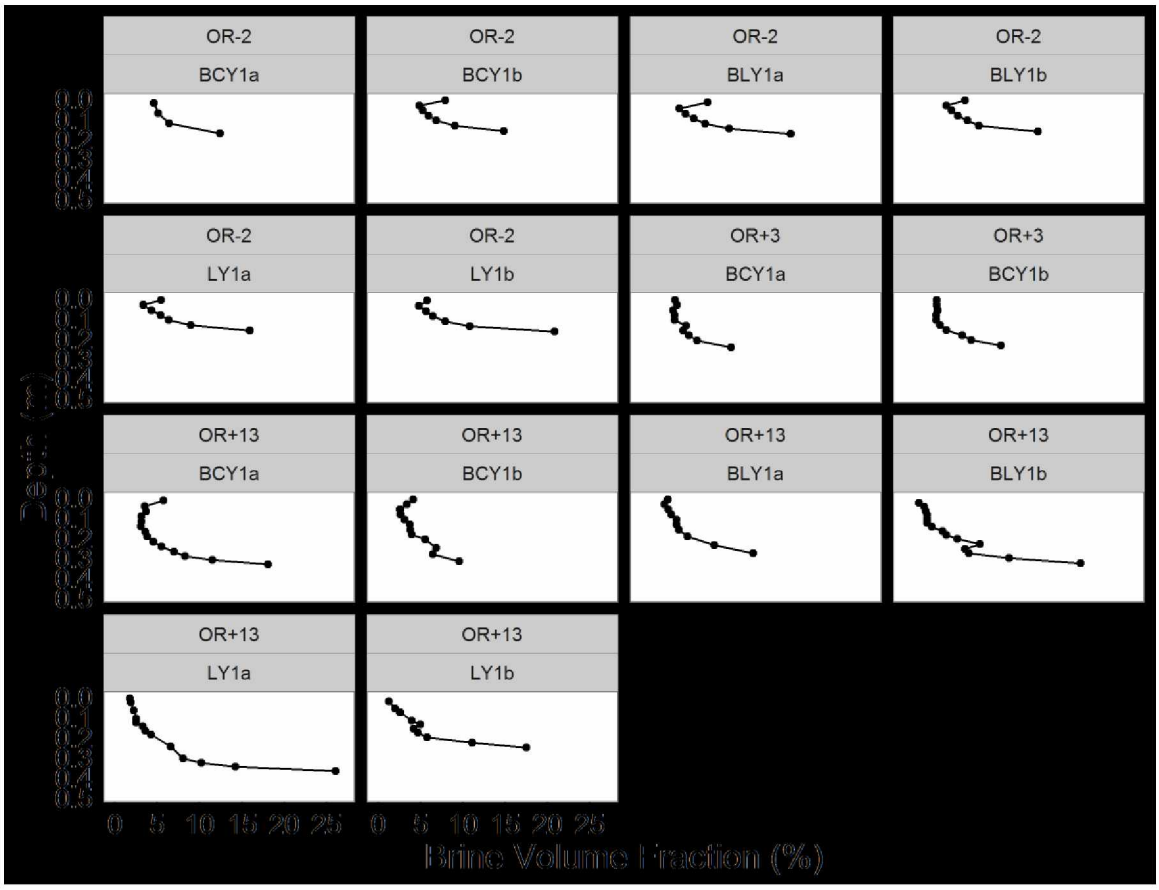

Figure 10. Brine Volume Fraction (BVF) profile of each sea ice tank in year 1 (2014). BVF was calculated according to Cox and Weeks (1983). The letters a and b refer to replicates for each treatment in this and the following figures.

photons m^{-2} s^{-1} to account for increased attenuation by thicker ice. Under-ice irradiance was 15 µmol photons m^{-2} s^{-1} during the brief window of measurements early in the experiment (ending on day OR-8). Temperature profiles were derived from linear interpolations of surface and water temperature as in year 1 (Fig. 11). Bulk salinity profiles in year 2 were incomplete because the abiotic ice above the inoculation layer was not sampled (Fig. 12). Calculated brine salinity was highest in the uppermost section of ice ranging from 71-99 at OR-2 and 107-136 at OR+10 (Fig. 13). Calculated BVF was always largest in the bottommost section of ice. The complete range of sections were 4.7-24.1% at OR-2 and 2.4-20.8% brine at OR+10 (Fig. 14).

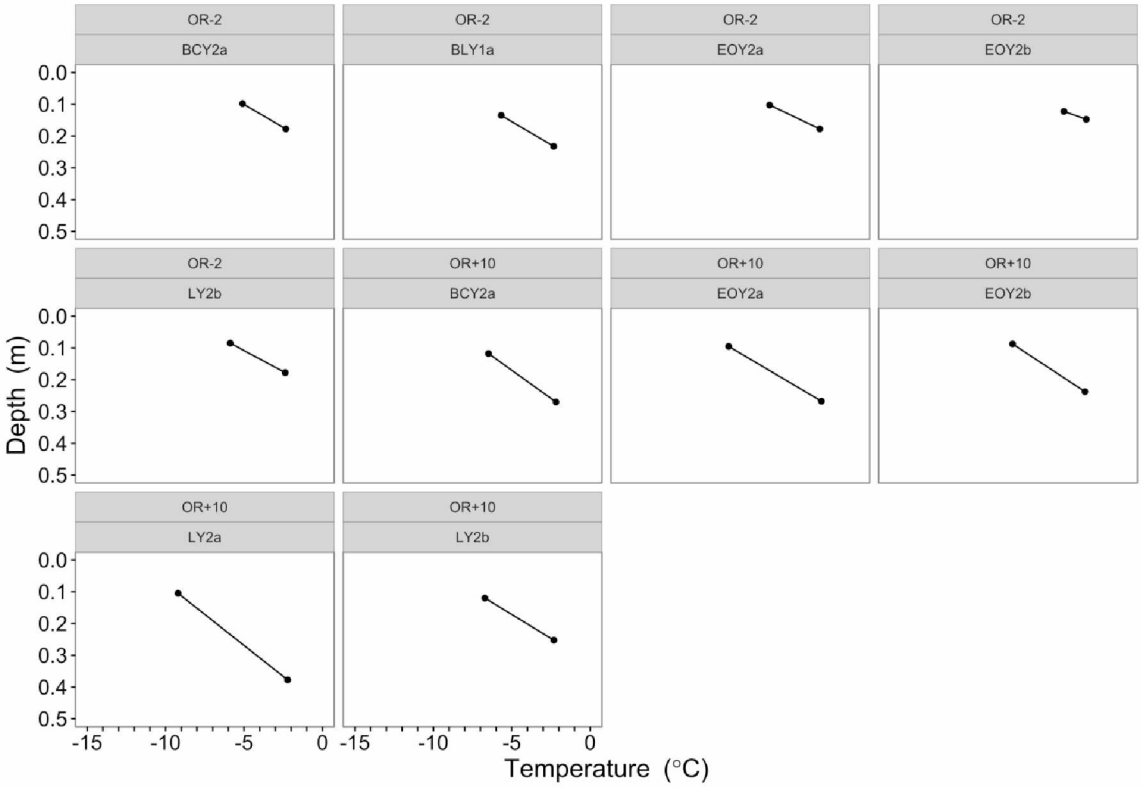

Figure 11. Temperature profile of each sea ice tank in year 2 (2015). Temperature was interpolated from the ice surface to the ice bottom. The letters a and b refer to replicates for each treatment in this and the following figures.

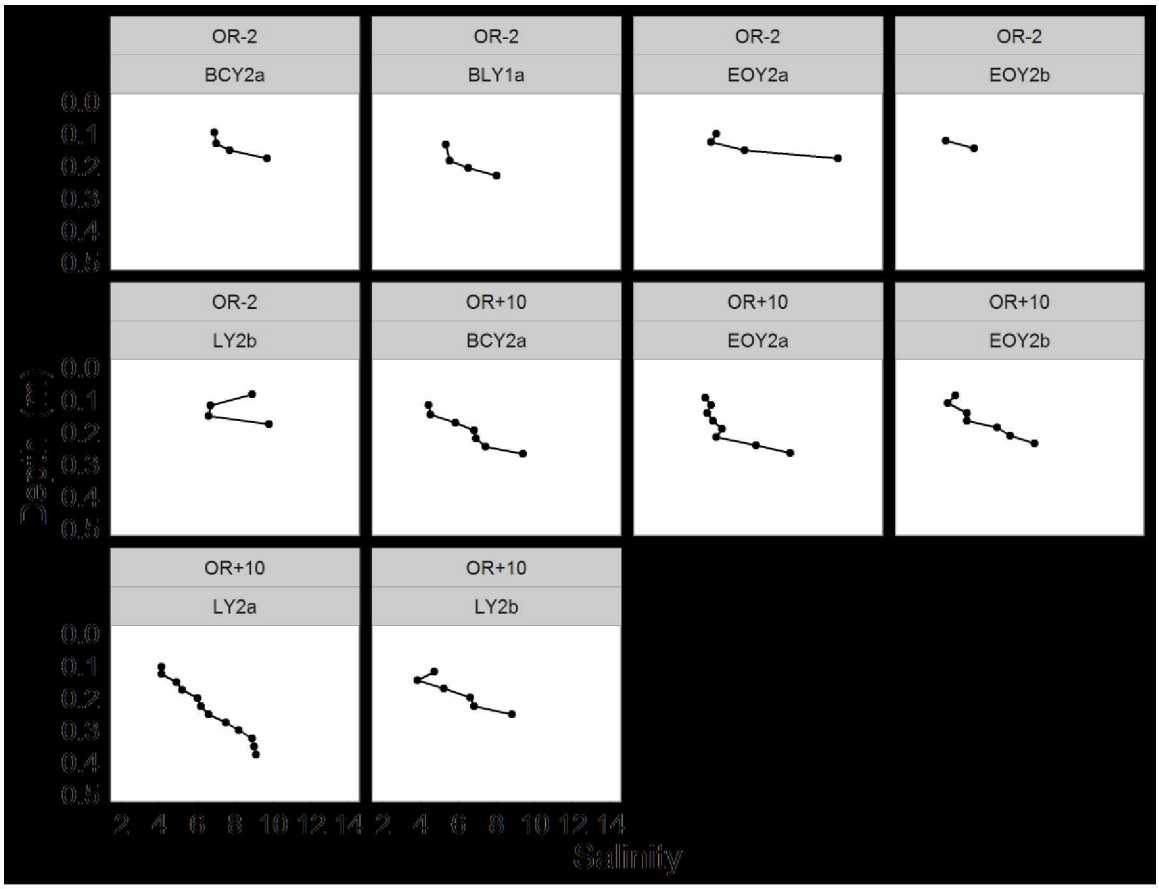

Figure 12. Bulk salinity profile of each sea ice tank in year 2 (2015). Bulk salinity was measured from directly melted samples at a 2.5 cm resolution. The letters a and b refer to replicates for each treatment in this and the following figures.

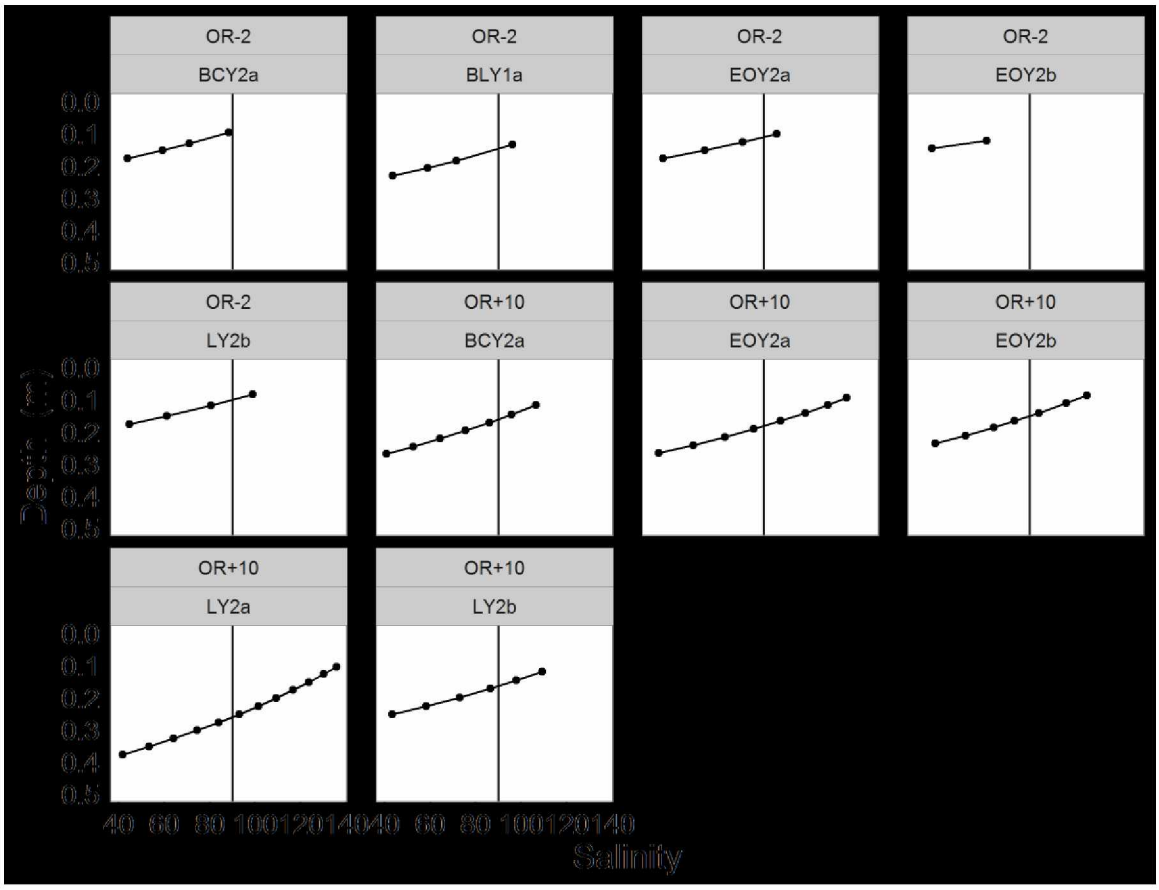

Figure 13. Brine salinity profile of each sea ice tank in year 2 (2015). Brine salinity was calculated according to Cox and Weeks (1983). Vertical line represents a salinity of 90 where algal growth declines can occur. The letters a and b refer to replicates for each treatment in this and the following figures.

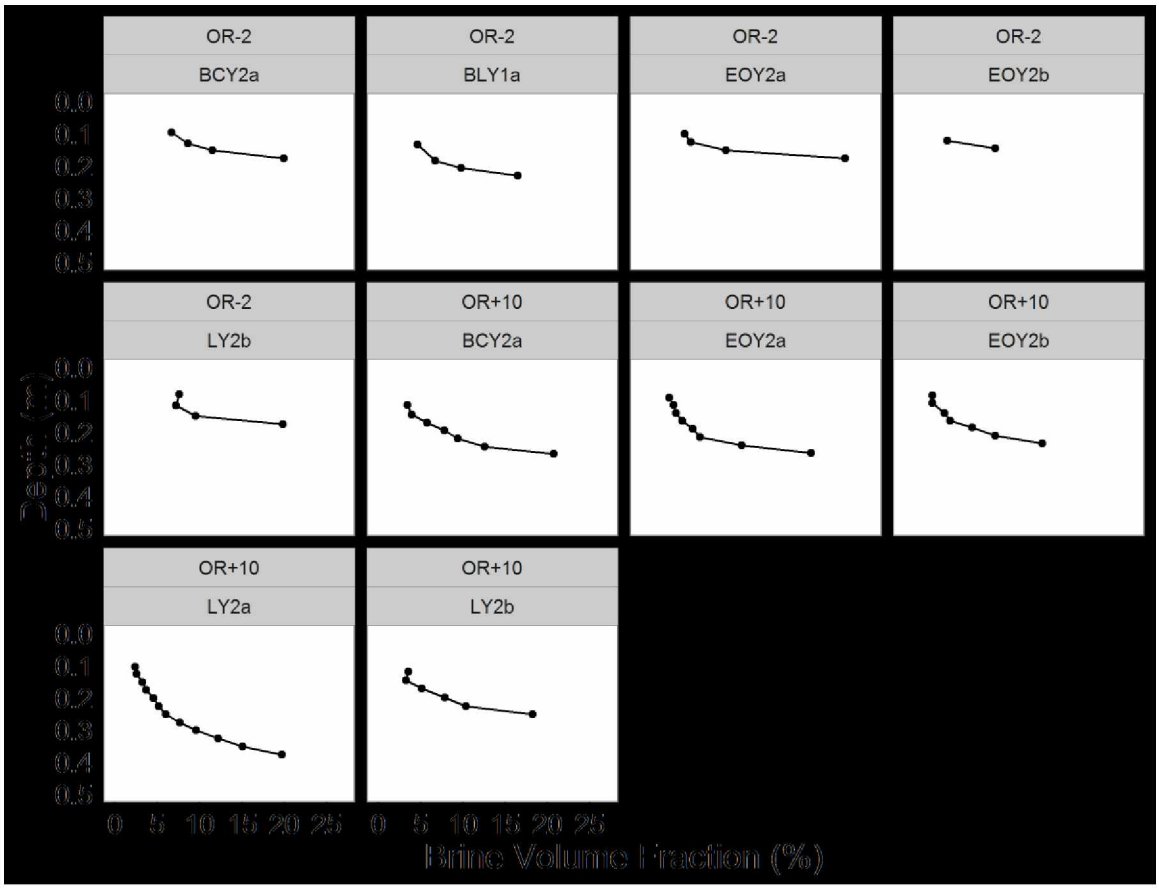

Figure 14. Brine Volume Fraction (BVF) profile of each sea ice tank in year 2 (2015). BVF was calculated according to Cox and Weeks (1983). The letters a and b refer to replicates for each treatment in this and the following figures.

3.2.2. Chlorophyll *a*

3.2.2.1. Year 1

In the BCY1 treatment, full core chl *a* concentration (Table 9) decreased by 40.5% from OR-2 (2.5 $\pm$ 0.5 µg l^{-1}) to OR+3 (1.5 $\pm$ 0.4 µg l^{-1}). Over the course of the entire experiment, full core chl *a* values decreased significantly from OR-2 to OR+13 in BCY1 and BLY1 (LMER, $p < 0.05$; Fig. 15a) by an average of 72.3 and 79.0% respectively. The dilution of the initial chl *a* concentration by passive dilution due to the increased volume of ice accounted for an average calculated decrease of 63.7 and 56.4% in BCY1 and BLY1 treatments, respectively. Chl *a* concentrations in the LY1 treatment were below the detection limit of 0.01 µg l^{-1} in all samples at all periods of sampling.

Table 9. Mean biological parameters in experiments for full ice cores in 2014 (year 1) and 2015 (year 2). Acronyms: Oil Release (OR), minus symbol (-) indicates days prior to oil release, plus sign (+) indicates days post oil release. Treatments include Biological Control Year 1 (BCY1), Biological Lens Year 1 (BLY1), Oil Lens Year 1 (LY1), Biological Control Year 2 (BCY2), Biological Lens Year 2 (BLY2), Emulsified Oil Year 2 (EOY2).

Year	Day	Treatment	Chlorophyll a (µg chl a l^{-1} ice)	Algal Abundance (Cells x 10^6 l^{-1} ice)	EPS (µg XGEQV l^{-1} ice)	Bacterial Abundance (Cells x 10^8 l^{-1} ice)
2014	OR-2	BCY1	2.5 + 0.5	na	556 + 130	3.2 + 1.3
		BLY1	3.5 + 1.4	na	616 + 368	2.6 + 1.8
		LY1	0.0 + 0.0	na	448 + 325	0.3 + 0.6
	OR+3	BCY1	1.5 + 0.4	na	314 + 114	1.3 + 0.7
	OR+13	BCY1	0.7 + 0.3	na	141 + 91	2.2 + 1.2
		BLY1	0.7 + 0.3	na	481 + 330	2.1 + 1.1
		LY1	n.d.	na	292 + 86	0.4 + 0.4
2015	OR-2	BCY2	3.5 + 0.8	4.1 + 0.7	632 + 30	0.7 + 0.3
		BLY2	2.7 + 0.9	2.6 + 0.9	620 + 36	0.4 + 0.1
		EOY2	4.0 + 2.0	3.3 + 1.3	722 + 158	0.7 + 0.3
	OR+10	BCY2	40.5 + 11.2	25.5 + 1.2	1006 + 211	0.5 + 0.2
		BLY2	5.5 + 5.6	3.4 + 1.4	576 + 195	0.5 + 0.1
		EOY2	5.1 + 5.1	4.2 + 3.2	527 + 86	0.3 + 0.0

* In Year 2, biota were released below already formed artificial ice; this portion of ice is not included in the full core values.

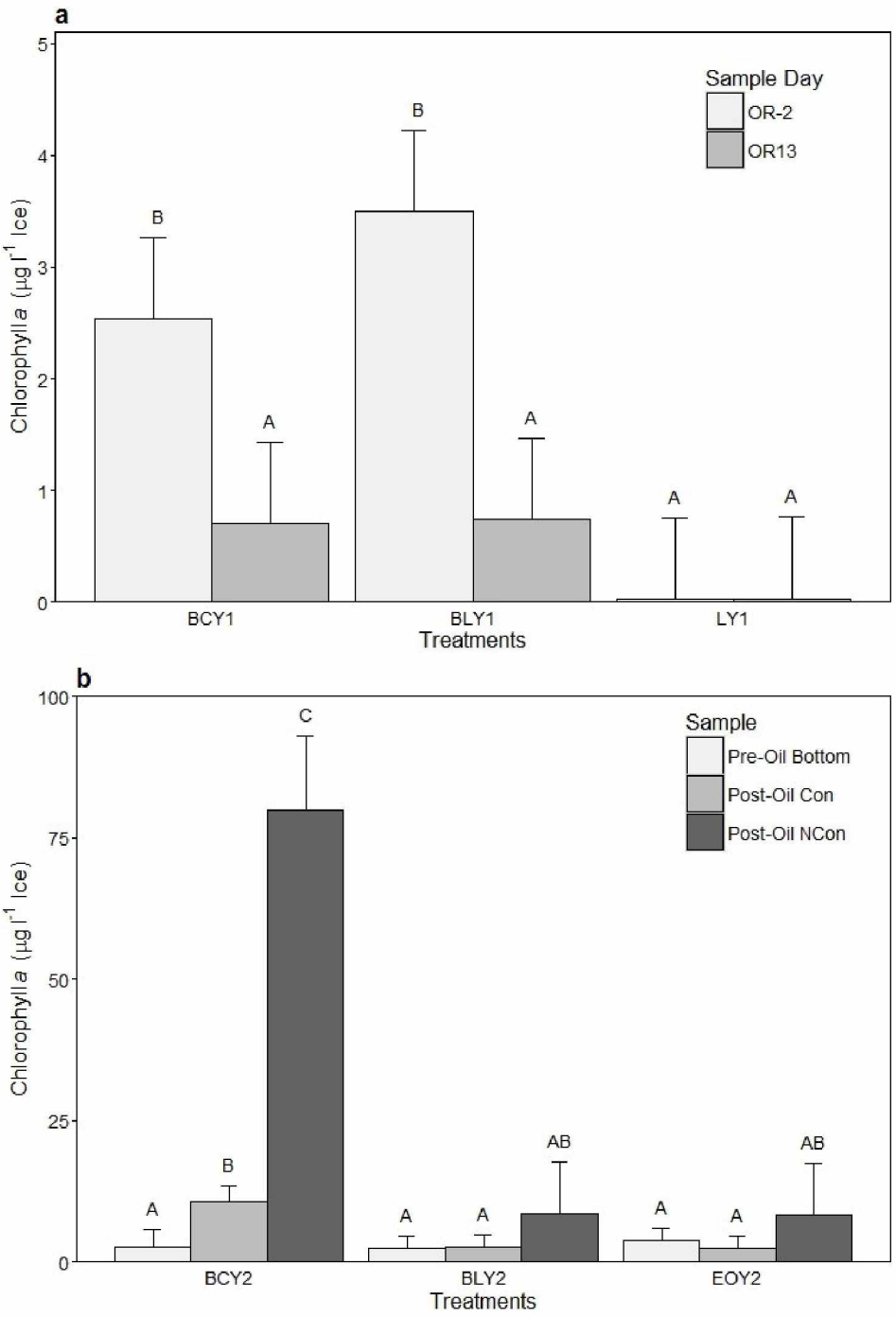

Figure 15. Mean chlorophyll *a* concentrations in a) full ice cores from 2014 (year 1) and b) 2015 (year 2) bottom ice sections. Conservative (Con) and Non-Conservative (Sections) are represented. Error bars represent the 95% confidence intervals. Letters above error bars represent Tukey's post hoc group assignment.

At OR-2, the BCY1 mean chl *a* concentration was higher in the top ice section (Table 10) relative to the bottom section by a factor of 3. In BLY1, chl *a* was also higher in the upper ice at OR-2 compared to the bottom ice section by a factor of 2. BCY1 and BLY1 bottom ice chl *a* concentrations significantly decreased between OR-2 and OR+13 (LMER, $p<0.05$) while the surface sections did not significantly differ (LMER, $p>0.05$). The mean chl *a* concentrations (LMER, $p>0.05$) for bottom ice sections did not differ significantly at OR+13 between treatments (LMER, $p>0.05$).

3.2.2.2. Year 2

Since chl *a* was measured two days before oil was released, the concentration at the day of oil release was calculated using a generation time determined by chl *a* concentration in BCY2, using measurements at OR-2 and OR+10, which was 0.3 doublings day^{-1} based on integrated full core concentrations (Table 9). Estimated chl *a* concentrations at the time of oil release in OLY2 and EOY2 treatments were calculated using OR-2 chl *a* concentrations for each treatment, the algal doubling rate based on the BCY2 data and the two day growth period prior to oil application. The resulting values of 4.1 and 6.1 µg chl *a* l^{-1} ice at time of oil release were not statistically different to the actual treatment means at OR+10 (T-test BLY2 $p=0.98$; EOY2 $p=0.51$). Assuming similar growth values projected at OR+10 using the same calculation were significantly greater than actual values (t-test BLY2 $p=<0.01$; EOY2 $p=0.01$)

At OR-2, chl *a* concentrations were highest in the upper ice section, adjacent to the inoculation layer. This pattern changed over the course of the experiment and highest concentrations at the ice-water interface for all treatments was established at OR+10 (Table 10). Chl *a* concentration in the topmost section of ice was not significantly different across treatments or sampling day (LMER, $p>0.05$). Bottom ice chl *a* concentration was significantly different in BCY2 compared to the other treatments (LMER, $p<0.05$; Fig. 15b). Comparing ice sections present at the time of oiling (OR-2) with new ice formed post oil release followed the same trend with BCY2 differing significantly from the other treatments (LMER, $p<0.05$; Fig. 15b).

Table 10. Mean biological parameters in experiments for ice sections in 2014 (year 1) and 2015 (year 2). In Year 2, biota was released below already formed artificial ice; this portion of ice is not included in the full core values. Acronyms: Oil Release (OR), minus symbol (-) indicates days prior to oil release, plus sign (+) indicates days post oil release. Treatments include Biological Control Year 1 (BCY1), Biological Lens Year 1 (BLY1), Oil Lens Year 1 (LY1), Biological Control Year 2 (BCY2), Biological Lens Year 2 (BLY2), Emulsified Oil Year 2 (EOY2). 0 cm represents the ice-water interface.

Year	Day	Treatment	Section	Chlorophyll *a* (µg chl *a* l^{-1} ice)	Algal Abundance (Cells x 10^6 l^{-1} ice)	EPS (µg XGEQV l^{-1} ice)	Bacterial Abundance (Cells x 10^8 l^{-1} ice)
2014	OR-2	BCY1	0-10.5	3.8 ± 0.8	na	667 ± 231	4.2 ± 2.5
			10.5-19.5	1.3 ± 0.5	na	456 ± 114	2.4 ± 2.3
		BLY1	0-9.5	5.0 ± 1.8	na	951 ± 558	4.2 ± 3.2
			9.5-17.5	2.4 ± 1.3	na	398 ± 134	1.2 ± 0.8
		LY1	0-8	*n.d*	na	686 ± 705	0.0 ± 0.1
			8-18	*n.d.*	na	245 ± 99	0.5 ± 1.1
	OR+3	BCY1	0-5	1.2 ± 0.3	na	935 ± 122	2.3 ± 1.4
			5-18.6	1.6 ± 0.5	na	332 ± 166	0.5 ± 0.9
			18.6-28.6	1.8 ± 1.1	na	202 ± 100	1.6 ± 1.7
	OR+13	BCY1	0-5	0.3 ± 0.2	na	394 ± 133	0.7 ± 1.3
			5-26.3	0.6 ± 0.4	na	192 ± 49	1.3 ± 1.1
			26.3-36.3	1.1 ± 0.4	na	223 ± 55	1.7 ± 1.7
		BLY1	0-5	1.0 ± 1.1	na	413 ± 139	1.5 ± 1.5
			5-19	0.8 ± 0.6	na	203 ± 133	0.3 ± 0.5
			19-26.2	0.9 ± 0.4	na	718 ± 718	0.1 ± 0.1
			26.3-33.2	0.3 ± 0.3	na	820 ± 835	8.6 ± 3.9
		LY1	0-5	*n.d*	na	731 ± 327	0.0 ± 0.0
			5-18.2	*n.d.*	na	94 ± 142	0.0 ± 0.0
			17.5-24.3	*n.d*	na	325 ± 96	0.0 ± 0.1
			24.3-30.6	*n.d.*	na	363 ± 231	2.0 ± 1.4
2015	OR-2	BCY2	9.1-13.3	4.3 ± 0.8	6.5 ± 1.8	744 ± 82	0.8 ± 0.4
			13.3-18.3	2.7 ± 2.0	4.8 ± 1.8	542 ± 71	0.9 ± 0.5
		BLY2	13.4-17.6	3.0 ± 1.2	2.6 ± 0.6	601 ± 39	0.4 ± 0.2
			17.6-22.6	2.4 ± 0.6	1.8 ± 0.6	638 ± 16	0.5 ± 0.3
		EOY2	9.8-14.3	4.4 ± 0.7	4.7 ± 1.8	764 ± 80	1.0 ± 0.5
			12.7-17.7	3.9 ± 1.8	2.5 ± 1.0	715 ± 113	0.4 ± 0.1
	OR+10	BCY2	16.6-20.9	3.0 ± 1.5	3.7 ± 2.9	885 ± 241	0.6 ± 0.2
			20.9-25.9	10.6 ± 5.9	12.3 ± 14.1	761 ± 49	0.6 ± 0.2
			25.9-33.6	79.9 ± 26.0	31.1 ± 31.2	1,257 ± 520	0.9 ± 0.4
		BLY2	16.3-21.3	1.5 ± 1.3	1.2 ± 0.1	463 ± 33	0.2 ± 0.2
			21.3-26.3	2.6 ± 0.4	3.1 ± 1.2	506 ± 35	0.3± 0.1
			26.3-35.75	8.3 ± 7.2	5.6 ± 3.7	577 ± 96	0.2 ± 0.1
		EOY2	18-22.6	1.2 ± 0.7	6.5 ± 2.1	549 ± 46	0.6 ± 0.3
			19.3-24.3	2.4 ± 0.9	3.8 ± 1.6	568 ± 135	0.3 ± 0.0
			24.3-28.9	10.2 ± 4.6	13.6 ± 11.6	655 ± 205	0.5 ± 0.2

3.2.3. Extracellular polymeric substances

3.2.3.1. Year 1

Full core EPS concentrations did not significantly differ across treatments from OR-2 to OR+13 (LMER, $p>0.05$; Fig. 16a). Values in the BCY1 samples decreased with time from 556 $\pm$ 130 μg l^{-1} ice at OR-2 to 314 $\pm$ 114 μg l^{-1} ice at OR+3 and 141 $\pm$ 91 μg l^{-1} ice at OR+13. (Table 9, Fig 16). EPS also decreased an average of 21.9% in the BLY1 treatment from OR-2 to OR+13. Assuming no change to the initial EPS concentration, initial EPS concentration was diluted by 62% due to ice thickening alone in BCY1. The calculated dilution in the BLY1 treatment, in contrast, estimated a higher (50%) decrease in EPS than the observed 22% decrease. Full core EPS in LY1 decreased by 35% from OR-2 to OR+13.

By section, the EPS concentrations exhibited the same pattern as chl *a* with higher mean concentrations in the topmost section of ice relative to the bottom section by a factor of 1.5, 2.4 and 2.8 in the BCY1, BLY1 and LY1 treatments (Table 10). EPS did not exhibit a significant difference across treatment or sampling day in the lowermost section of ice (LMER, $p>0.05$).

3.2.3.2. Year 2

No vertical gradient in EPS concentrations was found at OR-2. Top ice sections were not significantly different among treatments or sample days (LMER, $p>0.05$). Bottom ice EPS concentrations were not significantly different between treatments across sampling day (LMER, $p>0.05$). Ice formed after the oil introduction had significantly higher EPS concentrations in BCY2 than EOY2 or OLY2 (LMER, $p<0.05$; Fig. 16b).

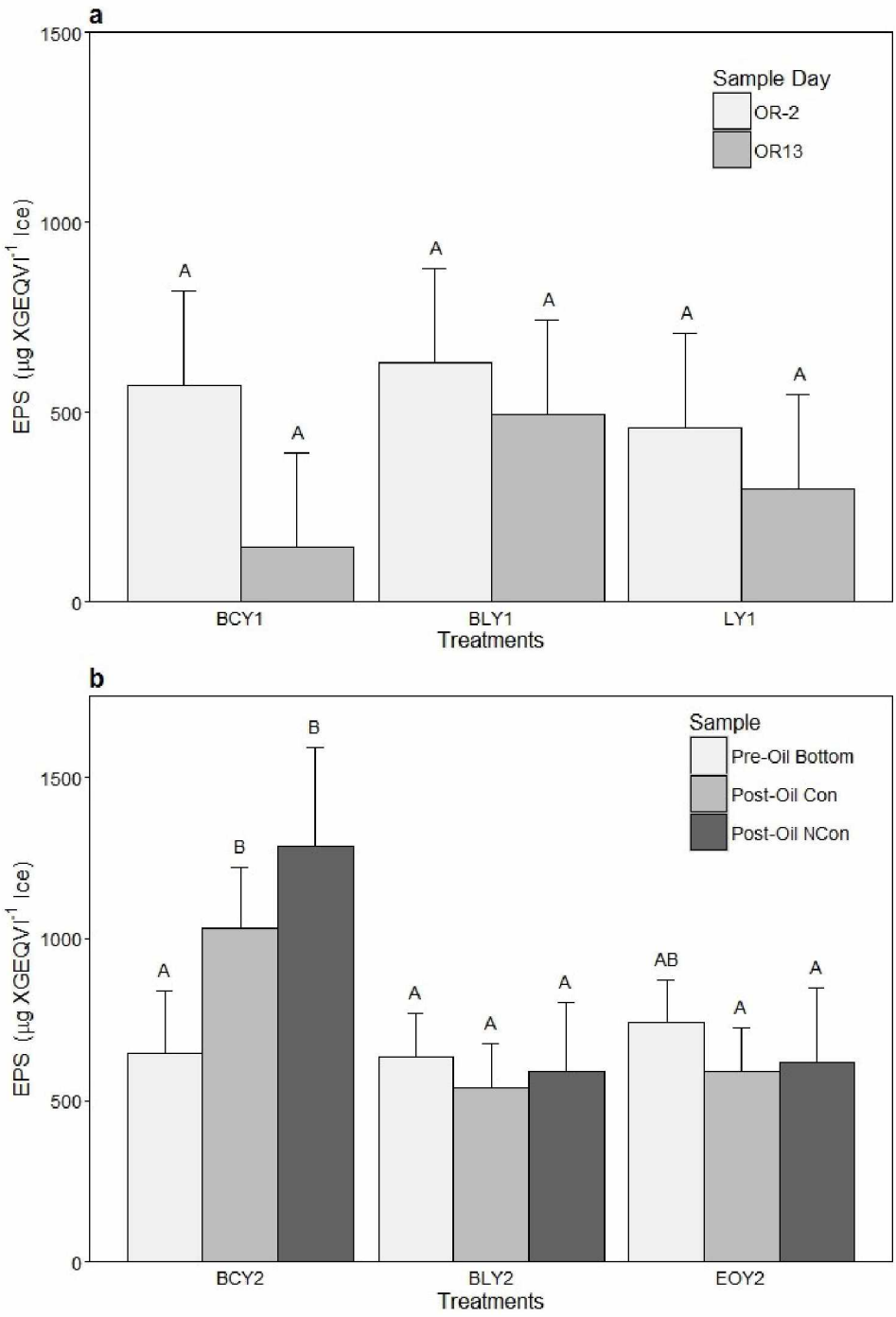

Figure 16. Mean Extracellular Polymeric Substances (EPS) concentrations in a) full ice cores from 2014 (year 1) and b) 2015 (year 2) bottom ice sections. Conservative (Con) and Non-Conservative (Sections) are represented. Error bars represent the 95% confidence interval. Letters above error bars represent Tukey's post hoc group assignment.

3.2.4. Algal abundance and species composition (year 2 only)

The algal community was dominated by the pennate diatoms *Nitzschia sp.* and *Ceratoneis closterium* at OR-2 across all tanks. *C. closterium* occurred in too low of an abundance to perform statistical analyses (<1%), therefore total diatom abundance was used for later statistical analysis. At OR+10, the algal community composition remained similar to OR-2, dominated by *Nitzschia sp.* with low abundance of *C. closterium* (<1%). BCY2 algal cell abundance at OR+10 in bottom ice and non-conserved bottom ice were significantly different from all other treatments across time (LMER, $p<0.05$; Fig. 17). Based on cell counts in the BCY2 treatment only at the beginning and end of the experiment, a generation time of 0.2 doublings day^{-1} was calculated for algae, which was 33% lower than the estimate based on chl *a*.

At OR-2, mean empty frustule abundance in full cores was low, representing 1.4% of all algal cells with high variability across tanks and cores. Empty frustule abundance at OR+10 increased across all treatments (Fig. 18) but was not significantly different between treatments at OR+10 (LMER, $p>0.05$). Full core empty frustule abundance in BCY2 and BLY2 treatments did not significantly differ between sample days (LMER, $p>0.05$) while EOY2 had significantly more empty frustules at OR+10 than OR-2 (LMER, $p<0.05$). Empty frustule abundance was higher in the section bordering the inoculation layer by a factor of 1.4 compared to the lower ice section. Algal cell abundance was significantly greater in bottom and non-conserved bottom ice sections at OR+10 in the BCY2 treatment (LMER, $p<0.05$; Fig. 17).

Cells deemed intact based on the epifluorescence observations (Fig. 19) dominated algal cell abundance at OR-2 with 97-100% of all diatoms in full cores across treatments in year 2. In the BCY2 treatment, intact algal cells were most abundant in the ice section nearest the ice-water interface and lowest in the uppermost ice section at OR+10. In oiled treatments, intact algal cells were in lowest abundance in the ice formed post- oil release, comprising 24-27% of total diatom abundance. Intact algal cells were significantly greater in the BCY2 treatment compared to the oil treatments at OR+10 (LMER, $p<0.05$).

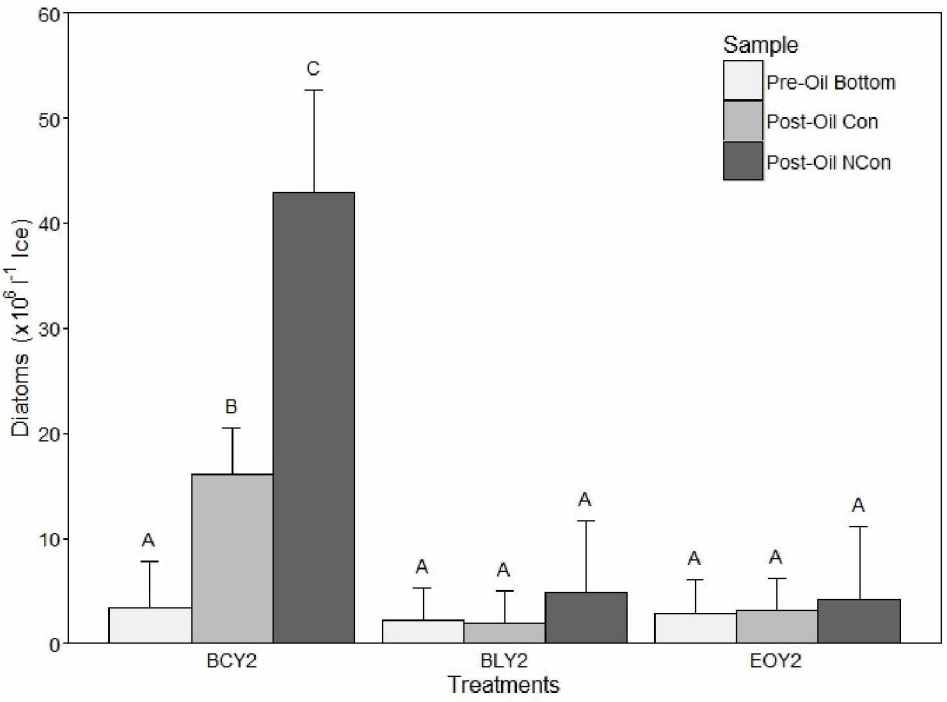

Figure 17. Mean total diatom abundance (excluding frustule counts) in bottom ice from 2015 (year 1) experiment. Conservative (Con) and Non-Conservative (Sections) are represented. Error bars represent the 95% confidence interval. Letters above error bars represent Tukey's post hoc group assignment.

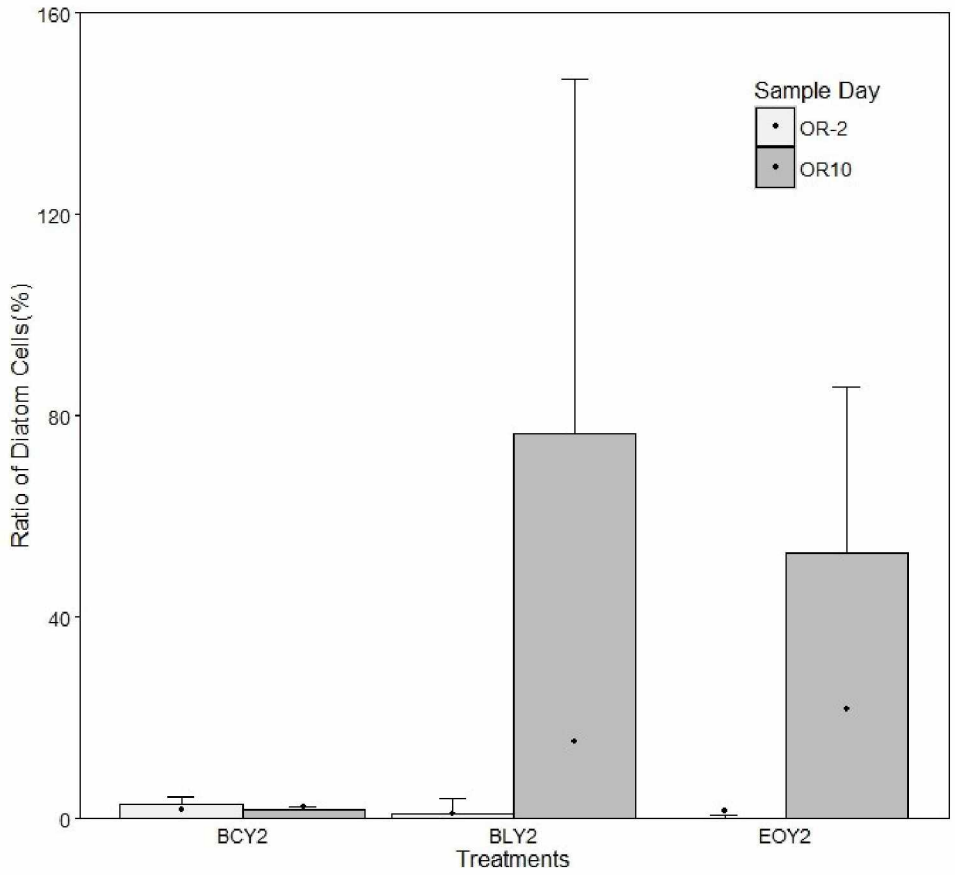

Figure 18. Full core mean percent "damaged" algae in 2015 (year 2), as determined epi-fluorescently (bars) overlaid with ratio of empty versus full diatom cells (%) (Frustules/Total Diatoms (excluding frustules)*100) (points). Error bars represent the 95% confidence interval.

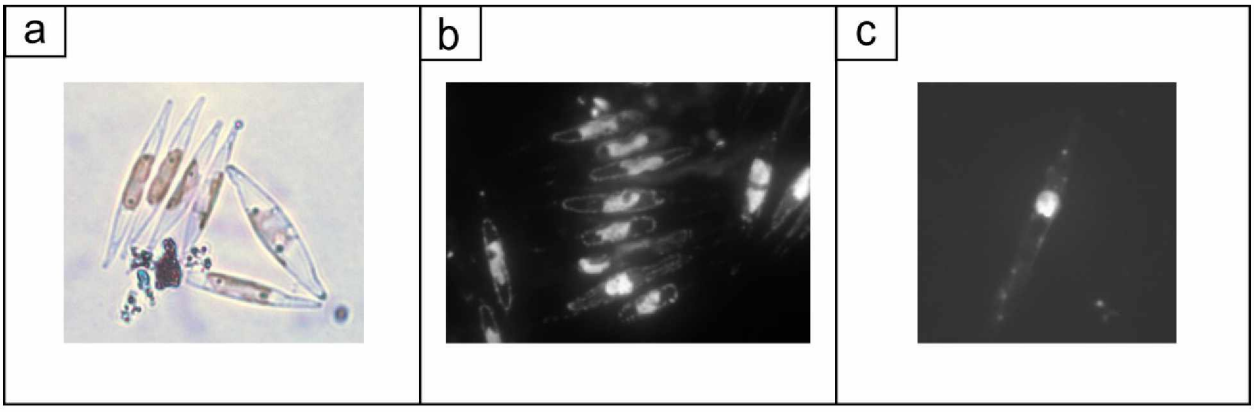

Figure 19. a) Light transmittance image of *Nitzschia sp.* from unoiled tank at OR+10. b) Epifluorescent image of "healthy" diatom cells from unoiled tank at OR+10 with elongated nucleus and intact plasma membrane. c) Epifluorescent image of an "unhealthy" diatom cell from an oiled tank at OR+10 with tightly bundled nucleus and dissolved plasma membrane.

3.2.5. Bacteria

3.2.5.1. Year 1

The mean full core bacterial abundance in BLY1 decreased to 39% of OR-2 concentrations (2.6 x 10^8 bacteria l^{-1} ice) by OR+3, but later increasing again to 69% of the initial concentration at OR+13 (Table 9). The variability in bacterial concentrations was large. Bacterial abundance decreased from OR-2 to OR+13 in BLY1 by 19%. Bacterial abundance was significantly lower in LY1 at OR-2 relative to the other treatments with a mean of 0.3 x 10^8 bacteria l^{-1} ice (LMER, $p<0.05$; Fig. 20a) but increased by 28% in the LY1 treatment. Concentrations did not significantly differ among treatments at OR+13 (LMER, $p>0.05$).

Vertical differences in sections reflected those of chl *a* and EPS, with highest abundances occurring in the uppermost ice section, which were 1.8 and 3.5 times greater than bottom ice at OR-2 in BCY1 and BLY1 respectively (Table 10). LY1 had a greater abundance in the bottom layer of ice. Full core bacterial abundance decreased in BCY1 and BLY1 but increased in LY1 with time from OR-2 to OR+13. Bacterial abundance in bottom ice was significantly higher in BLY1 at OR+13 than LY1 and to all treatments at OR-2 (LMER, $p<0.05$; Fig 20b) while BCY1 was not significantly different from either BCY1 or LY1 (LMER, $p>0.05$).

3.2.5.2. Year 2

Bacterial abundance was nearly identical between upper and lower ice sections prior to the oil release at OR-2 (Table 10) and lower than at the initiation of the experiment in year 1. When comparing top, bottom and non-conservative bottom ice sections, bacterial abundances did not significantly differ between treatments or sample periods (LMER, $p>0.05$).

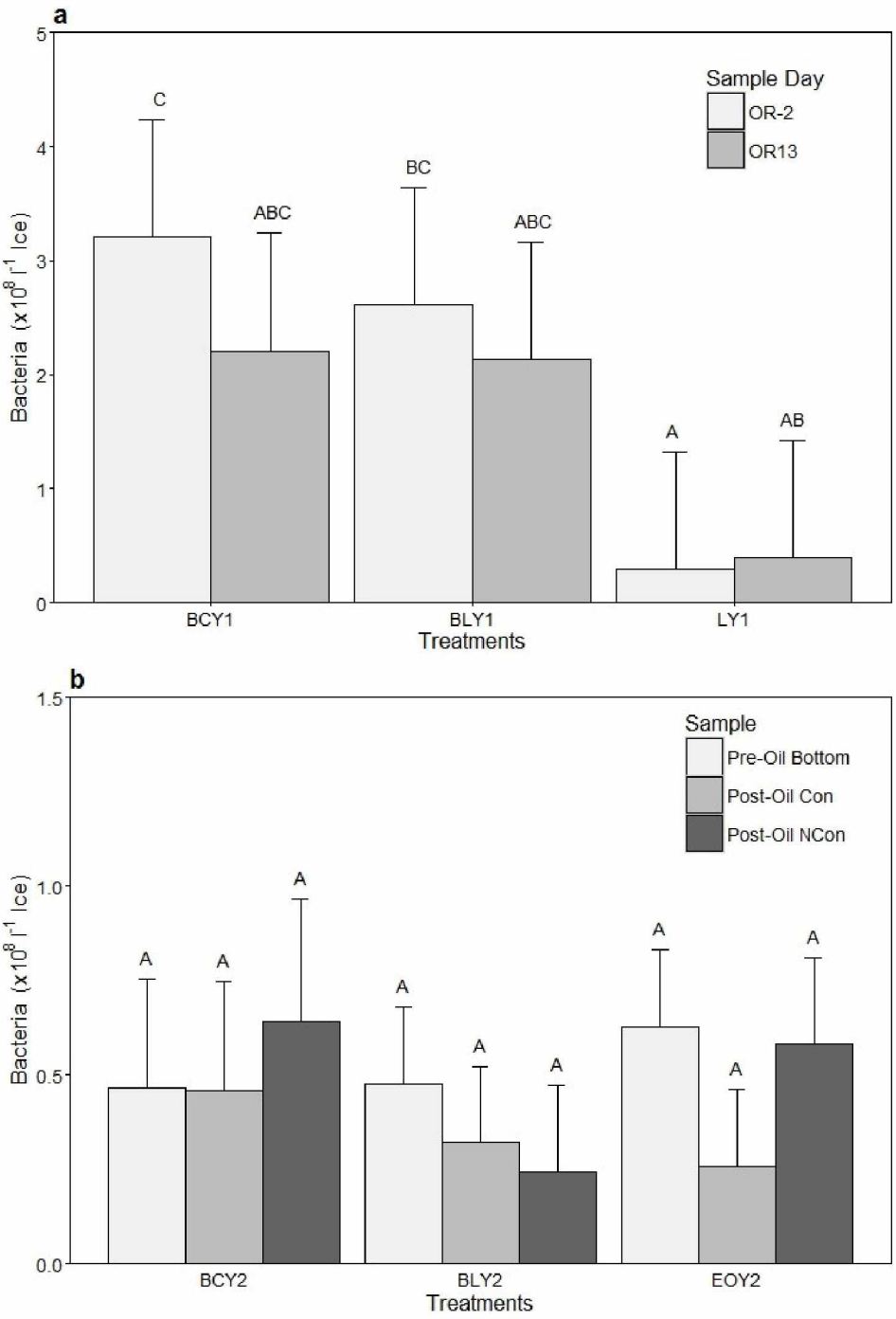

Figure 20. Mean bacteria abundance in a) full ice cores from 2014 (year 1) and b) 2015 (year 2) bottom ice sections. Conservative (Con) and Non-Conservative (Sections) are represented. Error bars represent the 95% confidence interval. Letters above error bars represent Tukey's post hoc group assignment.

4. Discussion

4.1. Methodological considerations

To achieve the objective of this study we needed to develop a mesocosm that closely simulated the growth of sea ice and sea-ice biota in Alaskan landfast ice conditions, including an evaluation of effects of under-ice crude oil on biota. During the course of this experiment, equipment requirements were identified and protocols were refined regarding the use of illumination, control of ice growth rates, pressure releases and methods of oil exposure and biota inoculation. Our experiment mimicked undeformed first-year ice (FYI) during thermodynamic growth. It did not simulate dynamic ice growth processes leading to, *e.g.* pancake ice, rubble fields or ridges.

Mesocosms designed for this experiment were successfully employed to quickly grow sea ice with physical properties and biomass representative of early to mid-spring landfast ice found along coastal Arctic Alaska. These ice tanks not only afforded close control and monitoring of experimental conditions but also allowed for containment of the hazardous compounds not advisable or permitted for environmental release, in our case crude oil (Cross and Martin 1987; Petrich et al. 2013). We chose medium-sized tanks for our experiment; tank size has varied markedly between studies ranging from < 10 l microcosms to 216 m^3 environmental test basins (Weissenberger 1998; Aslam et al. 2012b; Garneau et al. 2016), each with their own caveats. Small-scale microcosms may provide an easy way to achieve high treatment replication with minimal construction time and cost but restricts the ice thickness capable of being grown. Large environmental test basins provide a massive amount of ice for experiments but logistics become increasingly complex and sterility becomes nearly impossible. Large test basins also challenge the biologist to provide enough biological material to populate the ice and achieve homogenous environmental conditions for algal growth. This experiment utilized 360-l tanks with a corresponding surface area of 0.36 m^2, which was a compromise between a desire for replicate cores and treatments, to capture intra- and inter-tank variability, and constraints imposed by the cooling capacity and space of the cold room. Limitations of this tank size, specifically its area, included a small number of pseudo-replicate cores per tank and a low tank replication per treatment.

Light quality and quantity controls algal growth both in tanks and in the field and was adequate for growing abundant ice algae during the course of the experiment, specifically in year 2. Incident irradiance spectra in the Arctic exhibit the greatest energy in the PAR range under varying atmospheric conditions, with a parabolic shape and peak near 500 nm under clear and varying cloud conditions (Grenfell and Perovich 2008). The incident irradiation spectrum from the LED lights used during this

experiment is shown in Figure 21. Of the 55 light emitting diodes comprising the LED light source, 28 emitted narrow band light focused at 450 nm where microalgae exhibit a major peak in photosynthetic action (Lewis and Warnock 1985). It is clear that the parabolic shape seen in the field was not reproduced by our lights, but is more representative of the photosynthetic action spectrum of phytoplankton (Fig. 22), which is acceptable for our study as we wanted to provide sufficient light in the PAR range to sustain algal growth.

In the field, light quantity at the bottom of sea ice is largely controlled by season, snow depth and ice thickness. Snow attenuates light, and can cause light limitation of ice algal productivity under thick snow cover (Mundy et al. 2005), or allow damage by excessive high-intensity light (Robinson et al. 1997) under low snow cover. Often, ice algal biomass maxima can be found at intermediate snow depths of 6 to 20 cm (Mundy et al. 2005). We therefore selected our environmental collection site of ice biota as a flat portion of ice with an intermediate snow depth to increase our chance of encountering high algal biomass. Although snow depth was 2-3 times lower in year 2 compared to year 1, sampling was conducted earlier in year 2 when incident radiation was reduced (Leu et al. 2015). For the tank experiments, we chose to mimic the under-ice conditions rather than the incident irradiance, keeping light conditions typical for spring and low to intermediate snow cover. Under-ice PAR measured in year 1 and 2 was typical of Arctic FYI in late April (Gosselin and Legendre 1990; Manes and Gradinger 2009; Gradinger et al. 2009). Under-ice irradiance in the nearshore Alaska environment varies seasonally, spanning an order of magnitude from December (0 $\mu E\ m^{-2}\ s^{-1}$) to May (>30 $\mu E\ m^{-2}\ s^{-1}$), typically remaining in the single digit fluxes until March and reaching double digits by May (Manes and Gradinger 2009; Gradinger et al. 2009).

Wall effects represent an unnatural aspect of all tank experiments, and their impact is dictated by the size, shape and internal color of the tank (Martín-Robichaud and Peterson 1998). Tank wall color was a major variable influencing the light field relevant to biological processes. The white tank walls in year 1 reflected light and increased the upwelling radiation, which contributed to the overall measured light transmittance. The black liners used in year 2 absorbed part of the incident light and reduced the measured light intensity under the ice by a factor of 8 at similar LED settings. To achieve comparable under-ice growth conditions for ice algae with black tank liners, it was therefore necessary to increase the LED provided irradiance at the ice surface, leading to a stronger light intensity gradient through the ice and water column, similar to open ocean environments (Nicolaus et al. 2013). In conclusion, white tank walls allow for higher light intensities, whereas black tank walls allow for more natural light gradients through the ice layer, but require stronger LED intensities. Black tank walls might be

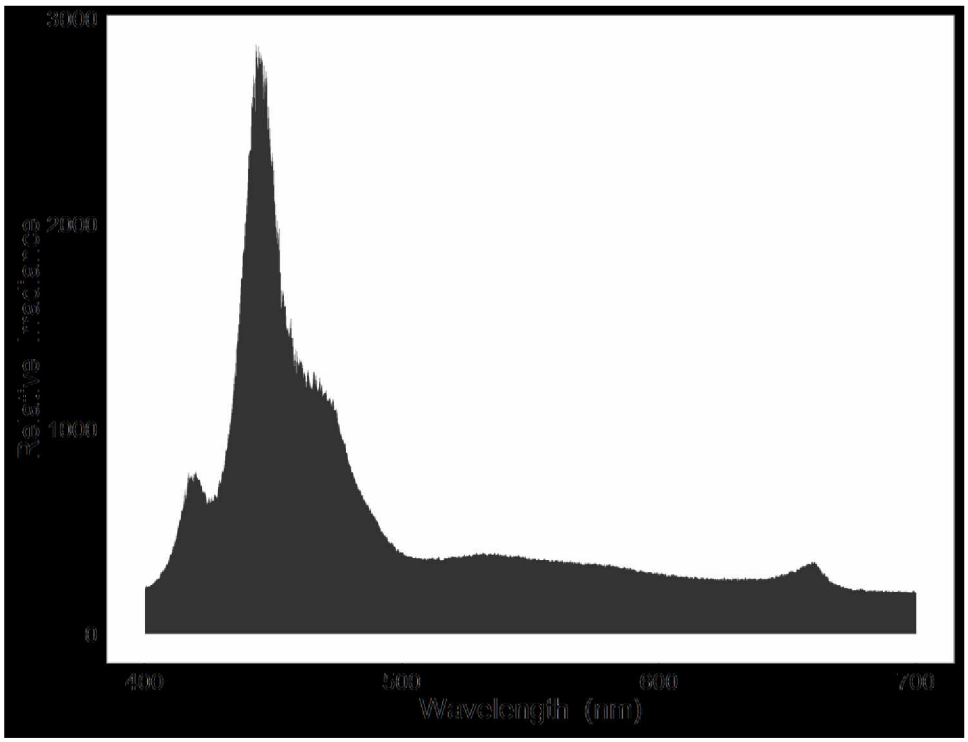

Figure 21. Light spectrum of the LED lights used in this experiment in the Photosynthetically Active Radiation (PAR) range (400-700nm).

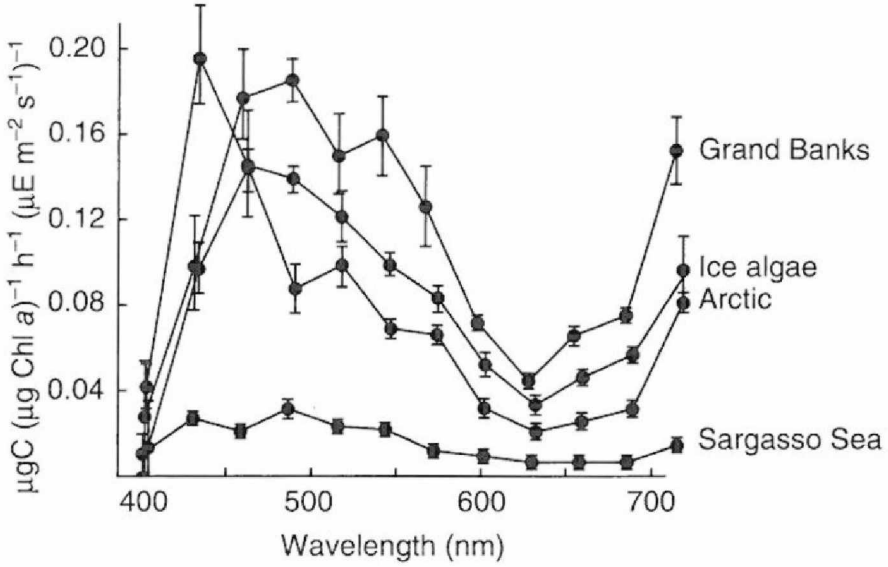

Figure 22. Photosynthetic action spectra from four natural populations, error bars represent one standard error. Reprinted from Miller and Wheeler (2012).

specifically recommended for conducting experiments with phototactic biota, while white walls could be beneficial to studies where simulating a natural light field is deemed less important than achieving an adequate light quantity.

Sea ice grown under quiescent and turbulent conditions results in differing microstructure of surface ice (Perovich and Gow 1996), which can be important to oil distribution and migration within the brine channel system (Karlsson et al. 2011). Different ice growth conditions not only influence the type of sea ice formed but also how oil (Martin et al. 1977; Wilson and Mackay 1986) and organisms (Weissenberger and Grossmann 1998) are incorporated into sea ice. Our experiments were designed to focus on ice in thermodynamic growth as this is representative of landfast ice during most of its life prior to breaking out in the summer (Mahoney et al. 2007). Ice and water movements can lead to dynamic ice growth processes and can alter the physical environment important to biota such as temperature, light and salinity. Different sea ice types and processes have been simulated in laboratory settings including frazil ice suspended in water and accumulated at the surface, *i.e.* grease ice (Reimnitz et al. 1993; Weissenberger and Grossmann 1998; Smedsrud Henrik 2001; Wang and Shen 2010), with most experiments focusing on level ice in thermodynamic growth (Weissenberger 1998; Krembs et al. 2001; Aslam et al. 2012b; Eronen-Rasimus et al. 2014) or decay (Weissenberger 1998; Krembs et al. 2001; Tison et al. 2002; Karlsson 2009; Hazen et al. 2010; Zhou et al. 2014). Studying dynamic processes requires large scale tanks like the Arctic Environmental Test Basin of the Hamburg Ship Model Basin which can generate frazil, pancake, broken, rafted and ridged ice with the ability to implement thermodynamic decay through atmospheric warming (Hamburg Ship Model Basin 2016). Unless modified, the tanks developed for this study are limited to quiescent ice growth.

When dealing with biological ice tank studies, care should be taken to ensure that the ice growth rate does not exceed the motile capacity of the biota. Ice growth rate affects salt retention (Nakawo and Sinha 1981), and subsequently the brine volume fraction (BVF) which has implications for brine channel geometry and the movement of sea ice biota (Krembs et al. 2000). The rate of ice growth is largely driven by the temperature difference between water and air and the thickness of the ice cover. Growth rates of Arctic FYI predominately range from 0.5-2 cm d^{-1} (Nakawo and Sinha 1981). In year 1, the ice growth rate in the tank at the time of biological inoculation was 5 cm day^{-1} and was slowed in year 2 to 1 cm day^{-1}. Most studies on laboratory grown sea ice experiments do not provide ice growth rates, but Krembs et al. (2001) reported a growth rate of 1.7-2.4 cm day^{-1} indicating our improvement in line with a previously successful experiment. Biological processes can also be affected by the rate of ice growth. If ice grows too fast, ice biota can become encapsulated within the ice sheet where they might

be exposed to low temperatures and high brine salinities (Cox and Weeks 1983; this study in year 1). They are more likely to maintain their position in the ice at low ice growth rates, but would necessitate active motion. The gliding rate of the sea ice diatom *Cylindrotheca closterium* was on average 14.4 cm day^{-1} at a temperature of 0°C (Aumack et al. 2014). Freshwater diatoms have gliding rates even higher than that, ranging from 35-109 cm day^{-1} at their optimum temperature and much lower speeds at cooler temperatures (Cohn et al. 2003). Our ice growth rates were within the range of these diatoms' gliding rates, yet we found a layer of dead cells in the inoculation layer of year 1. This may have been attributed to unaligned crystals representative of granular ice creating a tight network of interlocking crystals with minimal connectivity of brine pockets (Bock and Eicken 2005). It is not until congelation ice forms that vertically aligned crystals, and brine channels, would have allowed for easier navigation by ice algae.

By controlling the maximum thickness of ice in our tanks we ensured that algae remained capable of continued growth in the water and in the bottom ice layer. In experiments, ice growth can be controlled by modifying the air temperature, through water heating with submersible heaters, or a combination of the two. The restricted range of cold room temperature settings of our experimental chamber limited our ability to slow initial ice growth. The use of submersible in-tank heaters was applied to control ice growth rate. Lateral cooling along the tank walls was successfully limited by insulation surrounding the tank (Fig. 3). Water heating systems in both years were somewhat unsatisfactory. The final use of multiple heaters in each tank in year 2 allowed for variable heating, but likely caused the larger variability of ice thicknesses across tanks (Table 6). Our target ice thickness of 35 cm in the tank experiments was a compromise between forming sufficiently thick ice for algal growth, but limiting the increase in water salinity below the ice (due to ice desalination) since algal growth rates decrease with increasing salinities (Zhang et al. 1999). Sea ice algae exhibit maximum growth rates at salinities between 30 and 50 while most taxa become inhibited around 90 (Zhang et al. 1999).

The thermal and salinity profiles of sea ice define the environment in which sea ice organisms reside, including the available attachment surfaces (Krembs et al. 2000), brine channel diameter, which constricts movement (Weissenberger et al. 1992), and local salinity, which affects osmotic regulation and growth (Cox and Weeks 1983; Zhang et al. 1999). By determining tank ice properties, we were able to compare our ice to natural ice in the environment. Incomplete salinity profiles were collected in year 2 because the biological inoculation was done under already formed ice which was not sampled. While we observed the typical C-shaped (Malmgren 1927) bulk salinity profiles of FYI in our experiments, those profiles were modified by the additions of oil (year 1 & 2) and biota (year 2). The bulk salinity profiles in

artificially grown sea ice were variable but not outside the range of natural ice profiles (Weeks and Lee 1958). A subsurface C-shaped salinity distribution was observed in year 1 in direct correspondence with the oil layer. Karlsson (2009) reported a higher bulk salinity for oil-infiltrated ice, but did not offer an interpretation. EPS has been shown to reduce desalination of growing ice by physically inhibiting brine expulsion (Krembs et al. 2011). A similar mechanism may operate for oil infiltrated channels. Profiles in year 2 changed from partially C-shaped (OR-2) to linear profiles (OR+10). The reduced volume of oil released in year 2 compared to year 1 could have allowed for continuous growth of the bottom skeletal layer in year 2 in contrast to year 1 if the ice lamellae were in contact with the water. Low salinities at the surface, specifically at the end of the experiment in year 1 could represent an artefact resulting from desalinated ice coring shavings from earlier ice coring events in the tanks. Desalination due to heating of the ice from LED lights is unlikely, as ice surface temperatures remained near -10°C.

Sea-ice algae in the tanks, and the field, likely experienced osmotic stress as a result of high brine salinities in the upper ice sections. Brine salinity and relative volume (BVF) are calculated based on the temperature and bulk salinity profiles (Cox and Weeks 1983; Leppäranta and Manninen 1988). Consequently, brine salinity profiles track the temperature profiles in both field (Fig. 6) and tank data (Figs. 9 & 13). Brine salinities within the tanks fell within the range of natural landfast ice with highest salinities near the cold surface and low values in the lowermost sections spanning from 41-160. Maximum ice algal photosynthesis occurs at salinities between 35 and 51 (Ralph et al. 2007), while salinity in excess of 90 can inhibit algal growth (Zhang et al. 1999). Ice samples collected throughout the experiments contained segments above the salinity inhibition threshold of 90 (Figs. 9 & 13). Brine volume fraction (BVF) profiles under thermodynamic growth exhibited an L-shape (Figs. 10 & 14). Field and tank brine salinity profiles were similar to one another in shape and magnitude of values, disregarding a spike in BVF at the ice-air interface in 2014 at OR-2. This spike was likely due to upward brine expulsion during freeze up resulting in a hypersaline fluid on the surface of the ice (Perovich and Richter-Menge 1994). The brine volume fraction and its associated geometry controls the degree of movement and spatial availability for microbial occupation (Krembs et al. 2000). BVF will have an impact on oil infiltration in sea ice which makes it inherently important to have realistic BVF profiles for this oil in ice experiment; however this oil and ice interaction will not be discussed further in this thesis given its biological focus.

Foresight is required for all ice tank experiments regarding pressure and floating ice. Within the tanks, the sea ice layer was allowed to freeze to the sides to avoid the spilling of released oil to the ice surface. Pressurizing the tank water by downward growth of a confined ice sheet that is displacing a

disproportionately larger volume of water would have negative impacts on our experiments, as this can lead to upward flushing of brine and oil, or platelet ice formation under rapid depressurization in the tanks (Zhu et al. 2003). Our counter-acting mechanism to release pressure (Fig. 3) functioned well in most tanks except for a single catastrophic failure in year 2. Other studies have treated this issue of pressure with varying release mechanisms, or not at all. Floating ice, like natural sea ice, circumvents the pressure issue completely and might be tolerated in study designs where less or no oil is released. Weissenberger (1998) did not implement a pressure release device. Weekly coring, along with daily water column mixing by use of an airstone, suggests unsealed regions around the ice were present and could have reduced a buildup of pressure. Martin et al. (1995) found no evidence of brine flushing the surface of their thin ice experiments (only 10 cm thickness) when studying frost flower development with and without pressure release. They suggest pressure was released along the ice-wall interface, which was specifically avoided in our experiment. Aslam et al. (2012b) and Eronen-Rasimus et al. (2014) used a PVC tube for pressure release which needed to be cleared of ice daily, but also provided access to the underlying water for sampling. In tanks at the Cold Regions Research and Engineering Laboratory, an area of open water is maintained for deployment of instruments under the ice and uses overflow vents to capture the displaced water during ice growth (Marc Oggier, pers. comm.).

Successful inoculation of ice tanks with sea ice biota is the prerequisite for conducting the type of experiment presented here, and was in hindsight the most significant challenge in this experiment. Our initial goal was to mimic the processes in nature, where Arctic sea ice is populated with a diverse assemblage of bacteria, algae and metazoans in two major steps: initial seeding followed by succession. These organisms are incorporated into the ice during freeze up (Reimnitz et al. 1993; Gradinger and Ikävalko 1998) or recruit to the ice after it has already formed (McConnell et al. 2012). Subsequently, the sea ice community changes over time as flora and fauna are exposed to temperatures less than the freezing point (-1.8 °C at a salinity of 35) and salinities 2-7 times greater than seawater. Previous experiments have taken different approaches in regards to organism collection and incubation. The most relevant inoculum source for sea ice studies is arguably from the sea ice itself. Krembs et al. (2001) utilized both melted ice cores and brine collected from sea ice, and incubated the samples for three months to aid in biomass development. Weissenberger (1998) utilized sea ice brine along with natural seawater to inoculate the tanks, while Mock et al. (2002) solely relied on large cultures of sea ice derived algae grown in the lab. An alternative to sea ice derived biota is to utilize natural seawater (Zhou et al. 2014). Common to all of these experiments was the method of inoculation, which involved biota being suspended in the tank water prior to freezing. Since our experiment also attempted to establish a

diverse and natural sea ice community, we added communities from landfast sea ice, supplemented in year 2 with laboratory grown ice algae cultures (Table 2). The initial pouring of the inoculum over a slush ice layer was ineffective as biota froze into the ice, remained trapped in the surface ice and led to low biota concentrations near the ice-water interface. Such freeze-in events have also been observed in natural and experimental sea ice during freeze up when frazil ice rises through the water column entraining biota (Gradinger and Ikävalko 1998; Weissenberger and Grossmann 1998). A frazil layer was added below already formed sea ice of a thickness of 10 cm, to provide the biota an environment of slow ice growth and reduced the risk of rapid freezing. The coarse ice crystals used in our experiment fell into the natural frazil ice crystal size that can span several orders of magnitude from 1×10^{-2} to 1×10^{2} mm with a common range of 2-3mm (Smedsrud Henrik 2001). A secondary inoculation was conducted 24 hours later with a slow release of the biota just below the ice in a density stratified layer acted to hold the biota in contact with the ice. The combination of these two methods was indeed successful and ice algae grew in the ice bottom layer with little initial variability among tanks (Table 9). However, a limitation of this method is the interruption of columnar ice growth and potential disruption of brine channel connectivity.

Dispersive processes can influence the way oil interacts with sea-ice biota. Oil spilled under level sea ice will initially accumulate in pools under the ice, and can be redistributed laterally or entrained into the brine channel system (Fig. 1). The nature of the oil spill will have an effect on its interaction with sea ice, such that a spill during calm conditions can create an oil lens under ice, while physical dispersion created by turbulent conditions might introduce small droplets, or the dissolved oil phase, into the brine channel system. We, therefore, simulated two under-ice oil spill scenarios, one where oil lens formation occurs and one with dispersed oil. Though low energy oil release under sea ice is conducted differently in the field and in experiments, the most desirable approach combines a controlled release mechanism as possible in scuba diver studies *in situ* (Cross and Martin 1987) with the ability to maintain replicate mesocosms, for example obtained by curtains frozen into the ice in an environmental test basin (Bassett et al. 2016). We developed an injection method that was clean and efficient, distributed oil equally across the test area, and was practical in our small-scale experiments. We rejected Karlsson's (2009) approach to remove the entire ice cover and redeploy it after oil introduction, because it introduced large amounts of air, and probably allowed for considerable brine drainage. A second approach with a cannula still resulted in air introduction and freezing of the tube. We built on Karlsson's third approach, in which oil was introduced gravimetrically through a funnel and 5 cm diameter J-shaped tube, while carefully monitoring water displacement during the release. Modifications to the Karlsson method

included use of smaller tubes in year 2 and creating an airtight fit around each of the two tubes inserted below the ice by using precisely sized drill bits; water and slush also froze in around the tube. This method allowed us to load the oil into a funnel above the ice where it remained until a hand pump was used to remove water from the tank. Our mode of physical dispersion using a submerged pump created very fine oil droplets which were incorporated into a 2 cm thick band. Assuming an ice growth rate of 1 cm day^{-1} this implies incorporation of oil into ice over two days. This calculation, however, does not account for any post-incorporation redistribution that may have occurred.

Oil viscosity is a critical property that can determine oil redistribution within the brine channel system (Karlsson 2009). The oil used in this experiment had a pour point which we were unable to identify. However, oil remained fluid at -73 °C, in disagreement with the lab report provided by SL Ross Environmental Research Ltd. (Table 4). It exceeded the pour points of 59 diverse oils whose properties were compiled by the International Tanker Owners Pollution Federation Limited (ITOPF 2011). This temperature dependent property suggests that the ANS oil used in this experiment could have penetrated farther into the brine channel system than other oils would be capable of at similar temperatures, potentially influencing biological processes.

4.2. Comparison of biological measurements in the ice tanks to experiments and natural landfast ice

The sea ice mesocosms developed for this study provided habitat which generated various biological characteristics (e.g. algal biomass, EPS, algal and bacterial abundance) representative of early spring FYI, with similar concentrations to previous sea ice tank experiments. Below I compare my results to conditions in the natural environment, and to similar ice tank experiments to gauge the success of the biological inoculation. Unless otherwise noted, the following refers only to the data of year 2 because the year 1 inoculation was largely unsuccessful and lacked enough algal biomass for further biological interpretations.

Chl *a* concentration in ice cores is the most frequently reported biological measurement in field studies and ice tank experiments, and thus provides a good basis for comparison of ice biota development among studies. Chl *a* concentrations measured in our tanks fell within the range of values reported for other sea ice tank experiments (Table 11), as well as for natural environments (Table 8). The highest recorded chl *a* value of 106 µg l^{-1} ice for a tank experiment was documented after 35 days in 180 l outdoor tanks (Weissenberger 1998). Although our experiments were run for considerably shorter time periods, the observed algal growth suggests that higher biomass could have been achieved

with longer incubations. The chl *a* values in year 2 test tanks prior to oil inoculation were similar to FYI at the beginning of spring, February-March in coastal Alaska waters (Lee et al. 2008; Manes and Gradinger 2009). Other experiments (Krembs et al. 2001; Mock et al. 2002) were conducted with similar initial chl *a* concentrations to our own but differed in incubation period. The final chlorophyll concentrations in our tanks were similar to the beginning ice algal spring bloom conditions in the field, and exceeded most summer pack ice values (Gradinger 1999; Lee et al. 2008; Manes and Gradinger 2009; Gradinger et al. 2009).

Similar to chl *a*, EPS concentration in the ice tanks increased with time and reached values similar to early spring landfast ice levels. EPS in sea ice are largely produced by sea ice algae and bacteria and may have a cryoprotective role (Krembs et al. 2002; Nichols et al. 2005; Aslam et al. 2012b). The initial EPS concentrations in the tanks were below most reported field data for bottom ice by one order of magnitude. Riedel et al. (2006) report similar concentrations prior to the spring ice algal bloom, *i.e.* up to mid-March under low snow cover or mid-May under high snow (Riedel et al. 2006). The moderate correlation between diatom abundance and EPS concentrations (R^2=0.43) in unoiled samples indicates that diatoms are likely the source for the bulk of EPS production in our study as suggested by Krembs and Engel (2001) and Riedel et al. (2006) (Fig. 23).

Bacterial abundances established in the experimental tanks fell within the range of literature data for field and experimental studies (Table 11 & Table 12). In Arctic fast ice, bacterial abundances span several orders of magnitude from 10^7 to 10^9 cells l^{-1} ice from early spring into summer with no temporal trends (Krembs et al. 2002; Riedel et al. 2006). Other experimental studies reported either similar bacterial abundances (Aslam et al. 2012b) or substantially higher abundance

Table 11. Literature review of relevant sea ice tank studies which cultivated biota comparable to this study. Bold values indicate the maximum value during the experiment.

Study	Reservior Type	Tank Volume (m^3)	Section (cm)	Ice thickness (cm)	Incubation (days)	Chlorophyll *a* (µg l ice^{-1})	Algal Abundance (cells l ice^{-1})	Bacterial Abundance (cells l ice^{-1})
Weissenberger 1998	Tank	0.18	Full Core	15	35	**106**	**$37x10^6$**	0.6×10^{12}
			Full Core	**29**	42	49	24×10^6	0.6×10^{12}
			Full Core	22	91	80	$14x\ 10^6$	**$0.7x10^{12}$**
Krembs et al. 2001	Basin	180	All Sections	21	17	0.1-2	**0.79×10^6**	na
Mock et al. 2002	Tank	4	All Sections	15	10	**3-4**	na	na
Aslam et al. 2012a	Basin/Dividers	216/1.2	All Sections	10	**5**	na	na	**$0.8x10^9$**

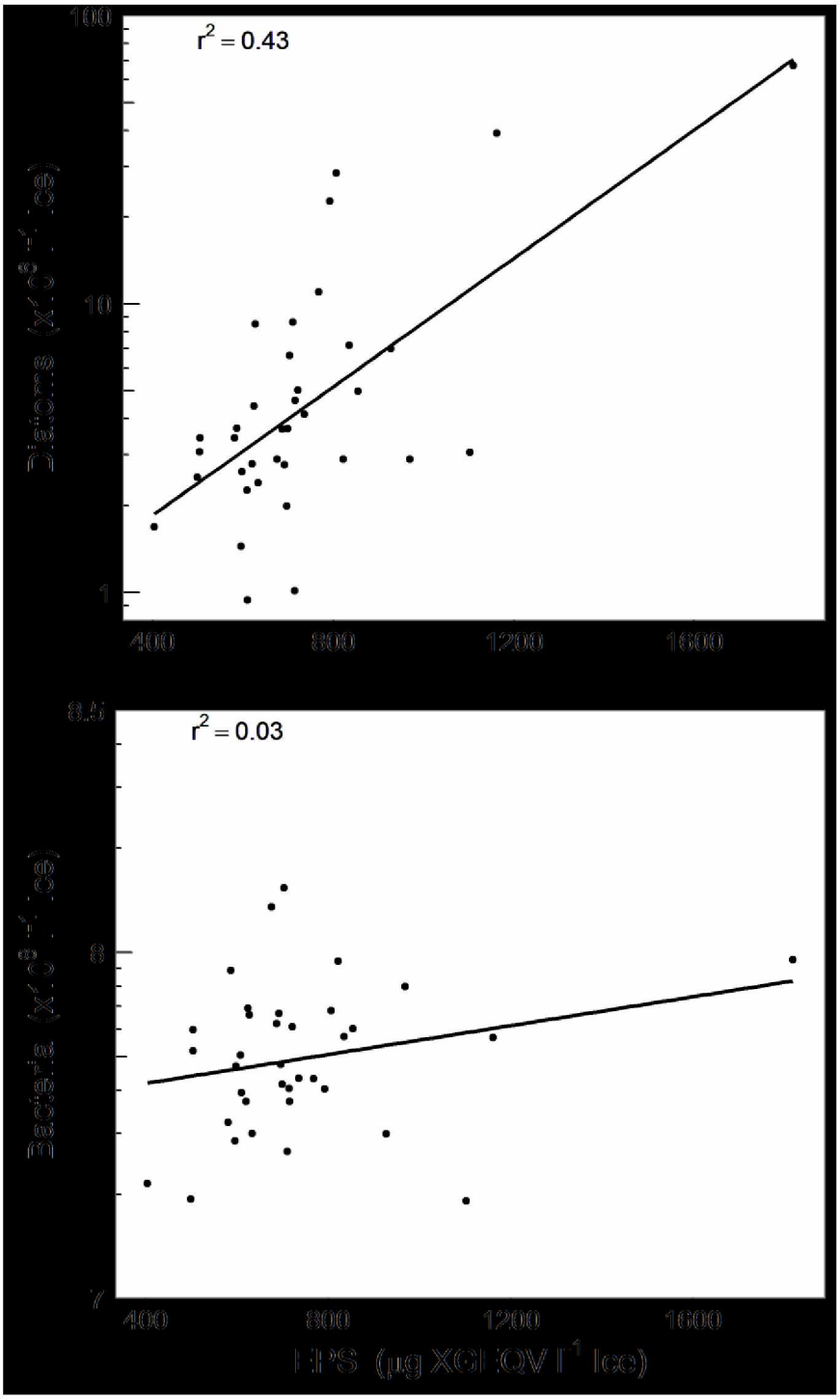

Figure 23. Regression analysis of diatom and bacterial abundance with EPS as recorded in µg Xanthum Gum Equivalents (XGEQV). Sections from oiled tanks at OR+10 are not included. Adjusted r^2 values are reported.

Table 12. Literature review of relevant sea ice field studies that measured biota comparable to this study.

Study	Ice Type	Location	Year	Ice Thickness (m)	Chlorophyll *a* (µg l ice^{-1})	Algal Abundance (cells l ice^{-1})	Bacterial Abundance (cells l ice^{-1})	EPS (mg XGEQV l ice^{-1})
Gradinger et al. 1999	Pack Ice	Greenland Sea	1994					
Gradinger 1999	Pack Ice	Greenland Sea	1991 & 1994	01-6.7	0-109 mean	0.4 -18.0 x 10^6 mean		
Gradinger et al. 2005	Pack Ice	Beaufort Sea	2002 & 2003	0.9-2.7	0-11			
Lange et al. 2015	FYI	Lincoln Sea	2010-2012	0.83-1.77	0.01-15.4 mean 0.6			
	MYI	Lincoln Sea	2010-2012	2.23-3.11	<0.01-14.1 mean 0.2			
Krembs et al. 2002	Fast Ice	Barrow, Alaska	1999	0.4-1.65	<0.1-16 (March Only)		2.5-7 x10^7 (March only)	1-7.7
Riedel et al. 2006	Fast Ice	Beaufort Sea	2005	1.3-2.0	0.3-711 median 88.4		0.3-4.3 x10^9 median 1.7 x10^9	<0.1-10.5 median 1.36
Lee et al. 2008	Fast Ice	Barrow, Alaska	2002 & 2003					
Gradinger et al. 2009	Fast Ice	Barrow, Alaska	2002 & 2003		15-340			
Krembs et al. 2011	Fast Ice	Barrow, Alaska	2001 & 2002	1.57-1.62	12.3-55.1			2.0-5.5
Manes & Gradinger 2009	Fast Ice	Barrow, Alaska	2005 & 2006	0.47-1.59	0.3-696			
Hsiao 1980	Fast Ice	Canada	1971-1978					

(Weissenberger 1998). The high abundances of bacteria in the non-seeded LY1 treatment could have resulted from contamination from other tanks, non-sterilized water supplies and/or the artificial sea water salts used, a problem that cannot be excluded in open tanks in standard cold rooms and environmental chambers.

Algal cell concentrations in the tank experiments were generally within the range of reported values of environmental samples and previous tank studies (Tables 11 & 12) reaching maximum abundances of over 30 $x10^6$ cells l ice^{-1} in our tanks. Further growth of algae, as result of sufficient light and inorganic nutrient conditions, led to increased abundances over time in the tanks, with final values exceeding field data from central Arctic pack ice by a factor of roughly 2 (Gradinger 1999), though lower than our field sample concentrations in spring. By growing algae within the sea ice to environmentally relevant concentrations, meaningful data relating to oil spills was collected.

Algal diversity in Arctic sea ice varies greatly between locations and with time, but is typically dominated by pennate diatoms (*e.g.* Poulin et al. 2011). The importance of biodiversity in contributing to ecosystem resilience after a trauma, *e.g.* oil spill, has been well documented (Folke et al. 2004). Despite incubation with natural ice biota, tank algal diversity was low and the community was almost exclusively dominated by the single pennate diatom *Nitzschia sp.* (99%), followed by *Cylindrotheca closterium* (1%). The pennate diatom genus *Nitzschia* (Hassall 1845) is commonly associated with sea ice (Suzuki et al. 1997; Ratkova and Wassmann 2005) both in Arctic and Antarctic marine systems. Other longer lasting tank experiments had higher observed diversity. Weissenberger (1998) identified 26 species of diatoms and Krembs et al. (2001) found 11 during their experiments. In Krembs et al. (2001), flagellates were numerically dominant for the duration of the study, but we detected only a single cell over the course of our experiment. A possible explanation of our low algal diversity is that the supplementation of biota with laboratory grown cultures could have led to an overwhelming inoculation of culture/tank adapted algae which were capable of out-competing other algae for resources. It should however be noted that *in situ* species richness in individual ice floes is also considerably below the reported total of 1,027 species of algae reported in Arctic sea ice (Poulin et al. 2011). Hsiao (1980) reported 196 species of ice algae during his study of Canadian landfast ice, and 55 taxa were identified by Horner and Schrader (1982) in Beaufort Sea landfast ice. Thus field studies demonstrate local selection of limited number of species matching the current environmental conditions also observed in our study.

4.3. Effects of under-ice crude oil release on sea ice biota

We tested two types of oiling scenarios because oil released from a capsized vessel will behave differently than a vigorous wellhead blowout. Both scenarios are capable of contaminating sea ice at the ice-water interface. A full scale blowout, as witnessed during the Deepwater Horizon and Ixtoc 1 spills in the Gulf of Mexico, can emulsify the oil and produce droplets <300 µm in diameter (Masutani and Adams 2000). By contrast, a sunken vessel or a slow leaking pipeline will produce much larger droplets that can coalesce at the ice-water interface to form an oil lens (AMAP 2010). Even slow leaks can be mechanically dispersed by wave energy at the ocean surface to produce small droplets which will settle out over a prolonged period of time (Farmer and Li 1994; Zheng and Yapa 2000). Oil released under sea ice in our experiments had strong effects on ice algal growth (inhibited the division of algal cells, increased algal pigment concentration, and production of EPS) while the abundance of bacteria remained similar across treatments, regardless of the route of oil exposure.

4.3.1. Effects on sea ice algae

In year 2, algal biomass and abundance in the top layer of the ice, farthest from the oil lens, remained low across all cores (Table 10). This near-surface ice was also the coldest (Fig. 11), and had a corresponding low BVF, high brine density, and low permeability (Golden 2009). This means that brine theoretically existed mostly in discrete isolated pockets, rather than in a connected channel system, and could function as a refuge for cells by protecting them from oil exposure. The low algal density can be explained by high brine salinity (>85) and low temperature (<-4°C). An oil induced effect was therefore not able to be confirmed. Reduction of ice algal growth with increasing salinity is well studied, and Zhang et al. (1999) for example found a strong reduction in ice algal growth at a salinity of 90.8. It is likely the these unfavorable conditions in this ice section stifled growth in all treatments, masking any oil related effect, leading to the insignificant results for cell abundance and biomass across treatment and sample day. EPS production, however, is stimulated by high brine salinity and cold temperatures (Krembs et al. 2002) and the non-oiled tank was the only one to show an increase of EPS in top sections. The close to significant p-value ($p=0.06$) in the top ice layer suggests that an oil related effect might have influenced EPS production in the algae as far away from the oil layer as 10 cm despite the calculated decrease in BVF.

We did not find a significant difference in algal biomass, cellular abundance, or EPS concentration of the conserved bottom ice before and after oiling in the BLY2 and EOY2 treatments (Fig. 15b, 16b & 17b).

However, we also did not witness a decrease in any of these parameters, indicating oil effects may lead to inhibition of growth. Additional data collected at multiple time points and comparison to a reference site would be required to determine if this is the case.

Ice formed after oil introduction was expected to exhibit the most profound oil impact during this experiment. However, the algal parameter values at the end of the experiment were similar to those from the bottom ice layer at the time of oiling. In this layer at the end of the experiment, the BCY2 bottom layer had a high concentration of biomass, cell abundance and EPS. The lack of increase in algal pigment concentration (chl *a*) in the two oiled treatments can be explained by inhibition of cell growth and division (Hsiao 1978; Aksmann and Tukaj 2008; Gilde and Pinckney 2012) and/or through reductions in chl *a* per cell even with continued cell division (Cullen et al. 1993). Incorporation of algae from the water column might explain the stagnant chl *a* concentrations measured at the end of the experiment, rather than a decrease in cellular pigment content. It remains possible that algal growth continued after oil release, albeit, reduced.

Extracellular Polymeric Substance (EPS) production was inhibited after crude oil exposure. These mucilaginous secretions of algae and bacteria are found in sea ice at high concentrations (Krembs et al. 2002; Underwood et al. 2013). EPS protects diatoms and bacteria from freezing (Liu et al. 2013), hypersaline environments like high salinity brines (Aslam et al. 2012a; Liu et al. 2013) and could function similarly under hyposaline exposure such as meltwater flushing (Ozturk and Aslim 2010). EPS is also produced by algae as a stress response to nutrient limitation (Alcoverro et al. 2000), temperature and oxidative stress (Chen 2014). EPS can directly influence salt retention in sea ice by increasing the abundance and size of brine pores (Krembs et al. 2011). Such effects can impact the distribution of oil and its water soluble fraction within the ice, thus impacting oil exposure to the microorganism inhabitants of the ice. EPS contributions are typically contributed by algae and bacteria in sea ice (Riedel et al. 2006; Collins et al. 2010; Krembs et al. 2011). We demonstrate for the first time that EPS production is inhibited by crude oil exposure. Theoretically EPS production could reduce the crude oil exposure of cells, as has been found for bacteria exposed to heavy metals (Bitton and Freihofer 1978), by surrounding the cells and providing a diffusive barrier against crude oil compounds. A cessation of EPS production makes this protective mechanism unlikely to protect cells at high oil doses in the ice matrix. Reduced EPS concentrations also have an effect on sea ice microstructure and permeability (Krembs et al. 2011), potentially increasing the flow of oil into the brine channel network.

Our study clearly demonstrated biological effects of oil exposure in sea ice systems. Based on our observations, we propose two possible methods for determining cell damage and mortality in fixed

melted sea ice samples, which could be applied in field studies: the frequency of empty diatom frustules and fluorescent cell properties. We assume that within sea ice, empty silicate frustules are retained within the ice matrix after diatom cell death. The frustule abundance therefore represents at least a fraction of the total dead cells as a consequence of oiling. A similar relation between relative frequency of dead algal cells and oil exposure has been observed elsewhere (Echeveste et al. 2010; Gilde and Pinckney 2012). Empty frustules as an indicator of cell death certainly underestimate actual mortality. Nevertheless, we observed a clear signal in the relative empty frustule abundance as it increased after oil exposure (Fig. 18). Frustule abundance may be a specifically suitable metric for sea ice communities which are often dominated by diatoms as main primary producers. Echeveste et al. (2010) found that by using membrane permeability digestion assays, most marine algae showed increased mortality when exposed to two common PAHs and that natural communities showed significantly more cell death than lab cultures. Because most, if not all, of the algal growth in the artificial sea ice was derived from lab cultures, these impacts may be even greater in a natural setting.

A second measure became evident during the fluorescence studies of fixed samples. Two groups of cells could be clearly separated. Group 1 (determined intact) demonstrated strong fluorescence of its plasma membrane with an indiscernible nucleus shrouded by the chloroplasts while group 2 (determined damaged) lacked a fluorescent plasma membrane, weak or no chloroplast fluorescence but had a more defined nucleus (Fig. 19). The fluorescent dye DAPI is specific to DNA and partially to RNA and is known to stain chloroplasts (Selldén and Leech 1981), mitochondria (Williamson and Fennell 1979) and nuclear DNA (Porter and Feig 1980). So far, viability assays of phytoplankton rely on specific stains (Roth et al. 1997; Veldhuis et al. 2001) or digestive enzymes (Agusti and Sánchez 2002) that penetrate compromised cell membranes for easy viewing in unfixed samples. For example, Echeveste et al. (2010) utilized a membrane permeability test which digests the permeable membranes of dead cells. In this method, two sets of pseudo samples are enumerated; one yielding a total cell count of both live and dead cells, and one treated by the process yields only the living cells. These processes will not work with fixed field samples because once the cells are fixed in formaldehyde, the plasma membrane becomes permeabilized within 20 to 120 minutes (Veldhuis et al. 2001). We could not confirm whether the observation in our experiments indeed represents dead or damaged cells, nor determined its mechanistic action; the oiled tanks had higher proportions of intact cells than damaged cells. Veldhuis et al. (2001) determined that non-viable cells still possess their photopigments and that loss of membrane integrity occurs later as a process of unicellular automortality, synonymous to apoptosis in multicellular organisms. We suggest that the capacity to visualize cell damage at the time of formaldehyde fixation is

possible using only DAPI cell staining. We propose that the possible new methods be further developed and rigorously validated to determine the efficacy of this method to determine cell damage caused by oil. A post-fixation method for determining cell damage after an oil spill will enable investigators to ship samples from a location of incidence to an analytical lab, freeing valuable time during a critical and time sensitive period. Additionally, fluorescent dyes like primulin for proteins could be further used to strengthen the fixed-sample analyses by possibly highlighting other oil influenced biomarkers.

Biodiversity and community composition matters in regards to sensitivity to oil toxicity. Of the major microalgae groups, diatoms appear to be the most sensitive to the toxic effects of crude oils (Hsiao 1978; Perez et al. 2010; Podkuiko 2013) though cell volume plays an important role as well (Echeveste et al. 2010). Our experimental algal community was dominated by a diatom, *Nitzschia sp.,* with a small contribution (<1%) by *Cylindrotheca closterium.* Our findings support the sensitivity of diatoms to crude oil and are reflected in the reduced biomass accumulation and the elevated proportion of damaged cells. The dominant taxon in our experiment is a relatively small diatom (<20 µm). The allometric relationship of surface area to volume is also important in anticipating the toxic effects crude oil will have on a particular microalga (González et al. 2009; Echeveste et al. 2010). Smaller cells like the dominant *Nitzschia sp.* have a proportionally larger surface area to volume ratio than larger cells and therefore have more area to incorporate oil compounds, leaving them more sensitive to oil toxicity. González et al. (2009), however, found evidence in direct contrast to this where small diatoms, <20 µm, were stimulated by oil treatments while diatoms > 20 µm were negatively impacted by the high oil concentration treatment. This discrepancy expresses the importance to study species specific responses to oil dosing. The fact that the present study was a near monoculture is a limitation and leaves the possibility that not all ice algal species will respond similarly to *Nitzschia sp.* in this experiment. It also points to the limitation of simulated *in situ* experiments which cannot fully resolve the natural diversity and its associated changes with season.

4.3.2. Effects on bacteria

The temporal changes of bacterial abundance in oiled and controlled treatments varied markedly between experiments and ice sections. In year 1, when no algal growth occurred within the ice and nutrients were not supplemented, bacterial abundance increased significantly by a factor of seven in the BLY1 treatment over time in the bottom ice. This increase can possibly be explained by growth stimulation of oil-degrading microbes. Oil degrading microbes are ubiquitous (Margesin and Schinner

2001) and exposure to hydrocarbons causes rapid development of the oil degrading microbes (Margesin and Schinner 1999). Bacterial abundance was previously observed to increase after light dosing with diesel and crude oil in natural Antarctic landfast sea ice (Delille et al. 1997), Antarctic planktonic environments (Delille et al. 1998) and soils in the Antarctic (Delille 2000). Natural bacteria populations in Arctic water also actively respond to oil dosage by stimulation of a community shift in favor of oil degraders in an experimental lab setting (McFarlin et al. 2014). Despite the cold conditions, biodegradation of crude oil occurs at near freezing temperatures (-1 °C) without nutrient introduction, albeit slower than in temperate regions (McFarlin et al. 2014).

Bacterial abundances in year 2, where we observed substantial ice algal growth in the un-oiled treatment BCY2, were interestingly not enhanced by oil introduction in contrast to year 1. One reason could be the different duration of the oil incubation, which was three days longer in year 1 than in year 2. This period, though short, could have allowed for an additional 3.6-5 divisions of bacteria based on bacterial growth rates at 0 °C (Kuparinen et al. 2011), and could explain differences between year 1 and 2. Alternatively, bacteria and algae compete for inorganic nitrogen sources, and the enhanced algal growth in year 2 might have caused nutrient depletion for bacteria. Additional factors like grazing mortality or viral lysis (Thingstad and Lignell 1997) were not assessed in this study but could also have contributed to stimulating the microbial food web within the ice (Vézina et al. 1997). No difference was found in bacterial abundance between the two oil treatments (dispersed and non-dispersed). This lack of a difference was unexpected as dispersing oil into small droplets is the main principle behind the use of chemical dispersants to allow for enhanced biodegradation of spilled oil (Prince et al. 2013). By dispersing oil, more surface area is exposed for bacterial attachment. Bacteria have been shown to grow faster and to a greater abundance with the use of chemical dispersants at cooler temperatures (10 °C), relative to oiled controls. Here we suggest that nutrient competition or heterotrophic top-down control superseded the difference between the two oiled treatments. While only one heterotrophic nanoflagellate was identified in all of the epifluorescent samples, it does not eliminate the possibility of their contribution as the preparation of these samples is not specifically designed for their enumeration.

5. Conclusion

This study demonstrates that sea ice mesocosms can be used for controlled experimental studies of oil impacts on ice biota in walk-in freezers. Novel approaches for inoculation of growing artificial ice sheets with field sampled biota were developed and biological characteristics matching natural conditions, specifically ice algal biomass, were achieved and maintained. Two different and likely oil spill scenarios (oil lens underplating and dispersed oil droplets) were also successfully simulated inside the tanks. A comparison between tanks with and without oil exposure allowed studying biological effects on bacteria, algae and the production of EPS.

Findings demonstrated not only effects of oil on ice biota, but also the relevance of biological interactions in the outcome of exposure experiments. Both oil spill scenarios resulted in the reduction in accumulation of sea ice algal pigment concentration (a proxy for algal biomass) and diatom abundance. Also, oil exposure inhibited EPS production, a complex mixture of carbohydrates, most likely produced by diatoms in this study and thus likely a consequence of the reduced algal growth. The different responses of bacterial abundances to oil exposure in year 1 and 2 suggest that bacterial abundances can quickly increase after oil exposure (year 1) however could be limited in their growth potential by nutrient competition during seasonal phases of high algal biomass (year 2).

Counterintuitively, chl *a* did not decrease after exposure of ice to oil. The lack or delay of ice algal biomass increase (i.e. reduction in growth rate) can be a useful metric in itself if the natural algal biomass trajectory of a reference site outside the immediately oil impacted area is known, monitored, or modeled. Changes in algal cell abundance (i.e. another indicator of change in growth rate), and in particular the observed algal fluorescence characteristics, were useful measures of algal health and its relation with time and oil exposure. The striking differences in algal growth between year 1 and 2 can be attributed to methodological differences in tank inoculation, but again highlight the need to look at several components of the ice biota, including bacteria and algae. In any case, it appears important under a real oil spill scenario to document the initial conditions when evaluating changes in abundances over time (growth rates) for both algae and bacteria. The observed differences in algal cell fluorescence properties should be further assessed as a tool to identify and detect effects of oil contamination in the field. More research is required to assess its consistent occurrence for different taxa and evaluate whether this phenomenon results from cellular damage or interference by oil with DAPI staining.

EPS production in sea ice was inhibited under oil-exposed conditions likely due to inhibition of the major EPS source, the sea ice diatoms. Further research is required to determine if sub-lethal oil

concentrations could actually increase EPS production by ice algae as a physiological response to protect against exposure to soluble toxic compounds and direct oil contact.

Bacterial abundances appeared to respond not only to oil exposure but also to nutrient competition with sea ice algae. Here we suggest that bacterial response might be highest during the dark winter season with limited algal biomass and growth, while no abundance increase might occur after oil spills during the ice algal spring bloom. Other complex biological relationships, not addressed in this study, may affect bacterial biomass, including species selective oil toxicity or bacterial grazing by flagellates and ciliates. Here genomic sequencing may elucidate the potential increase of oil degrading microbes under oil spill scenarios.

In the case of an actual spill, the Natural Resource Damage Assessment of NOAA (https://darrp.noaa.gov/about-darrp/natural-resource-damage-assessment) requires identification of the damage, as well as an assessment and plan for restoration and monitoring. In terms of damage, this study suggests that oil spills during the ice algal bloom season can disrupt ice algal growth, which could lead to effects within the Arctic ecosystem on higher trophic levels as ice algae provide an abundant and early food source for pelagic zooplankton (Michel et al. 2006; Søreide et al. 2010; Durbin and Casas 2014) and benthic fauna (Boetius et al. 2013). Furthermore, ice algae may seed the annual phytoplankton bloom (Haecky et al. 1998; Jin et al. 2007; Szymanski and Gradinger 2016), which could be delayed or reduced under an oil spill scenario. Coupling measurements of both the pelagic and benthic ecosystem after an oil spill in icy conditions will be crucial for determining impacts to these realms. Advection of phytoplankton into the area of an oil spill may act to mitigate the loss of a localized phytoplankton seed population. If an oil spill were to occur during peak bloom the ice algae could become contaminated by the crude oil source and enter the food web either through adsorption or as an accumulation of toxic PAHs in the thylakoid membranes of algal cells (Marwood et al. 1999; Sargian et al. 2005). Early additions of inorganic nutrients to boost bacterial growth response and oil breakdown might be used to mitigate oil effects.

Currently three oil inhibition pathways have been suggested for algae in general: 1) direct adsorption to individual cells reducing nutrient and gas exchange (Jiang et al. 2010), 2) toxicological interactions with cell membranes and photosystem components (Singh and Gaur 1988; Aksmann and Tukaj 2008; Perez et al. 2010), and 3) reduction of light transmittance. We propose a fourth interaction unique to sea ice in which an oil lens will plug brine channels from below, isolating them from sea water exchange and reducing or eliminating replenishment of inorganic nutrients, oxygen and CO_2 from the underlying water mass. All four mechanisms would be most pronounced in the basal 1-2 cm where most

of the biological interactions occur in natural ice habitats. The toxicological impact could extend further into the ice due to fluid convection, dependent on brine channel connectivity.

Our study highlights the need for further investigations of oil exposure effects on diverse sea ice algal and bacterial communities. Such experiments could include interactions between light availability, algae and bacteria to elucidate if oil-degrading bacteria might be more efficient biological clean-up agents in the absence of algal growth (i.e. in the absence of light) as our results suggest. Also addition of inorganic nutrients might increase the biological clean-up by sea ice microbes to avoid nutrient limitation as factor. A wide range of species should be tested, as algal diversity in our tanks was limited. Furthermore we suggest studying the complete microbial network within such experiments, as bacterial loss terms could be important factors. Lower and varying oil concentrations should be utilized to study the biological response to sub-lethal oil concentrations. Clearly, future tank studies using the experimental and scientific insights gathered during this set of experiments can provide a solid scientific background to develop and improve adequate responses in case of oil spills in Arctic waters.

6. References

Agusti S, Sánchez MC (2002) Cell variability in natural phytoplankton communities quantified by a membrane permeability probe. Limnol Ocean 47:818–828.

Aksmann A, Tukaj Z (2008) Intact anthracene inhibits photosynthesis in algal cells: A fluorescence induction study on Chlamydomonas reinhardtii cw92 strain. Chemosphere 74:26–32. doi: 10.1016/j.chemosphere.2008.09.064

Alcoverro T, Conte E, Mazzella L (2000) Production of mucilage by the Adriatic epipelic diatom Cylindrotheca closterium (Bacillariophyceae) under nutrient limitation. J Phycol 36:1087–1095. doi: 10.1046/j.1529-8817.2000.99193.x

AMAP (2010) Assessment 2007: Oil and gas activities in the Arctic- effects and potential effects. Volume 1. Oslo, Norway

Arar EJ, Collins GB (1997) Method 445.0. in vitro determination of chlorophyll a and phaeophytin a in marine and freshwater by fluorescence. Natl Expo Res Lab Off Res Dev US Environ Prot Agency 1–22.

Arctic Council (2009) Arctic Marine Shipping Assessment 2009 Report.

Aslam SN, Cresswell-Maynard T, Thomas DN, Underwood GJC (2012a) Production and characterization of the intra- and extracellular carbohydrates and polymeric substances (EPS) of three sea-ice diatom species, and evidence for a cryoprotective role for EPS. J Phycol 48:1494–1509. doi: 10.1111/jpy.12004

Aslam SN, Underwood GJC, Kaartokallio H, et al (2012b) Dissolved extracellular polymeric substances (dEPS) dynamics and bacterial growth during sea ice formation in an ice tank study. Polar Biol 35:661–676. doi: 10.1007/s00300-011-1112-0

Aumack CF, Juhl AR, Krembs C (2014) Diatom vertical migration within land-fast Arctic sea ice. J Mar Syst 139:496–504. doi: 10.1016/j.jmarsys.2014.08.013

Bassett C, Lavery AC, Maksym T, Wilkinson JP (2016) Broadband acoustic backscatter from crude oil under laboratory-grown sea ice. J Acoust Soc Am 140:2274–2287. doi: 10.1121/1.4963876

Bates D, Mächler M, Bolker B, Walker S (2014) Fitting Linear Mixed-Effects Models using lme4. Submitt to J Stat Softw 67:51. doi: 10.18637/jss.v067.i01

Bender ML, Frantzen M, Vieweg I, et al (2016) Effects of chronic dietary petroleum exposure on reproductive development in polar cod (Boreogadus saida). Aquat Toxicol 180:196–208. doi: 10.1016/j.aquatox.2016.10.005

Bitton G, Freihofer V (1978) Influence of extracellular polysaccharides on the toxicity of copper and cadmium toward Klebsiella aerogenes. Microb Ecol 4:119–125.

Bock C, Eicken H (2005) A magnetic resonance study of temperature-dependent microstructural evolution and self-diffusion of water in Arctic first-year sea ice. Ann Glaciol 40:179–184. doi: 10.3189/172756405781813645

Boetius A, Albrecht S, Bakker K, et al (2013) Export of algal biomass from the melting Arctic sea ice. doi: 10.1126/science.1231346

Bragg JR, Prince RC, Harner EJ, Atlas RM (1994) Effectiveness of bioremediation for the Exxon Valdez oil spill. Nature 368:413–418. doi: 10.1038/367532a0

Brakstad OG, Nonstad I (2008) Responses of microbial communities in Arctic sea ice after contamination by crude petroleum oil. 540–552. doi: 10.1007/s00248-007-9299-x

Buist IA, Dickins DF (1987) Experimental spills of crude oil in pack ice. Int Oil Spill Conf Proc 1987:373–381. doi: 10.7901/2169-3358-1987-1-373

Buist I, Potter S, Nedwed T, Mullin J (2011) Herding surfactants to contract and thicken oil spills in pack ice for in situ burning. Cold Reg Sci Technol 67:3–23. doi: 10.1016/j.coldregions.2011.02.004

Chen J (2014) Factors affecting carbohydrate production and the formation of transparent exopolymer particles (TEP) by diatoms. Texas A&M

Cohn SA, Farrell JF, Munro JD, et al (2003) The effect of temperature and mixed species composition on diatom motility and adhesion. Diatom Res 18:225–243. doi: 10.1080/0269249X.2003.9705589

Collins RE, Rocap G, Deming JW (2010) Persistence of bacterial and archaeal communities in sea ice through an Arctic winter. Environ Microbiol 12:1828–1841. doi: 10.1111/j.1462-2920.2010.02179.x

Cota GF, Smith REH (1991) Ecology of bottom ice algae: II. Dynamics, distributions and productivity. J Mar Syst 2:279–295. doi: 10.1016/0924-7963(91)90037-U

Cox GFN, Weeks WF (1983) Equations for determining the gas and brine volumes in sea ice samples. J Glaciol 29:306–316. doi: 10.3198/1983JoG29-102-306-316

Cox GFN, Weeks WF (1975) Brine drainage and initial salt entrapment in sodium chloride ice.

Cross WE (1987) Effects of oil and chemically treated oil on primary productivity of high Arctic ice algae studied in situ. Arctic 40:266–276.

Cross WE, Martin CM (1987) Effects of oil and chemically treated oil on nearshore under-ice meiofauna studied in situ. Arctic 40:258–265.

Cullen JJ, Geider R, Ishizaka J, et al (1993) Toward a general description of phytoplankton growth for biogeochemical models. Towar. a Model Ocean Biogeochem. Process. 153–67.

Delille D (2000) Response of Antarctic soil bacterial assemblages to contamination by diesel fuel and crude oil. Microb Ecol 40:159–168. doi: 10.1007/s002480000027

Delille D, Bassères A, Dessommes A (1997) Seasonal variation of bacteria in sea ice contaminated by diesel fuel and dispersed crude oil. Microb Ecol 33:97–105. doi: 10.1007/s002489900012

Delille D, Bassères A, Dessommes A (1998) Effectiveness of bioremediation for oil-polluted Antarctic seawater. Polar Biol 19:237–241. doi: 10.1007/s003000050240

DuBois M, Gilles K a., Hamilton JK, et al (1956) Colorimetric method for determination of sugars and related substances. Anal Chem 28:350–356. doi: 10.1021/ac60111a017

Durbin EG, Casas MC (2014) Early reproduction by Calanus glacialis in the Northern Bering Sea: The role of ice algae as revealed by molecular analysis. J Plankton Res 36:523–541. doi: 10.1093/plankt/fbt121

Echeveste P, Agustí S, Dachs J (2010) Cell size dependent toxicity thresholds of polycyclic aromatic hydrocarbons to natural and cultured phytoplankton populations. Environ Pollut 158:299–307. doi: 10.1016/j.envpol.2009.07.006

Elarbaoui S, Richard M, Boufahja F, et al (2015) Effect of crude oil exposure and dispersant application on meiofauna: an intertidal mesocosm experiment. Environ Sci Process Impacts 17:997–1004. doi: 10.1039/C5EM00051C

Eronen-Rasimus E, Kaartokallio H, Lyra C, et al (2014) Bacterial community dynamics and activity in relation to dissolved organic matter availability during sea-ice formation in a mesocosm experiment. Microbiologyopen 3:139–156. doi: 10.1002/mbo3.157

Faksness LG, Brandvik PJ (2008) Distribution of water soluble components from oil encapsulated in Arctic sea ice: Summary of three field seasons. Cold Reg Sci Technol 54:106–114. doi: 10.1016/j.coldregions.2008.03.006

Faksness LG, Hansen BH, Altin D, Brandvik PJ (2012) Chemical composition and acute toxicity in the water after in situ burning - A laboratory experiment. Mar Pollut Bull 64:49–55. doi: 10.1016/j.marpolbul.2011.10.024

Farmer D, Li M (1994) Oil dispersion by turbulence and coherent circulations. Ocean Eng 21:575–586. doi: 10.1016/0029-8018(94)90007-8

Fiala M, Delille D (1999) Annual changes of microalgae biomass in Antarctic sea ice contaminated by crude oil and diesel fuel. Polar Biol 21:391–396. doi: 10.1007/s003000050378

Folke C, Carpenter SR, Walker B, et al (2004) Regime shifts, resilience, and biodiversity in ecosystem management. Annu Rev Ecol Evol Syst 35:557–581. doi: 10.2307/annurev.ecolsys.35.021103.30000021

Gardiner WW, Word JQ, Word JD, et al (2013) The acute toxicity of chemically and physically dispersed crude oil to key Arctic species under Arctic conditions during the open water season. Environ Toxicol Chem 32:2284–300. doi: 10.1002/etc.2307

Garneau M-È, Michel C, Meisterhans G, et al (2016) Hydrocarbon biodegradation by Arctic sea-ice and sub-ice microbial communities during microcosm experiments, Northwest Passage (Nunavut, Canada). 1–18. doi: 10.1093/femsec/fiw130

Garrisson D, Buck K (1989) The biota of Antarctic pack ice in the Weddell Sea and Antarctic peninsula regions. Polar Biol 10:211–219.

Gautier DL, Bird KJ, Charpentier RR, et al (2009) Assessment of undiscovered oil and gas in the Arctic. Science (80-) 324:1175–1179.

Gerdes B, Brinkmeyer R, Dieckmann G, Helmke E (2005) Influence of crude oil on changes of bacterial communities in Arctic sea-ice. FEMS Microbiol Ecol 53:129–139. doi: 10.1016/j.femsec.2004.11.010

Gilde K, Pinckney JL (2012) Sublethal effects of crude oil on the community structure of estuarine phytoplankton. Estuaries and Coasts 35:853–861. doi: 10.1007/s12237-011-9473-8

Glaeser JL, Vance GP (1972) A Study of the Behavior of Oil Spills in the Arctic. In: Offshore Technology Conference. Offshore Technology Conference,

Golden KM (2009) Climate change and the mathematics of transport in sea ice. Not Am Math Soc 56:562–584.

González J, Figueiras FG, Aranguren-Gassis M, et al (2009) Effect of a simulated oil spill on natural assemblages of marine phytoplankton enclosed in microcosms. Estuar Coast Shelf Sci 83:265–276. doi: 10.1016/j.ecss.2009.04.001

Gosselin M, Legendre L (1990) Light and nutrient limitation of sea-ice microalgae (Hudson Bay, Canadian Arctic). J. Phycol. 37:1125.

Gosselin M, Levasseur M, Wheeler PA, et al (1997) New measurements of phytoplankton and ice algal production in the Arctic Ocean. Deep Res Part II Top Stud Oceanogr 44:1623–1644. doi: 10.1016/S0967-0645(97)00054-4

Gradinger R (1999) Vertical fine structure of the biomass and composition of algal communities in Arctic pack ice. Mar Biol 133:745–754. doi: 10.1007/s002270050516

Gradinger R, Friedrich C, Spindler M (1999) Abundance, biomass and composition of the sea ice biota of the Greenland Sea pack ice. Deep Sea Res Part II Top Stud Oceanogr 46:1457–1472. doi: 10.1016/S0967-0645(99)00030-2

Gradinger R, Ikävalko J (1998) Organism incorporation into newly forming Arctic sea ice in the Greenland Sea. J Plankton Res 20:871–886. doi: 10.1093/plankt/20.5.871

Gradinger R, Kaufman M, Bluhm B (2009) Pivotal role of sea ice sediments in the seasonal development of near-shore Arctic fast ice biota. Mar Ecol Prog Ser 394:49–63. doi: 10.3354/meps08320

Gradinger R, Zhang Q (1997) Vertical distribution of bacteria in Arctic sea ice from the Barents and Laptev Seas. Polar Biol 17:448–454. doi: 10.1007/s003000050139

Gradinger R, Meiners K, Plumley G, Zhang Q, Bluhm BA (2005) Abundance and composition of the sea-ice meiofauna in off-shore pack ice of the Beaufort Gyre in summer 2002 and 2003. Polar Biol 28.3:171-181.

Grenfell TC, Perovich DK (2008) Incident spectral irradiance in the Arctic Basin during the summer and fall. J Geophys Res Atmos 113:1–13. doi: 10.1029/2007JD009418

Haecky P, Jonsson S, Andersson A (1998) Influence of sea ice on the composition of the spring phytoplankton bloom in the northern Baltic Sea. Polar Biol 20:1–8. doi: 10.1007/s003000050270

Hamburg Ship Model Basin (2016) Arctic Environmental Test Basin. http://www.hsva.de/our-facilities/arctic-environmental-test-basin.html.

Hansen BH, Lie KK, Størseth TR, et al (2016) Exposure of first-feeding cod larvae to dispersed crude oil results in similar transcriptional and metabolic responses as food deprivation. J Toxicol Environ Heal - Part A Curr Issues 79:558–571. doi: 10.1080/07317131.2016.1171985

Harsem Ø, Heen K, Rodrigues JMP, Vassdal T (2013) Oil exploration and sea ice projections in the Arctic. Polar Rec (Gr Brit) 51:91–106. doi: 10.1017/S0032247413000624

Hassall AH (1845) A history of the British freshwater algæ, including descriptions of the Desmidæ and Diatomaceæ with upwards of one hundred plates, illustrating the various species. 1:1–462.

Hazen TC, Dubinsky E a, DeSantis TZ, et al (2010) Deep-sea oil plume enriches indigenous oil-degrading bacteria. Science 330:204–208. doi: 10.1126/science.1195979

Horner R, Schrader GC (1982) Relative contributions of ice algae, phytoplankton, and benthic microalgae to primary production in nearshore regions of the Beaufort Sea. Arctic 35:485–503. doi: 10.14430/arctic2356

Hsiao SC (1978) Effects of crude oils on the growth of Arctic marine phytoplankton. Environ Pollut 93–107.

Hsiao SIC (1980) Quantitative composition, distribution, community structure and standing stock of sea ice microalgae in the Canadian Arctic. Arctic 33:768–793. doi: 10.14430/arctic2595

ITOPF (2011) Fate of marine oil spills. 2:London:ITOPF.

Jiang Z, Huang Y, Xu X, et al (2010) Advance in the toxic effects of petroleum water accommodated fraction on marine plankton. Acta Ecol Sin 30:8–15. doi: 10.1016/j.chnaes.2009.12.002

Jin M, Deal C, Wang J, et al (2007) Ice-associated phytoplankton blooms in the southeastern Bering Sea. Geophys Res Lett 34:1–6. doi: 10.1029/2006GL028849

Karlsson J (2009) A laboratory study of fixation, release rates and small scale movement of oil in sea ice. Univesrity of Copenhagen

Karlsson J, Petrich C, Eicken H (2011) Oil entrainment and migration in laboratory grown saltwater ice. 10.

Kotovitch M, Moreau S, Zhou J, et al (2016) Air-ice carbon pathways inferred from a sea ice tank experiment. Elem Sci Anthr 4:112. doi: 10.12952/journal.elementa.000112

Krembs C, Eicken H, Deming JW (2011) Exopolymer alteration of physical properties of sea ice and implications for ice habitability and biogeochemistry in a warmer Arctic. Proc Natl Acad Sci U S A 108:3653–8. doi: 10.1073/pnas.1100701108

Krembs C, Eicken H, Junge K, Deming JW (2002) High concentrations of exopolymeric substances in Arctic winter sea ice: Implications for the polar ocean carbon cycle and cryoprotection of diatoms. Deep Res Part I Oceanogr Res Pap 49:2163–2181. doi: 10.1016/S0967-0637(02)00122-X

Krembs C, Engel A (2001) Abundance and variability of microorganisms and transparent exopolymer particles across the ice-water interface of melting first-year sea ice in the Laptev Sea (Arctic). Mar Biol 138:173–185. doi: 10.1007/s002270000396

Krembs C, Gradinger R, Spindler M (2000) Implications of brine channel geometry and surface area for the interaction of sympagic organisms in Arctic sea ice. J Exp Mar Bio Ecol 243:55–80. doi: 10.1016/S0022-0981(99)00111-2

Krembs C, Mock T, Gradinger R (2001) A mesocosm study of physical-biological interactions in artificial sea ice: Effects of brine channel surface evolution and brine movement on algal biomass. Polar Biol 24:356–364. doi: 10.1007/s003000000219

Kuparinen J, Autio R, Kaartokallio H (2011) Sea ice bacterial growth rate, growth efficiency and preference for inorganic nitrogen sources in the Baltic Sea. Polar Biol 34:1361–1373. doi: 10.1007/s00300-011-0989-y

Lange B a., Michel C, Beckers JF, et al (2015) Comparing springtime ice-algal chlorophyll a and physical properties of multi-year and first-year sea ice from the Lincoln Sea. PLoS One 10:e0122418. doi: 10.1371/journal.pone.0122418

Lee SH, Whitledge TE, Kang SH (2008) Spring time production of bottom ice algae in the landfast sea ice zone at Barrow, Alaska. J Exp Mar Bio Ecol 367:204–212. doi: 10.1016/j.jembe.2008.09.018

Leppäranta M, Manninen T (1988) The brine and gas content of sea ice with attention to low salinities and high temperatures. Finnish Inst. Mar. Res. Intern. Rep. 2:1–14.

Leu E, Mundy CJ, Assmy P, et al (2015) Arctic spring awakening - Steering principles behind the phenology of vernal ice algal blooms. Prog Oceanogr 139:151–170. doi: 10.1016/j.pocean.2015.07.012

Lewis MR, Warnock RE (1985) Measuring photosynthetic action spectra of natural phytoplankton populations. J Phycol 21:310–315. doi: 10.1111/j.0022-3646.1985.00310.x

Li M, Garrett C (1998) The relationship between oil droplet size and upper ocean turbulence. Mar Pollut Bull 36:961–970. doi: 10.1016/S0025-326X(98)00096-4

Liu SB, Chen XL, He HL, et al (2013) Structure and ecological roles of a novel exopolysaccharide from the Arctic sea ice bacterium Pseudoalteromonas sp. strain SM20310. Appl Environ Microbiol 79:224–230. doi: 10.1128/AEM.01801-12

MacNeill MR, Goodman RH (1987) Oil motion during lead closure. Environmental Studies Resolving Funds Report No. 053.

Mahoney A, Eicken H, Gaylord AG, Shapiro L (2007) Alaska landfast sea ice: Links with bathymetry and atmospheric circulation. J Geophys Res Ocean. doi: 10.1029/2006JC003559

Mahoney AR, Eicken H, Gaylord AG, Gens R (2014) Landfast sea ice extent in the Chukchi and Beaufort Seas: The annual cycle and decadal variability. Cold Reg Sci Technol 103:41–56. doi: 10.1016/j.coldregions.2014.03.003

Malmgren F (1927) On the properties of sea-ice. Norw North Pol Exp Sci Res 1:1-6.

Manes SS, Gradinger R (2009) Small scale vertical gradients of Arctic ice algal photophysiological properties. Photosynth Res 1–14. doi: 10.1007/s11120-009-9489-0

Margesin R, Schinner F (2001) Biodegradation and bioremediation of hydrocarbons in extreme environments. Appl Microbiol Biotechnol 56:650–663. doi: 10.1007/s002530100701

Margesin R, Schinner F (1999) Biological decontamination of oil spills in cold environments. J Chem Technol Biotechnol 74:381–389. doi: 10.1002/(SICI)1097-4660(199905)74:5<381::AID-JCTB59>3.0.CO;2-0

Martín-Robichaud D, Peterson RH (1998) Effects of light intensity, tank colour and photoperiod on swimbladder inflation success in larval striped bass, Morone saxatilis (Walbaum). Aquac Res 29:539–547. doi: 10.1046/j.1365-2109.1998.00234.x

Martin S, Drucker R, Fort M (1995) A laboratory study of frost flower growth on the surface of young sea ice. J Geophys Res 100:7027–7036. doi: 10.1029/94JC03243

Martin S, Kauffman P, Welander PE (1977) A laboratory study of the dispersion of crude oil within sea ice grown in a wave field. In: Proceedings of the Twenty-Seventh Alaska Science Conference.

Marwood C a, Smith RE, Solomon KR, et al (1999) Intact and photomodified polycyclic aromatic hydrocarbons inhibit photosynthesis in natural assemblages of Lake Erie phytoplankton exposed to solar radiation. Ecotoxicol Environ Saf 44:322–327. doi: 10.1006/eesa.1999.1840

Masutani SM, Adams EE (2000) Experimental study of multi-phase plumes with application to deep ocean oil spills.

McConnell B, Gradinger R, Iken K, Bluhm B (2012) Growth rates of Arctic juvenile Scolelepis squamata (Polychaeta: Spionidae) isolated from Chukchi Sea fast ice. Polar Biol 35:1487–1494. doi: 10.1007/s00300-012-1187-2

McFarlin KM, Prince RC, Perkins R, Leigh MB (2014) Biodegradation of dispersed oil in Arctic seawater at -1°C. PLoS One 9:1–8. doi: 10.1371/journal.pone.0084297

Michel C, Ingram RG, Harris LR (2006) Variability in oceanographic and ecological processes in the Canadian Arctic Archipelago. Prog Oceanogr 71:379–401. doi: 10.1016/j.pocean.2006.09.006

Miller CB, Wheeler PA (2012) Biological Oceanography, 2nd ed. Oregon State University

Mock T, Dieckmann GS, Haas C, et al (2002) Micro-optodes in sea ice: A new approach to investigate oxygen dynamics during sea ice formation. Aquat Microb Ecol 29:297–306. doi: 10.3354/ame029297

Mock T, Gradinger R (1999) Determination of Arctic ice algal production with a new in situ incubation technique. Mar Ecol Prog Ser 177:15–26. doi: Doi 10.3354/Meps177015

Mundy CJ, Barber DG, Michel C (2005) Variability of snow and ice thermal, physical and optical properties pertinent to sea ice algae biomass during spring. J Mar Syst 58:107–120. doi: 10.1016/j.jmarsys.2005.07.003

Nakawo M, Sinha NK (1981) Growth rate and salinity profile of first-year sea ice in the high Arctic. J Glaciol 27:313–328.

Nichols CM, Bowman JP, Guezennec J (2005) Effects of incubation temperature on growth and production of exopolysaccharides by an Antarctic sea ice bacterium grown in batch culture. Appl Environ Microbiol 71:3519–3523. doi: 10.1128/AEM.71.7.3519

Nicolaus M, Petrich C, Hudson SR, Granskog MA (2013) Variability of light transmission through Arctic land-fast sea ice during spring. Cryosphere 7:977–986. doi: 10.5194/tc-7-977-2013

NORCOR Engineering and Research Ltd. (1975) The Interaction of Crude Oil with Arctic Sea Ice.

Overland JE, Wang M (2013) When will the summer Arctic be nearly sea ice free? Geophys Res Lett 40:2097–2101. doi: 10.1002/grl.50316

Özhan K, Miles SM, Gao H, Bargu S (2014) Relative phytoplankton growth responses to physically and chemically dispersed South Louisiana sweet crude oil. Environ Monit Assess 186:3941–3956. doi: 10.1007/s10661-014-3670-4

Ozturk S, Aslim B (2010) Modification of exopolysaccharide composition and production by three cyanobacterial isolates under salt stress. Environ Sci Pollut Res 17:595–602. doi: 10.1007/s11356-009-0233-2

Perez P, Fernandez E, Beiras R (2010) Fuel toxicity on Isochrysis galbana and a coastal phytoplankton assemblage: Growth rate vs. variable fluorescence. Ecotoxicol Environ Saf 73:254–261. doi: 10.1016/j.ecoenv.2009.11.010

Perovich DK, Gow AJ (1996) A quantitative description of sea ice inclusions. J Geophys Res 101:18327. doi: 10.1029/96JC01688

Perovich DK, Richter-Menge JA (1994) Surface characteristics of lead ice. J Geophys Res 99:16341–16350. doi: 10.1029/94JC01194

Petrich C, Karlsson J, Eicken H (2013) Porosity of growing sea ice and potential for oil entrainment. Cold Reg Sci Technol 87:27–32. doi: 10.1016/j.coldregions.2012.12.002

Podkuiko L (2013) The effects of two crude oil solutions to phytoplankton species. Dissertation, University of Tartu, Tartu, Estonia.

Porter KG, Feig YS (1980) The use of DAPI for identifying aquatic microfloral. Limnol Oceanogr 25:943–948. doi: 10.4319/lo.1980.25.5.0943

Poulin M, Daugbjerg N, Gradinger R, et al (2011) The pan-Arctic biodiversity of marine pelagic and sea-ice unicellular eukaryotes: A first-attempt assessment. Mar Biodivers 41:13–28. doi: 10.1007/s12526-010-0058-8

Prince RC, McFarlin KM, Butler JD, et al (2013) The primary biodegradation of dispersed crude oil in the sea. Chemosphere 90:521–526. doi: 10.1016/j.chemosphere.2012.08.020

Ralph PJ, Ryan KG, Martin A, Fenton G (2007) Melting out of sea ice causes greater photosynthetic stress in algae than freezing in. J Phycol 43:948–956. doi: 10.1111/j.1529-8817.2007.00382.x

Ratkova TN, Wassmann P (2005) Sea ice algae in the White and Barents seas: Composition and origin. Polar Res 24:95–110. doi: DOI 10.1111/j.1751-8369.2005.tb00143.x

Reimnitz E, Clayton JR, Kempema EW, et al (1993) Interaction of rising frazil with suspended particles: tank experiments with applications to nature. Cold Reg Sci Technol 21:117–135. doi: 10.1016/0165-232X(93)90002-P

Riedel A, Michel C, Gosselin M (2006) Seasonal study of sea-ice exopolymeric substances on the Mackenzie shelf: Implications for transport of sea-ice bacteria and algae. Aquat Microb Ecol 45:195–206. doi: 10.3354/ame045195

Robinson DH, Kolber Z, Sullivan CW (1997) Photophysiology and photoacclimation in surface sea ice algae from McMurdo Sound, Antarctica. Mar Ecol Prog Ser 147:243–256. doi: 10.3354/meps147243

Roth BL, Poot M, Yue ST, et al (1997) Bacterial viability and antibiotic susceptibility testing with SYTOX green nucleic acid stain. 63:2421–2431.

Sargian P, Mostajir B, Chatila K, et al (2005) Non-synergistic effects of water-soluble crude oil and enhanced ultraviolet-B radiation on a natural plankton assemblage. Mar Ecol Prog Ser 294:63–77. doi: 10.3354/meps294063

Selldén G, Leech RM (1981) Localization of DNA in mature and young wheat chloroplasts using the fluorescent probe 4'-6-Diamidino-2-phenylindole. Plant Physiol 68:731–734. doi: 10.1104/pp.68.3.731

Singh AK, Gaur JP (1988) Effect of assam crude on photosynthesis and associated electron transport system in Anabaena doliolum. Bull Environ Contam Toxicol 41:776–780. doi: 10.1007/BF02021033

Siron R, Pelletier E, Delille D, Roy S (1993) Fate and effects of dispersed crude oil under icy conditions simulated in mesocosms. Mar Environ Res 35:273–302. doi: 10.1016/0141-1136(93)90098-K

Smedsrud Henrik LH (2001) Frazil-ice entrainment of sediment: Large-tank laboratory experiments. J Glaciol 47:461–471. doi: 10.3189/172756501781832142

SOKI Wiki (2014) Carbohydrate analysis. http://soki.aq/display/StandMeth/Carbohydrate+Analysis. Accessed 2014.

Søreide JE, Leu E, Berge J, et al (2010) Timing of blooms, algal food quality and Calanus glacialis reproduction and growth in a changing Arctic. Glob Chang Biol no-no. doi: 10.1111/j.1365-2486.2010.02175.x

Suzuki Y, Kudoh S, Takahashi M (1997) Photosynthetic and respiratory characteristics of an Arctic ice algal community living in low light and low temperature conditions. J Mar Syst 11:111–121. doi: 10.1016/S0924-7963(96)00032-2

Szymanski A, Gradinger R (2016) The diversity, abundance and fate of ice algae and phytoplankton in the Bering Sea. Polar Biol 39:309–325. doi: 10.1007/s00300-015-1783-z

Thingstad TF, Lignell R (1997) Theoretical models for the control of bacterial growth rate, abundance, diversity and carbon demand. Aquat Microb Ecol 13:19–27. doi: 10.3354/ame013019

Tison J-L, Haas C, Gowing MM, et al (2002) Tank study of physico-chemical controls on gas content and composition during growth of young sea ice. J Glaciol 48:177–191. doi: 10.3189/172756502781831377

Tkalich P, Chan ES (2002) Vertical mixing of oil droplets by breaking waves. Mar Pollut Bull 44:1219–1229. doi: 10.1016/S0025-326X(02)00178-9

Underwood GJC, Aslam SN, Michel C, et al (2013) Broad-scale predictability of carbohydrates and exopolymers in Antarctic and Arctic sea ice. Proc Natl Acad Sci U S A 110:15734–9. doi: 10.1073/pnas.1302870110

van der Merwe P, Lannuzel D, Nichols C a M, et al (2009) Biogeochemical observations during the winter-spring transition in East Antarctic sea ice: Evidence of iron and exopolysaccharide controls. Mar Chem 115:163–175. doi: 10.1016/j.marchem.2009.08.001

Veldhuis M, Kraay G, Timmermans K (2001) Cell death in phytoplankton: correlation between changes in membrane permeability, photosynthetic activity, pigmentation and growth. Eur J Phycol 36:167–177. doi: 10.1080/09670260110001735318

Vézina AF, Demers S, Laurion I, et al (1997) Carbon flows through the microbial food web of first-year ice in resolute passage (Canadian High Arctic). J Mar Syst 11:173–189. doi: 10.1016/S0924-7963(96)00037-1

Wang M, Overland JE (2012) A sea ice free summer Arctic within 30 years: An update from CMIP5 models. Geophys Res Lett 39:n/a-n/a. doi: 10.1029/2012GL052868

Wang R, Shen HH (2010) Experimental study on surface wave propagating through a grease-pancake ice mixture. Cold Reg Sci Technol 61:90–96. doi: 10.1016/j.coldregions.2010.01.011

Weeks WF, Lee OS (1958) Observations on the physical properties of sea ice at Hopedale, Labrador. Arctic 11:134–155.

Weissenberger J (1998) Arctic Sea ice biota: Design and evaluation of a mesocosm experiment. Polar Biol 19:151–159. doi: 10.1007/s003000050228

Weissenberger J, Dieckmann G, Gradinger R, Spindler M (1992) Sea ice: A cast technique to examine and analyze brine pockets and channel structure. Limnol Oceanogr 37:179–183. doi: 10.4319/lo.1992.37.1.0179

Weissenberger J, Grossmann S (1998) Experimental formation of sea ice: Importance of water circulation and wave action for incorporation of phytoplankton and bacteria. Polar Biol 20:178–188. doi: 10.1007/s003000050294

Williamson DH, Fennell DJ (1979) Visualization of yeast mitochondrial dna with the fluorescent stain "DAPI." Methods Enzymol 56:728–733. doi: 10.1016/0076-6879(79)56065-0

Wilson D, Mackay D (1986) The behaviour of oil in freezing situations. Manuscript Report EE92, Environment Canada, Ottawa, ON.

Zhang Q, Gradinger R, Spindler M (1999) Experimental study on the effect of salinity on growth rates of Arctic-sea-ice algae from the Greenland Sea. High Temp 1–8.

Zheng L, Yapa PD (2000) Buoyant velocity of spherical and nonspherical bubbles/droplets. J Hydraul Eng 126:852–854. doi: 10.1061/(ASCE)0733-9429(2000)126:11(852)

Zhou J, Delille B, Kaartokallio H, et al (2014) Physical and bacterial controls on inorganic nutrients and dissolved organic carbon during a sea ice growth and decay experiment. Mar Chem 166:59–69. doi: 10.1016/j.marchem.2014.09.013

Zhu S, Bail AL, Ramaswamy HS (2003) Ice crystal formation in pressure shift freezing of atlantic salmon (Salmo Salar) as compared to classical freezing methods. J Food Process Preserv 27:427–444. doi: 10.1111/j.1745-4549.2003.tb00528.x